Kirti Thesis new.pdf

Delhi Technological University

Document Details

Submission ID
trn:oid:::27535:128400783

Submission Date
Feb 16, 2026, 4:58 PM GMT+5:30

Download Date
Feb 16, 2026, 5:07 PM GMT+5:30

File Name
Kirti Thesis new.pdf

File Size
3.2 MB

217 Pages

49,163 Words

264,506 Characters

6% Overall Similarity

The combined total of all matches, including overlapping sources, for each database.

Filtered from the Report

- Bibliography
- Quoted Text
- Cited Text
- Small Matches (less than 10 words)
- Crossref database

Match Groups

187 Not Cited or Quoted 6%
Matches with neither in-text citation nor quotation marks

0 Missing Quotations 0%
Matches that are still very similar to source material

0 Missing Citation 0%
Matches that have quotation marks, but no in-text citation

0 Cited and Quoted 0%
Matches with in-text citation present, but no quotation marks

Top Sources

4% Internet sources
1% Publications
3% Submitted works (Student Papers)

Integrity Flags

1 Integrity Flag for Review

Replaced Characters
123 suspect characters on 50 pages
Letters are swapped with similar characters from another alphabet.

Our system's algorithms look deeply at a document for any inconsistencies that would set it apart from a normal submission. If we notice something strange, we flag it for you to review.

A Flag is not necessarily an indicator of a problem. However, we'd recommend you focus your attention there for further review.

Match Groups

187 Not Cited or Quoted 6%
Matches with neither in-text citation nor quotation marks

0 Missing Quotations 0%
Matches that are still very similar to source material

0 Missing Citation 0%
Matches that have quotation marks, but no in-text citation

0 Cited and Quoted 0%
Matches with in-text citation present, but no quotation marks

Top Sources

4% Internet sources
1% Publications
3% Submitted works (Student Papers)

Top Sources

The sources with the highest number of matches within the submission. Overlapping sources will not be displayed.

1	Internet	dspace.dtu.ac.in:8080 <1%
2	Submitted works	Delhi Technological University on 2017-02-09 <1%
3	Internet	docs.neu.edu.tr <1%
4	Submitted works	IIT Delhi on 2013-10-18 <1%
5	Internet	pdffox.com <1%
6	Submitted works	Delhi Technological University on 2024-04-26 <1%
7	Internet	hdl.handle.net <1%
8	Internet	coek.info <1%
9	Internet	link.springer.com <1%
10	Submitted works	University of Mustansiriyah on 2014-11-01 <1%

11 Internet
tudr.thapar.edu:8080 <1%

12 Internet
ndl.ethernet.edu.et <1%

13 Internet
repository.ju.edu.et <1%

14 Internet
gyan.iitg.ernet.in <1%

15 Internet
www.karlin.mff.cuni.cz <1%

16 Submitted works
National Institute of Technology, Rourkela on 2022-05-11 <1%

17 Internet
www.eudoxuspress.com <1%

18 Internet
repository.nwu.ac.za <1%

19 Submitted works
BML Munjal University on 2025-08-21 <1%

20 Submitted works
Jamia Milia Islamia University on 2017-04-10 <1%

21 Publication
Kaya, Serap. "Korovkin şartlarını gerçekleyen Genel Bir Lineer Pozitif operatörler ... <1%

22 Publication
Bhadurali, Sadik Amin. "Analysis of Airbnb Pricing in Lisbon: A Machine Learning ... <1%

23 Submitted works
Eastern Mediterranean University on 2014-09-15 <1%

24 Publication
Moeini, Mohammad. "Computational Analysis and Data-Driven Modeling of Hurri... <1%

25 Publication
Abdelwahab Kharab, Abdelwahab Kharab, Ronald B. Guenther. "An Introduction t... <1%

26 Internet
ijnao.um.ac.ir <1%

27 Internet
www.unioviedo.es <1%

28 Submitted works
Atilim University on 2017-05-11 <1%

29 Submitted works
Bülent Ecevit Üniversitesi on 2017-08-25 <1%

30 Publication
Cenk Temizel, Salih Tutun, Celal Hakan Canbaz, Ekrem Alagoz et al. "Artificial Inte... <1%

31 Submitted works
University of Bristol on 2023-03-20 <1%

32 Internet
www.researchgate.net <1%

33 Submitted works
Indian Institute of Technology Guwahati on 2018-04-24 <1%

34 Publication
Santanu Saha Ray, Prakash Kumar Sahu. "Novel Methods for Solving Linear and ... <1%

35 Internet
dspace.bits-pilani.ac.in:8080 <1%

36 Submitted works
Jamia Milia Islamia University on 2018-08-04 <1%

37 Publication
Bayati, Mohamed. "Interaction at the Solid-Water Interface of 0d and 2d Carbon ... <1%

38 Submitted works
Sardar Vallabhbhai National Inst. of Tech.Surat on 2018-02-23 <1%

39 Submitted works
Middle East Technical University on 2017-06-23 <1%

40 Submitted works
National Institute of Technology, Rourkela on 2018-04-05 <1%

41 Internet
docplayer.net <1%

42 Internet
dokumen.pub <1%

43 Publication
Khan, Danish. "Improved Interpolation and Extrapolation Across Chemical Comp... <1%

44 Publication
Shah, Jayvir Harishbhai. "Optimizing Gasoline Engines for Complying to Future E... <1%

45 Publication
Chatterjee, Abhishek. "Tribological behavior of CVD-grown hafnium diboride thin ... <1%

46 Submitted works
Indian Institute of Technology Guwahati on 2018-04-24 <1%

47 Submitted works
Phuket Rajabhat University on 2021-12-30 <1%

48 Publication
Riaz, Bilal. "Applications of Computational Optimal Transport in Machine Learnin... <1%

49 Internet
doi.org <1%

50 Internet
ebin.pub <1%

51 Internet
etd.uwc.ac.za <1%

52 Internet
gyan.iitg.ac.in <1%

53 Submitted works
Addis Ababa University on 2025-09-12 <1%

54 Publication
Cai, Yaoyuan. "Fast Operator Splitting Algorithms for Spatial Fractional Diffusion ... <1%

55 Submitted works
Eastern Mediterranean University on 2021-08-16 <1%

56 Submitted works
LNM Institute of Information Technology on 2022-03-11 <1%

57 Publication
Mariesa L. Crow. "Computational Methods for Electric Power Systems", CRC Press... <1%

58 Publication
Mark S. Gockenbach. "Finite-Dimensional Linear Algebra", CRC Press, 2019 <1%

59 Submitted works
National Institute of Technology, Rourkela on 2018-10-25 <1%

60 Submitted works
North West University on 2020-09-24 <1%

61 Submitted works
Panjab University on 2015-02-25 <1%

62 Submitted works
Panjab University on 2016-08-23 <1%

63 Submitted works
Universiti Sains Malaysia on 2017-05-17 <1%

64 Submitted works
Utah Education Network on 2018-01-12 <1%

65 Publication
Yilik, Özlem Öksüzer. "Bazı lineer pozitif operatörlerin varyasyon yarınormunda y... <1%

66 Internet
ir.library.nitw.ac.in:8080 <1%

67 Internet

pubs.sciepub.com <1%

NUMERICAL AND MACHINE LEARNING APPROACH FOR SINGULARLY PERTURBED PROBLEMS WITH APPLICATION TO CYCLONE MODELING

A thesis submitted to

DELHI TECHNOLOGICAL UNIVERSITY

in partial fulfillment of the requirements of the award of the degree of

DOCTOR OF PHILOSOPHY

in

MATHEMATICS

by

KIRTI BENIWAL

under the supervision of

Dr. Vivek Kumar Aggarwal

DEPARTMENT OF APPLIED MATHEMATICS

DELHI TECHNOLOGICAL UNIVERSITY

BAWANA ROAD, DELHI-110 042, INDIA.

February 2026 **Enroll. No. : 2K21/PhDAM/06**

DECLARATION

I hereby declare that the research work presented in this thesis entitled "**Numerical and Machine learning approach for singularly perturbed problems with application to cyclone modeling**" submitted to the Delhi Technological University, Delhi for the award of the degree of *Doctor of Philosophy in Mathematics* has been carried out by me under the supervision of *Dr. Vivek Kumar Aggarwal*, Department of Applied Mathematics, Delhi Technological University, Delhi, India.

The research work embodied in this thesis, except where otherwise indicated, is my original research. I have not previously submitted any portion or all of this thesis to any other university/institution for the purpose of receiving a degree/diploma. Unless otherwise stated, this thesis contains no other person's data, graphs, or other content.

February 2026

(KIRTI BENIWAL)
Enrollment No.: 2K21/PhDAM/06
Department of Applied Mathematics
Delhi Technological University
Delhi-110042.

CERTIFICATE

This is to certify that the thesis entitled "**Numerical and Machine learning approach for singularly perturbed problems with application to cyclone modeling**" submitted by **Ms. KIRTI BENIWAL** in the Department of Applied Mathematics, Delhi Technological University, Delhi, India for the award of degree of *Doctor of Philosophy in Mathematics*, is an original contribution and a faithful record of research work carried out by her under my supervision.

I have studied this thesis and believe it to be totally suitable in quality level as a thesis for the Doctor of Philosophy degree.

To the best of my knowledge, the work carried out in this thesis is original but it has not been presented in any form to any other university/institution for the purpose of receiving a degree or certification.

(Dr. Vivek Kumar Aggarwal)
Supervisor
Department of Applied Mathematics
Delhi Technological University
Delhi.

(Dr. R. Srivastva)
Professor & Head
Department of Applied Mathematics
Delhi Technological University
Delhi.

ACKNOWLEDGEMENTS

To start with, I express my sincere gratitude to Almighty God for strength, wisdom, and perseverance throughout the doctoral thesis. This research work would never possible without the guidance, encouragement, and support of many individuals who contributed directly or indirectly to my academic journey.

I express my heartfelt gratitude to my respected supervisor, Dr. Vivek Kumar Aggarwal, Department of Applied Mathematics, Delhi Technological University (DTU), Delhi, for his patience, guidance, and valuable suggestions. His academic insight and constructive feedback played a valuable role in shaping this research work. It is a great privilege to work under his supervision, and I sincerely thank him for the academic freedom and his confidence he laid in me to pursue my research interests.

I am sincerely thankful to Prof. R. Srivastva, Head of Department of Applied Mathematics, DTU, for offering valuable guidance and support which greatly contributed to the successful completion of this work.

I extend my sincere thanks to my SRC members, Prof. Anil Kumar, Department of Applied Chemistry, and Dr. Nilam, Department of Applied Mathematics, for their constructive feedback and academic accumen which improved the quality of this research.

I also express my gratitude to Prof. Naokant Deo, Department of Applied Mathematics, DTU, and all the members of the DRC of the Department of Applied Mathematics for their continuous support and motivation throughout my work.

I would like to thanks Dr. Ruchika (IMI, Delhi), Dr. Sudhakar (DU), and Dr. Shashi kant (IMD), Ms. Anshu, Ms. Rachna, Ms. Brahmvidhya, and Mr. Krishna Mishra (IMD) for their cooperation and assistance which made this work possible. I am grateful for their assistance and good wishes.

I gracefully acknowledge the Academic Branch, Administration of Delhi Technological University and office staff of the Department of Applied Mathematics for their cooperation and continuous support to create such progressive environment.

I owe my deepest gratitude to my family for their trust, and emotional support. I am sincerely thankful to my father, Mr. Subhash Beniwal and Mr. Yudhvir Dahiya, and my mother, Mrs. Sunil and Mrs. Amita, for their belief in my abilities and aspiration. I am specially grateful to my beloved Surya Dahiya, and my brother

Ankit for their constant support, strength and motivation throughout this journey.

I gratefully thanks Delhi Technological University for awarding me a fellowship, with financial support and made this research work smoother.

Finally, I would like to give my vote of thanks to all those who have not been mentioned here by name but have supported me in various ways during my Ph.D. journey.

February 2026 **(KIRTI BENIWAL)**

To my late Grand Father

Contents

Preface

This thesis contributes to numerical methods and ML approach for singularly perturbed differential and its application in cyclone modelling. The purpose of this research is to approximate singularly perturbed differential equations using approximation methods. We investigate, develop, and analyse numerical methods, as well as their implementations, for such challenging problems. A chapter-by-chapter structure of the thesis is as follows:

Chapter 1 is introductory in nature which gives a brief review of SPPs and survey on numerical analysis of SPDDEs and numerical techniques. Objectives, Literature survey and a brief summary of the present work is also included in this chapter.

Chapter 2 is about the numerical collocation methods based on Bernstein collocation method using equispaced nodes and Chebyshev-Gauss-Lobatto Nodes for solving linear and non linear singularly perturbed differntial equations, and results are then compared with traditional methods and error analysis is carried out.

In *chapter 3*, is devoted to Szasz Mirakyan operator . In this chapter we solved both linear and non linear singularly perturbed differntial equations and compared with traditional Methods Stability Analysis and error analysis is carried.

In *chapter 4*, This chapter presents a novel framework combining the Bernstein-Chlodowsky operator with neural networks termed as Bernstein-Chlodowsky Neural Network (BNN) and Bernstein-Chlodowsky collocation method (CCM) for solving singularly perturbed differential equations (SPDEs) in the context of atmospheric science and cyclone modeling. We solve linear and nonlinear SPDEs using the Bernstein-Chlodowsky collocation method and BNN, emphasizing how well these methods captures the convection dominated processes observed in cyclonic systems. The operator's superior convergence and boundary layer resolution make it an effective tool for cyclone modeling.

Chapter 5 This chapter focuses on predicting the Accumulated Cyclone Energy

(ACE) in the NIO during monsoon using an optimized Artificial Neural Network (ANN) model. The permutation feature is essential in finding the most influential features to improve model performance

Chapter 6 This chapter aims to forecast, using yearly cyclone data, the Accumulated Cyclone Energy (ACE) values for the North Indian Ocean (NIO) area. We study a predictive framework for estimating Accumulated Cyclone Energy (ACE) in the North Indian Ocean (NIO) using historical cyclone data from 1982 to 2023, en- compassing the Arabian Sea (AS) and Bay of Bengal (BOB) basins. Interpolation was performed using the Szász-Mirakyan operator, which preserves the statistical properties of the underlying distribution while reconstructing missing and zero values more effectively than conventional methods. XGBoost and neural networks are two machine learning methods compared in the study.

Chapter 7 Finally, this Chapter is devoted to conclusion of the study and discussion on some future directions of the current research work.

2 Finally, the bibliography and list of author's publications have been given at the end of the thesis.

List of Abbreviations

ODE	Ordinary Differential equation
PDE	Partial Differential equation
SPDE	Singularly Perturbed Differential Equations
SPP	singular perturbation problems
SPBVP	Singularly Perturbed Boundary value problem
BVP	Boundary Value Problem
IVP	Initial Value Problem
FDM	Finite Difference Method
FEM	Finite Element Method
FVM	Finite Volume Method
SMK	Szász–Mirakyan–Kantorovich
OMM	Operational Matrix Methods
ANN	Artificial Neural Network
ML	Machine Learning
IBVP	Initial Boundary Value Problem
DDM	Domain Decomposition Method
NSPPDE	Non Linear Singularly Perturbed Partial Differential Equation
VIM	Variational Iteration Method
PINN	Physics informed Neural Network
BCM	Bernstein Collocation Method
VM	Variational Method
ES	Equispaced
CN	Chebyshev Nodes

RMSE	Root Mean Square Error
BNN	Bernstein Chodowsky Neural Network
CCM	Bernstein Chlodowsky Collocation Method
ACE	Accumulated Cyclone Energy
PDI	Power Dissipation Index
VF	Velocity Flux
NIO	North Indian Ocean
AS	Arabian sea
BOB	Bay of Bengal
IMD	India Meteorological Department

List of Figures

List of Tables

Chapter 1

Introduction and Literature Survey

This chapter establishes the conceptual, mathematical, and computational foundations of the thesis by situating singularly perturbed differential equations within the broader framework of multiscale physical modelling, with particular emphasis on atmospheric dynamics and tropical cyclone systems. It begins by tracing the central role of differential equations—ordinary, partial, and perturbed forms. By highlighting the limitations of classical analytical and numerical techniques in the presence of small perturbation parameters, the chapter motivates the need for specialised theoretical tools capable of capturing sharp gradients, boundary layers, and solution behaviour.

Cyclone formation and intensification are interpreted as multiscale processes involving inner–outer solution structures analogous to those encountered in classical singular perturbation theory. This mathematical analogy provides a unifying perspective for modelling cyclone boundary layers, and energy dissipation. Building upon this theoretical foundation, the chapter critically examines the numerical challenges inherent in solving singularly perturbed problems. Issues such as stiffness, loss of stability, mesh inadequacy, and ε dependent error growth are systematically analysed. While traditional mesh-based approaches—including Shishkin meshes, fitted finite difference schemes, and finite element methods—have achieved partial success, their computational complexity and sensitivity to parameter tuning motivate the exploration of alternative paradigms. In response, the chapter introduces operator-based approximation methods rooted in classical approximation theory. Bernstein, Szász–Mirakyan, and Szász–Mirakyan–Kantorovich operators are presented as mathematically stable, positive linear operators capable of uniformly approximating both smooth solutions and rapidly varying bound-

ary layers without explicit mesh refinement. Their convergence properties, moment conditions, and suitability for unbounded or semi-infinite domains are discussed in detail, establishing their relevance for atmospheric and cyclone-related models. The integration of machine learning into numerical analysis represents a further conceptual advance addressed in this chapter. By framing machine learning models as function approximators analogous to numerical operators, the chapter highlights a natural convergence between data-driven and operator-based methodologies. Recent hybrid approaches that combine operator-theoretic stability with machine learning's predictive capacity are reviewed, particularly in the context of cyclone energy indices such as Accumulated Cyclone Energy (ACE). These developments underscore the growing importance of interdisciplinary computational frameworks for complex geophysical systems.

1.1 Introduction

1.1.1 Background and Mathematical Foundation

Mathematics plays a role in nearly every aspect of our daily lives. Advances in applied mathematics have been driven by the development and extension of numerous important methods and techniques [1]. Differential equations, in particular, represent a vast and crucial area of mathematics in the modern world. Calculus has historically been a foundational field for both theoretical understanding and practical applications, and it continues to hold this significance today.

Definition 1.1.1. An equation which involves differentials or differential coefficients is called a differential equation i.e an equation involving dependent and independent variable and the derivative of dependent variable w.r.t independent variable

There are two primary categories into which differential equations fall, and each of them is further split into different forms. Ordinary differential equations and partial differential equations are the two most significant subcategories.

Definition 1.1.2. Ordinary differential equations are differential equations that include the ordinary derivatives of one or more dependent variables with respect to a single independent variable.

Example 1.1.1.

$$2\frac{d^2y}{dx^2} + xy^2\frac{dy}{dx} = 0 \tag{1.1}$$

Definition 1.1.3. A partial differential equation is a differential equation that includes partial derivatives of one or more dependent variables with respect to more than one independent variable.

Example 1.1.2.

$$\frac{\delta v}{\delta x} - 2\frac{\delta v}{\delta t} = v^2 \tag{1.2}$$

Next, the differential equations that are linear and non-linear are separated. The derivatives and dependent variable are in the first degree when a differential equation is expressed as a polynomial, and the coefficients of the different terms are either constants or functions of the independent variable. In contrast, when a nonlinear differential equation is expressed as a polynomial, the dependent variable and derivatives are in one or more degrees, and the coefficients of

the various terms are either constants or functions of the independent variable.
After dividing differential equations into several categories, let's examine their origins. This gives us an idea of the vast array of applications for differential equations and their techniques.

Differential equations are utilized in many scientific and technical fields to solve numerical equations. Here, we highlight several of these problems.

1. The dilemma of assessing the velocity of a satellite, rocket, planet, or projectile.

2. Determining the charge or current in an electric car may be difficult.

3. The examination of the rate of population expansion or the rate of breakdown of the radioactive material.

4. The challenge of recognizing curves with particular geometrical characteristics.

Such difficulties are mathematically formulated as differential equations. Applications for ordinary differential equations (ODE) with variable coefficients are numerous. These equations include, for example, the Euler, Bessel, Legendre, and Laguerre equations. Numerous nonlinear ODEs with variable coefficients, including the Duffing equation, Thomas-Fermi equation, and Van der Pol equation, have also been examined in the literature[2, 3]. In practical mathematics, physics, and engineering, both linear and nonlinear ordinary differential equations with variable coefficients are crucial.
The goal of the research was to provide precise techniques for solving a variety of linear and nonlinear equations without the need to discretize the variables or make any concrete assumptions.
In the 1940s, the phrase single disturbance was first used. In order to discover approximate solutions to difficult problems, the field and its related methodologies have changed over time.

Such issues are frequently expressed in terms of differential equations with at least one minor parameter. J.H. Poincare is likely the first to discuss mathematical problems that heavily utilize tiny parameters [1].

In the natural sciences and engineering, mathematical equations are used to simulate a wide range of events. These mathematical equations have a variety of parameters. Small adjustments to these parameters have an impact on the answers of these equations. This slight change is referred to as perturbation, and the associated parameter is called the perturbation parameter.
These mathematical problems have hard-to-find precise solutions. Consequently, determining their approximate solutions is an other method. The approximation approaches are used to reach these results. The path to perturbation theory is further paved by these perturbation techniques.

The core idea behind perturbation theory is to solve an issue by figuring out how to solve its neighboring problems. The theory looks at how solutions behave locally. This may be accomplished by adding the perturbation parameter (ϵ), a tiny dimensionless quantity, to the problem. A formal power series of the perturbation parameter may then be used to express the problem's approximate solution. Therefore, the impact of minor perturbations is measured via perturbation theory.The two kinds of perturbations are singular perturbations and regular perturbations.

This classification depends on the effect of such disturbances when the effect is small, then perturbation is termed as regular and when the effect is large, then perturbation is termed as singular perturbation.
A precise definition of the regularly and singularly perturbed problem is as follows-

Definition 1.1.4. A problem $f(u(x), \epsilon) = 0$ is said to be Regular Perturbation Problem if it depends on the perturbation parameter ϵ in such a way that its solution $u_\epsilon(x)$ converges uniformly to the solution $u_0(x)$ of the limiting case $(f(u(x), 0))$ over the domain of existence as $\varepsilon \to 0$.

Definition 1.1.5. A problem $f(u(x), \epsilon) = 0$ is said to be a Singular Perturbation Problem if it depends on the perturbation parameter ϵ in such a way that its solution $u_\epsilon(x)$ is not uniformly convergent to the solution $u_0(x)$ of the limiting case

$(f(u(x),0))$ as $\varepsilon \to 0$.

1.1.2 Singularly Perturbed Differential Equations(SPDE)

We look at two-point boundary value problems that are singularly perturbed

$$\epsilon u''(t) + p(t)u'(t) + q(t)u(t) = f(t), \quad t \in [a,b] \tag{1.3}$$

with boundary conditions

$$u(a) = \gamma \quad u(b) = \alpha \tag{1.4}$$

Where γ and α are real constants whereas ϵ is small positive parameter $(0 < \epsilon \leq 1)$. On $[a,b]$, we conclude $p(t), q(t),$, $f(t)$ are the continuously differentiable functions. Two-point boundary value issues are found in the fields of fluid mechanics, chemical reactor theory, reaction-diffusion processes, and geophysics (1.3,1.4). In these cases, the largest derivative is multiplied by a minor parameter. Whereas the answer varies gradually in some places, it changes quickly in others. In thin transition boundary or interior layers where solution can shift quickly, but the solution behave consistently and change very slowly away from the layers. There are several methods for solving singular perturbation issues.

Analytical and Numerical Challenges

The study of SPDEs involves several key difficulties:

1. Solutions are multi-scale and often non-uniformly convergent.

2. Standard numerical methods (finite difference, FEM) yield oscillations or large errors for small ε.

3. Accurate resolution requires special ε-uniform methods or operator-based approximations.

Operator families such as Bernstein, Szász–Mirakyan, and Szász–Mirakyan–Kantorovich (SMK) provide mathematically stable frameworks for approximating smooth and layer-type solutions without fine mesh refinement.

1.2 Numerical Methods

1.2.1 Numerical Analysis

There are three approaches to numerical analysis, which is the creation and study of algorithms for numerical computations:

i) It may entail creating strategies for resolving certain computational issues that stem from mathematical applications.

ii) Developing and evaluating algorithms for basic mathematical estimations that are shared by many applications or conducting theoretical study on issues that are essential to algorithm success.

iii) It performs research in a number of fields, including function approximation, data fitting and smoothing, optimisation, matrix calculations, ordinary, partial, and functional differential equations, computational aspects of dynamical systems, theory of orthogonal polynomials, and special functions.

1.2.2 Numerical Method for Singular Perturbation Problems

Singularly perturbed differential equations have multi-scale characteristics in their solutions. When the solution changes quickly over a portion of the independent variable, the region is called a boundary layer. The answer gradually shifts in the outer region. As a result, singular perturbation problems (SPPs) acquire their "two-time-scale" feature. The phrase "boundary layer" is taken from the field of physics. From the standpoint of approximating the solution, the problem is "stiff" since the slow and fast phenomena coexist. To far, a number of approaches have been put out to determine the approximate solution of singular perturbation issues, which fall into the following categories:

i) Finite Difference Methods (FDM),

ii) Finite Element Methods (FEM),

iii) Finite Volume Methods (FVM),

iv) Collocation Methods,

v) Operational Matrix Methods (OMM),
vi) Iterative methods and
vii) Asymptotic Approach.

Only the limited class of issues can be solved using asymptotic methods. When it comes to two-dimensional problems, they are not easily relevant. The asymptotic approaches are applicable to complex one-dimensional nonlinear situations for modest values of the singular perturbation parameter ε. The asymptotic technique yields semi-quantitative data regarding the solution of any individual member of the family as well as qualitative behaviour of the solution of a family of problems.

1.3 Literature Survey

1.3.1 Traditional numerical technique for linear Singularly Perturbed Differential Equation

The numerical technique, on the other hand, provides quantifiable data regarding the resolution of a particular issue. An outline of the numerical method for dealing with singular perturbations is provided in this section.
A comprehensive overview of SPPs and their theoretical and numerical application can be found in [4, 5, 6, 7, 8, 9, 10, 11] and the citations therein. Two survey papers were published as a result of the increase in research effort in the field of numerical treatment for solving singularly perturbed ODEs [12, 13]. Kadalbajoo and Reddy provided an overview of numerical techniques for one-dimensional SPPs in [12], beginning with Pearson's work [14, 15] from 1968 to 1984. A follow-up survey study on the numerical treatment of singularly perturbed ODEs was published by Kadalbajoo and Patidar [13]. It covers the work completed after 1984, ranging from Ascher's work [16] to Kopteva's work [17] in 1999. The work completed after 1999 is the main emphasis of this section.
Lengerink examines singularly perturbed BVPs of the one-dimensional convection-diffusion type in [18]. To solve these kinds of BVPs, the author has suggested, examined, and applied a centred difference or finite element discretisation. Discreti-

sation is done using a piecewise equally spaced mesh. In terms of the number of nodes in relation to the perturbation parameter, the author has demonstrated that the suggested method is second order convergent.

A ε-uniform error estimate for first-order upwind is calculated by Beckett and Mackenzie [19] using a model for inhomogeneous second-order SPB-VPs on a non-uniform grid. The equidistribution of a positive monitor function, which is a linear combination of a positive constant and a suitable power of the solution's second derivative, is used to discretise the mesh. The authors demonstrated how to select the constant in order to guarantee ε-uniform convergence.

Implementing a numerical approach for a singularly perturbed differential equation of reaction-diffusion type with a discontinuous source term is the goal of this research study [20]. The authors' numerical technique comprises of a non-standard Shishkin mesh (piece-wise uniform mesh) and a standard finite difference operator. The Shishkin mesh is designed to capture the interior and boundary layers that emerge within the problem's solution. With regard to singular perturbation parameters, the authors have demonstrated that the suggested approach is uniformly convergent. To illustrate how these issues arise in the context of models of basic semiconductor devices, a quick review is provided.

In order to solve convection-type singularly perturbed BVPs, the authors of this study [20] have suggested a defect correction technique based on the FDM on the piece-wise uniform mesh known as the Shishkin mesh. After doing a convergence analysis, the authors were able to determine uniform bounds for error in the perturbation parameter ε.

Research publications on the numerical approximation for SPDE solutions were published by Kopteva and Stynes in 2001. Kopteva and Stynes examine the singularly perturbed BVPs of the convection-diffusion type in conservative form in [21]. To address such BVPs, they offer an upwind conservative FDM. By dividing the differences of the calculated solution on every arbitrary mesh with the weight of the tiny diffusion coefficient, they set limitations for the mistakes in approximating the derivative of the exact solution. After that, these limits are clarified for the particular Shishkin and Bakhvalov mesh situations.

A two-point BVP of singularly perturbed kind is shown by Kadalbajoo and Patidar

[22], who also address the situations in which solutions to such BVPs reveal a peculiar "turning point" phenomenon. To solve such BVPs, the authors provide a numerical method based on the cubic spline methodology with non-uniform mesh. The convergence and stability of the suggested numerical system are examined. Numerical experiments are conducted to support the expected theory, and certain test problems are considered.

In order to solve singularly perturbed BVPs, Liu and Tang [23] proposed a Galerkin-spectral technique in 2001. This method uses a class of trial functions that are appropriate for coordinate stretching. The error analysis for the suggested spectrum approach has been completed by the authors. Using conventional spectral methods to solve SPPs, spectral precision is only achievable when $N = O(\varepsilon^{-f})$, where f is a positive constant and ε is the singular perturbation parameter. For advection-diffusion equations, they got comparable outcomes. The suggested method has two key characteristics: i) the singular perturbation parameter ε is not included in the coordinate transformation; ii) machine precision may be reached with N of the order of several hundred, even when ε is quite small.

MacMullen et al. propose a self-adjoint singularly perturbed ordinary differential equation in [24] and provide a parameter uniform numerical approach to approximate BVPs of this kind. An effectively designed discrete Schwarz approach based on maximum norm is shown to converge uniformly to the exact solution with respect to the singular perturbation parameter. The Second-order maximum norm convergence is present in the proposed system.

Aziz and Khan [25] examined singularly-perturbed BVPs and suggested a numerical strategy based on the quintic spline approach for these kinds of issue. A pentadiagonal linear system is the result of the strategy. In their paper, the authors assert that the suggested method has a fourth-order convergence.

Farrell et al. devised and examined numerical techniques based on upwind FDM for the solution of SSP in this study [26]. The convergence analysis in the maximal norm has been examined by the writers. For the numerical solutions derived from a suggested method applied to Prandtl's issue emerging from laminar flow via a thin flat plate, the authors use the method for estimating Reynolds-uniform error bounds in the maximum norm.

Together with Patidar, Kadalbajoo once more published a survey study [13] on numerical methods for solving singularly perturbed ODEs in 2002. The authors of this article provide an overview of the work completed after 1984, spanning from

Ascher's work [16] to 1999. In order to solve the BVPs for singularly perturbed linear and nonlinear ODEs, Kadalbajoo and Patidar (2002) proposed a number of numerical difference algorithms based on the cubic spline.

To get the numerical solution of SPBVPs, they take into account spline in . i) The reaction-diffusion type, ii) the convection-diffusion type without a reaction term, and iii) a more standard convection-diffusion type with a reaction term are the three problem types that the authors of this study examine. Using the continuity of the first derivative of the spline function, the authors solve these BVPs. Using tried-and-true procedures, the resulting spline creates a tridiagonal system that can be solved. For the numerical solution of these kinds of BVPs, the authors have obtained the error estimates. The nonlinear SPBVPs are the subject of this essay [27]. The authors of this paper suggest a numerical method for nonlinear SPBVPs that is based on cubic splines with non-uniform mesh. The quasilinearization technique first linearises the suggested nonlinear problem. The authors use a variable-mesh cubic spline to drive the difference schemes for linearised SPBVPs. The authors of [28] describe a spline-in-tension approach for the self-adjoint two-point SPBVPs. It is demonstrated that the suggested strategy has nearly second-order convergence. Kadalbajoo et al. examined a unique perturbation problem in [29] and created a B-spline collocation technique for these kinds of issues by employing artificial viscosity.

Under particular equilibration conditions, B. Zhang et al. examined reaction-diffusion type SPBVPs and obtained posterior error bounds for nonconforming finite element approximations to such problems.

Anisotropic meshes with reaction-diffusion type SPBVPs were described by J. Zhao and S. Chen [30]. Using the nonconforming finite element method over the anisotropic mesh, the authors have produced reliable a posteriori error estimates. The author of [31] suggests a numerical method for solving convection-diffusion type SPBVPs with a regular boundary layer. The method is an iterative approach based on the Schwarz alternating procedure over a nonuniform grid (Shishkin mesh). It is shown that the overlapping Schwarz technique does not yield ε uniform convergent numerical approximations with uniform meshes and arbitrarily fixed interface points. A numerical method utilising uniform meshes on overlapping meshes and Shishkin interface points must yield approximations that converge to accurate solutions. The authors conclude by looking at a non-overlapping approach for a two-dimensional elliptic issue with regular boundary layers that

makes use of uniform meshes, Shishkin interface positions, and artificial Dirichlet interface conditions.

C. Clavero et al. design an FDM to tackle such problems in [32] and provide a uniformly convergent alternating direction HODIE FDM for a 2D parabolic convection-diffusion partial differential equation. The authors use FDM in the space direction and an identity expansion to apply the Peaceman and Rachford approach in the time direction and (HODIE) high-order differences. Using piece-wise uniform mesh in space direction, the author discretises the mesh grid.
A 2D parabolic partial differential equation of the reaction-diffusion singly perturbed type is presented by C. Clavero et al. in [33]. The suggested approach entails applying the Peaceman and Rachford methodology in the time direction, the (HODIE) scheme, and the finite difference method in the space direction. The approach is third-order convergent in space and second-order convergent in time, as demonstrated by the authors.
A two-coupled system of singularly perturbed reaction-diffusion ODEs of Dirichlet type is the subject of Matthews et al. [34]. The authors have developed a numerical method that, regardless of the singular perturbation value, yields approximate solutions that converge point-wise at all domain locations.
Natesan and Ramanujam address singularly perturbed second-order ODEs of the Robin type in this work [35]. An asymptotic approximation solution and the answer derived from a numerical approach that includes an exponential FDM are appropriately integrated to approximate the multi-scale nature of such problems. The "transition point," which will be used as a border value for the boundary layer area problem, is selected inside the interval of integration when the reduced problem's solution is assessed. In order to carry out iterations, the authors gradually shift the transition point to the right until the solution stabilises. The reduced problem's solution is regarded as an approximation of the original problem in the outer region. Estimates of error are determined for the approximate solution.
A FEM for numerically approximating singularly perturbed systems of reaction-diffusion problems was presented by C. Xenophontos and L. Oberbroeckling . After doing an error analysis, the authors assert that the suggested approach converges at an exponential rate.
Two-point SPBVPs with milder boundary layers are suggested in [36], and a nu-

merical approach utilising the shooting technique is built. The outer area and the boundary layer, also known as the inner region, are the two subintervals of the domain that the authors split into consideration of the differential equation. An exponentially fitted FDM solves an IVP derived from the provided BVP in the boundary layer area. On the other hand, in the outer region, the authors have employed a traditional upwind approach. The convergence and error analysis are performed by the writers. It is described how the approach is implemented on parallel architectures.

The authors address the application of numerical integration techniques for solving SPBVPs in this article [37]. An approximation first-order differential equation with a term recurrence relationship is used by the authors in place of the original second ODE. The suggested approach builds upon the deviating argument in an iterative manner.

A family of convection-diffusion problems in one spatial dimension is presented by F. Celiker and B. Cockburn [38]. To investigate the superconvergence of various numerical systems, the author employs discontinuous Galerkin, discontinuous Petrov-Galerkin, and hybridised approaches. The superconvergence of order (2q + 1), where q is a polynomial's degree, has been demonstrated by the authors. The results of the suggested numerical test corroborate the theoretical conclusions.

Valarmathi and Ramanujam consider an asymptotic numerical fitted mesh method for singularly perturbed third-order ODEs of the reaction-diffusion type [39, 40] and fourth- order ODEs of the convection-diffusion type [41]. The authors transform the third-order singularly perturbed BVPs into an equivalent problem of a weakly coupled system of one first-order and one second-order ODE with the parameter ε multiplying the highest order derivative and a fourth-order SPBVPs into the equivalent problem of a weakly coupled system of two-second order ODEs, one with a small parameter and other without the parameter. A computational method based on asymptotic expansion is proposed to solve these systems. In [39], up to the transformation of the third order into the system of ODEs is the same as the authors did in [40]. The boundary layer area and the outer region are the two sub-intervals into which the authors of this study split the domain of the differential equation definition. The differential equation is now resolved independently in each of these locations. The solution for the entire interval is given by combining the solutions so acquired in these intervals. The authors primarily

employ the zeroth-order asymptotic expansion of the BVP solution or an appropriate asymptotic expansion solution to derive boundary conditions at the transition sites. Newton's approach of quasi-linearization is used to address the differential equation's semi-linearity.

The numerical analysis of the third-order singly perturbed ODE by Valarmathi and Ramanujam is still ongoing. The authors of [42] examine third-order convection-diffusion-type ODEs that are only disturbed. This article suggests a numerical approach to address these issues. By applying appropriate beginning and boundary conditions, this technique converts the provided BVPs into a weakly coupled system of two ODEs. The weakly linked system is reduced to a decoupled system by the authors. The domain of the differential equation specification is then split into two non-overlapping subintervals known as the inner and outer regions in order to numerically solve this decoupled system using a boundary value approach. These areas are then used as two-point BVPs to solve the decoupled system. The outside region uses a traditional FDM. whereas the inner region uses an exponentially fitted FDM. The zero-order asymptotic expansion approximation of the problem solution is used to determine the boundary conditions at the transition point.

Singularly perturbed third-order BVPs on a layer adaptive mesh are the subject of H. Zarin et al. [43]. An interior penalty finite element method on piece-wise uniform mesh (Shishkin mesh) was designed by the author. The suggested approach is found to be robust, and the error estimates are obtained in the energy norm.

The hp-version of the FEM is used to numerically solve problems of this kind. M. Melenk and C. Xenophontos [44] examine a singularly perturbed reaction-diffusion equation that is presented on a two-dimensional domain with an analytical boundary. The method is uniformly convergent with respect to the singular perturbation parameter, according to the authors' convergence analysis conducted in the balanced norm.

Heinrichs [45] introduced least squares spectral collocation for issues involving unique and discontinuous perturbations in 2003. The author divided the domain into subdomains for the first derivative operator, applying jumps at discontinuities to each subdomain and applying an equal order polynomial to each subdomain. For discretisation, he used spectral collocation using Chebyshev polynomials. Least squares can effectively solve the overdetermined system caused by the

collocation and interface conditions. Only symmetric positive definite linear systems are used in the solution approach. By using least-squares for stabilisation, the author expands this method to single perturbation situations. The boundary layer is resolved by a proper decomposition of the domain well.

A second-order global uniformly convergent numerical technique for the coupled system of singularly perturbed IVPs is designed by S.C.S. Rao and S. Kumar [46]. A robust numerical method with high-order parameters was proposed by M. Kumar and S.C.S. Rao [47] for the 1D singly perturbed time-dependent reaction-diffusion Dirichlet problem. The fourth-order high-order compact scheme is directly on a Shishin method in the space, and the Crank-Nicolson approach is on a uniform grid in the time direction.

In order to solve singularly perturbed two-point BVPs, the authors in [48] created a difference technique based on spline in compression on a non-uniform mesh. The proposed scheme is second-order accurate. A few numerical examples have been provided by the authors to reinforce the theoretical findings.

For SPPs with weak boundary layers, Natesan et al. [49] created and examined a numerical method. The authors of this paper separated the domain $[0, 1]$ into two distinct sub-domains, $[0, k\varepsilon]$ and $[k\varepsilon, 1]$, which do not overlap. To address the suggested problem, exponential FDM is used in the layer area $[0, k\varepsilon]$, subject to the transition boundary condition at $x = k\varepsilon$. The SPPs differential equation is approximated in the regular area $[k\varepsilon, 1]$ using a traditional FDM. The value of the asymptotic approximation is utilised to establish the boundary condition at the interior point $x = k\varepsilon$, also known as the transition point. The suggested method is shown to be convergent with respect to the perturbation parameter ε after the authors performed the error estimation.

Singularly perturbed third-order BVPs on a layer adaptive mesh are the subject of H. Zarin et al. [43]. Shishkin mesh is the name given to the author's interior penalty finite element method on layer adaptive mesh. The suggested approach is found to be robust, and the error estimates are obtained in the energy norm.

The hp-version of the FEM is used to numerically solve problems of this kind. J.M. Melenk and C. Xenophontos [44] examine a singularly perturbed reaction-diffusion equation that is presented on a two-dimensional domain with an analytical boundary. The approach is uniformly convergent with respect to the singular perturbation parameter, according to the authors' convergence study conducted in the balanced norm.

Heinrichs [45] introduced least squares spectral collocation for issues involving unique and discontinuous perturbations in 2003. The author divided the domain into subdomains for the first derivative operator, applying jumps at discontinuities to each subdomain and applying an equal order polynomial to each subdomain. Spectral collocation is what he utilises.

Chebyshev polynomials are used for discretisation. Least squares can effectively solve the overdetermined system caused by the collocation and interface conditions. Only symmetric positive definite linear systems are used in the solution approach. By using least-squares for stabilisation, the author expands this method to single perturbation situations. The boundary layer is resolved by a proper decomposition of the domain well.

A second-order global uniformly convergent numerical approach for the coupled system of perturbed IVPs is designed by S.C.S. Rao and S. Kumar [46]. A robust numerical method with high-order parameters was proposed by M. Kumar and S.C.S. Rao [47] for the 1D singularly perturbed time-dependent reaction-diffusion Dirichlet problem. The suggested approach combines the fourth-order high-order compact scheme directly on a Shishin method in space with the Crank-Nicolson technique on a uniform grid in the time direction.

In order to solve perturbed two-point BVPs, the authors in [48] created a difference technique based on spline in compression on a non-uniform mesh. The accuracy of the suggested strategy is second-order. To bolster the theoretical findings, the authors have included a few numerical examples.

A computational method to approximate non-turning-point SPBVPs for second-order ODEs subject to Dirichlet-type boundary conditions was created and examined by the authors in [50]. The authors of this paper suggested an asymptotic expansion of zeroth order for the numerical solution of SPBVPs. After that, an equivalent IVP for a first-order ODE is obtained by integrating the issue. After applying the zeroth order asymptotic expansion to approximate some of the terms in the differential equations, the IVP classical approach or a fitted operator method is used. By calculating the error estimate for the numerical solution, it is demonstrated that the suggested method is convergent of order h, where h is the mesh size.

Singularly perturbed second-order differential equations and their application to multi-point BVPs are the topics of Z. Du and L. Kong [51]. The suggested problem

is resolved by the authors using a hybrid approach that combines the Liouville-Green transform with asymptotic solutions.

A Richarchardson extrapolation method and FDM are developed by Natividad and Stynes [52] for numerically approximating singularly perturbed convection-diffusion problems over piecewise uniform Shishkin meshes. The authors of this study demonstrate how to create a Richardson extrapolant of the calculated solution and demonstrate that, when $N+1$ points are employed in the mesh, the extrapolation approach minimises the nodal errors from $O(N^{-1}lnN)$ to $O(N^{-2}ln2N)$. Vivek et al. [53] suggested a new adaptive mesh approach using second-order central difference techniques as a numerical method for solving convection dominated, convection-diffusion SSPs. The adaptation parameter for convection-diffusion issues in the suggested approach is a novel, entropy-like quantity. Prior knowledge of the location and breadth of the layers (interior and boundary) is not necessary for the suggested approach. Vivek Kumar created and examined a high-order compact finite-difference (HOCFD) method in [54] for resolving perturbed elliptic and parabolic reaction-diffusion problems in 1D and 2D. According to the author, parameter uniform convergence has occurred. A singularly disturbed star graph with $k+1$ nodes and k edges is examined by Vivek et al. in [55]. This results in a system of k distinct partial differential equations along the edges with coupling conditions at the common junction. The study of singularities and boundary layers produced by a convection-diffusion issue in a circle of incompatible data was started by C.Y. Jung and R. Temam [56]. There are two features of the circle's edge that are connected to incompatible data. The authors have meticulously examined a complicated single phenomena for extremely incompatible evidence.

A parabolic singularly perturbed partial differential equation of the convection type with a discontinuous (first-type discontinuity) source term and a degenerating convective term is examined by C. Clavero et al. [57]. To solve the suggested problem, the authors have created a piece-wise uniform mesh monotone finite difference approach. The 1d parabolic convection response partial differential equation of singly perturbed type is the subject of C. Clavero et al. [58]. Multiplying the convection term by the parameter μ makes the suggested issue more complicated, and the source term has a discontinuity. As a result, border and inner layers appear. To address these kinds of issues, the authors have developed an implicit Euler technique over the uniform grid in time direction and a finite differ-

ence approach over a Shishkin mesh in space direction. The suggested method is convergent with first order in time and second order in space, according to the authors.

A hybrid difference scheme for a singularly perturbed reaction-diffusion problem with a discontinuous (first-type discontinuity) source term was created and put into practice by the authors in [59]. The case of semiconductor modelling is also covered by the author. Second order convergence in the maximal norm has been demonstrated by the authors.

The singularly perturbed reaction-diffusion problems with $d \geq 2$ are examined by R. Lin and M. Stynes [60]. First, the authors demonstrated that the energy standard is insufficient to account for the layer part mistake. The authors demonstrated uniform convergence for $d \geq 2$ and provided a balanced norm.

Error limitations for the streamline diffusion finite element technique (SDFEM) for 2D convection-dominated BVPs with boundary layers were determined by J. Zhang et al. in [61]. The authors show that, regardless of the perturbation value ε, the approach converges with a point-wise accuracy of almost order $7/4$ away from the characteristic layers. These theoretical results are confirmed by numerical experiments. [62] For convection-diffusion BVPs with characteristic layers, J. Zhang and X. Liu presented SDFEM on hybrid meshes and Shishkin meshes. For 2D convection-diffusion BVPs over Shishkin mesh, Z. Zhang suggested a finite element and calculated the super-convergence in [63].

A.F. Hegarty and E. O'Riordan developed a consistent numerical approach in this paper [64] to address linear SPBVPs convection dominating across a circular region. The technique uses a monotone FDM over a Shishkin-type layer-adapted mesh.

A singularly perturbed parabolic periodic BVPs of the reaction advection-diffusion type are considered by N.N. Nefedov et al. [65]. By using the upper and lower solution method, the author has applied a modified asymptotic approach. For the suggested problem, the authors have determined the existence and asymptotic stability of periodic solutions.

A system of two connected singularly perturbed linear reaction-diffusion two-point BVPs is shown by Madden et al. [66], who also develop a numerical approach to address these issues. The leading term in each equation is multiplied by a small positive parameter, although the size of these parameters might vary. The system solutions have boundary layers that interact and overlap. The authors

created a piecewise-uniform Shishkin mesh by looking at the structure of these layers. Additionally, they demonstrate that central differencing on this mesh is uniformly accurate in both small parameters and nearly first-order. The anticipated theory is supported by numerical findings for a test problem.

A convection-diffusion issue on a unit square with Dirichlet boundary conditions is presented by H.-G. Roos and H. Zarin [67]. The conventional Galerkin FEM and an h-version of the nonsymmetric discontinuous Galerkin FEM with interior penalties are used to discretise the issue on a layer-adapted mesh with linear/bilinear components. Using carefully chosen penalty factors for edges from the mesh's coarse area, the authors show uniform convergence (in the perturbation parameter) in a related norm.

For convection-dominated diffusion BVPs, H. Zarin investigates and applies a numerical technique based on discontinuous FEM in [68]. The method combines standard Galerkin FEM with bilinear components with a high-performance variant of nonsymmetric discontinuous Galerkin FEM. Super closeness findings have been produced by the authors. It is discovered that the approach is reliable and effective.

The authors of [69] created a numerical method that combines regular Galerkin FEM with discontinuous Galerkin FEM. In the layer region, the author has applied the discontinuous Galerkin technique, and in the regular region, the Galerkin fem. Advection-diffusion reaction problems are used to determine the suggested method's stability and convergence.

A trustworthy technique for numerically approximating a nonlinear singularly perturbed IVPs was created by Z. Cen et al. [70]. The authors have also created a second order approach based on their analysis of the precise solution's behaviour.

The development of parameter-uniform numerical techniques for solving singly perturbed ordinary differential equations (BVPs) with two tiny parameters is discussed in [71]. The authors have obtained theoretical constraints on the derivatives of the solutions that are explicit in terms of parameters. An upwind finite difference operator and a suitable piecewise uniform mesh are used in a numerical approach. Convergence of the suggested approach is demonstrated, and parameter-uniform error limits for the problem's numerical solution are obtained. The theoretical conclusions are supported by the numerical data that were obtained.

M. Brdar and H. Zarin examined a two-parameter singularly perturbed differential equation in [72] and developed a numerical technique to solve it. On a Bakhvalov-type mesh, the authors show uniform convergence of a piecewise linear Galerkin FEM.

The error estimate for finite linear elements on Bakhvalov type meshes was developed by H.-G. Roos [73]. Convection-diffusion problems with exponential layers have the best error estimates for finite linear elements on Shishkin-type meshes. The first energy norm optimum convergence result for a Bakhvalov-type mesh is presented by the author.

In order to numerically estimate singularly perturbed two parameter problems with non-smooth data, M. Chandru, T. Prabha, and V. Shanthi [74] devised a numerical approach. The theoretical constraints on the derivatives have been derived by the authors. The authors have created a hybrid difference scheme using a Shishkin mesh.

To solve a singularly perturbed parabolic partial differential equation, J.L. Gracia and E. O'Riordan [75] suggested an effective numerical method that consists of a finite difference operator on a piecewise-uniform Shishkin mesh.

A trustworthy numerical technique was created and examined by S. Kumar and B.V.R. Kumar [76]. for a parabolic singularly perturbed differential equation's numerical approximation. An algorithm created by the authors combines the Domain Decomposition Method with (DDM) based on the three-step Taylor Galerkin Finite Element and Schwarz alternating (3TGFE) technique. An examination of convergence has been performed.

Martin Stynes and Niall Madden create and evaluate numerical methods in [77]. to roughly represent the individually perturbed reaction-diffusion type's multi-scale nature BVPs. The weighted and balanced finite element method is the foundation of the suggested method. approach on a uniform piecewise grid. A parameter uniformity has been demonstrated by the authors. convergence and discovered that the suggested method converges almost first-order.

In order to address singularly perturbed convection-diffusion issues, S. Franz [78] constructed discontinuous Galerkin FEM. The author has solved the problem of stability with standard Galerkin FEM in this method.

To capture the boundary layer phenomena of the singly perturbed reaction-diffusion BVPs, the authors of [79] created a modified graded mesh. The convergence is examined in the energy norm using a modified graded mesh and a finite element

technique that the authors have constructed.

A Bernstein operator approach for approximating Volterra integral differential equations of singularly perturbed type was implemented by the authors in [80]. Analysis of convergence and error has been done by the author. Numerical findings demonstrate the suggested method's resilience and efficiency.

1.3.2 Traditional Numerical Techniques for Nonlinear singularly Perturbed Differential Equation

When transforming a real-world occurrence into a mathematical model, nonlinear singularly perturbed partial differential equations (NSPPDEs) are crucial. Compared to traditional nonlinear partial differential equations, the dynamics of NSPPDEs are completely different. These kinds of issues rely on a little positive parameter, which causes the solution to change slowly in the rest of the domain and quickly in small areas. This type of issue is known as SSPs, and the behaviour of the solution in small areas is referred to as layer phenomena. It is difficult to build computer techniques for these kinds of issues because a tiny positive parameter ε and a nonlinear component simultaneously contaminate the proposed problem's solution. We use numerical methods by linearising the nonlinear issues since only a small number of nonlinear systems can be solved openly. The quality of the estimated solution somehow degenerates as a result of the linearisation of the nonlinear issue, leading to misleading results, and we are forced to sacrifice the precision of the solution. An effort has been made to address the challenges posed by nonlinear issues in this thesis. Two numerical methods for solving the NSPPDEs without linearisation or discretisation have been described by the authors in this thesis. Thus far, there is a dearth of published research on nonlinear singularly perturbed differential equations (NSPDEs) and NSPPDEs.

A research work on BVPs for a nonlinear differential equation of convection type with a small parameter was published in 1952 by N. Levinson and E.A. Coddington [81]. The problem was examined by the writers in light of existence and uniqueness. In 1973, a nonlinear two-point BVP of singly perturbed type was examined by D.S. Cohen [82]. The existence and uniqueness of the suggested problem have been verified by the author.

A numerical method for numerically approximating a class of nonlinear singular perturbation two-point BVPs was proposed by M.K. Kadalbajoo and Y.N. Reddy

[83] in 1988. An iterative boundary value approach was created by the author. The analysis is done theoretically.

A semilinear singularly perturbed two-point BVP is addressed by Farrell et al. in [84], who also create an FDM on an equidistant mesh with nodal distance h. The authors of this article have demonstrated that because h goes to zero in the maximum norm, the suggested numerical method with a constant fitting factor cannot converge ε-uniformly to the solution of the given issue. A series of numerical experiments has been examined, and the numerical results with varied fitting factors support the theoretical conclusions. Miller, Shishkin, O'Riordan, and Farrell examine quasilinear singly perturbed BVPs displaying boundary layer phenomena in [85]. The authors of this paper create a special piecewise-uniform mesh called the Shishin mesh and an upwind difference operators approach that are suited to these boundary layers. Regarding the singular perturbation parameter, it is demonstrated that the convergence analysis is parameter uniform in a discrete maximum norm.

O'Malley, Jr. [86] wrote a study on the asymptotic solution for singularly perturbed BVPs in 2000. The BVPs for certain differential equations of the type "$\varepsilon x''(t) = f(x(t))g(x'(t))$ on $0 \leq t \leq 1$" whose solution displays an inner shock layer were examined in this study. For these BVPs, he developed an asymptotic solution.

Kadalbajoo and Patidar [87] address nonlinear BVP that is singularly disturbed. A numerical method based on cubic spline over Shishkin mesh is designed by the authors. Prior to using the suggested numerical procedure, the original nonlinear BVP is linearised using the quasilinearization technique. According to the authors' convergence calculations, the approach has a second order convergence rate and is parameter uniform.

A numerical technique for estimating the semi-linear singular perturbation BVPs was developed by VUlanovi´ c and Relja [88]. Sixth-order FDM has been created by the author. After deriving the theoretical estimates, it is discovered that the approach is parameter uniform.

The authors of this publication [89] expand on Stynes and O'Riordan's research on locally exponentially fitted FEM for singly perturbed two-point BVPs. The authors of this article examine a local exponentially fitted FEM where the normal continuous piecewise linear function is used in place of a singularly perturbed two-point BVPs, and exponential splines are only implemented in the layer por-

tion. They also derive an ε-uniform $h|lnh|^{1/2}$ order error estimate in the energy norm for this scheme, assuming that the mesh is quasi-uniform. The two higher-order numerical methods for approximating the solution of singularly perturbed two-point BVP are also taken into consideration by the authors.

A study on the numerical method for a quasilinear singularly perturbed elliptic reaction-diffusion equation in a vertical strip was published in this paper [90] by G.I. Shishkin and L.P. Shishkina. To improve the accuracy and pace of convergence, the authors have applied the Richardson extrapolation approach.

To get a close-form analytic solution of singularly perturbed IVPs and a system of these, Zhao et al. use a variant of the iteration approach in [91]. Convergence analysis was performed, and the method demonstrated convergence with respect to the singular perturbation parameter ε. The theoretical conclusion is supported by numerical data from a numerical experiment.

The author of [92] created and used the homotopy perturbation methodology, an iterative analytical method for numerically solving a nonlinear two-point singularly perturbed BVP. The approach appears to work better for quicker convergence when the absolute residual error concept is used to calculate the ideal convergence control settings. In this paper, the author examines three nonlinear test problems that were resolved using the suggested approach.

An iterative analytical approach for nonlinear singularly perturbed convection-diffusion problems was put out by the author of the article [93]. The technique is based on a Lagrange multiplier, which is assessed using variational theory and the Liouville-Green transformation.

The presence and uniqueness of the suggested problem have also been demonstrated by the author. Two linear and two nonlinear test problems have been examined in order to assess the effectiveness of the suggested approach, and the results show that it is reliable.

The authors of the paper [94] examine a quasilinear two-point BVP of the convection-diffusion type and offer a reliable adaptive technique based on an upwind FDM for approximating BVPs of this kind. The nodes of the employed mesh are adaptively shifted using a simple innovative technique based on the equidistribution of the arc length of the currently determined piecewise linear solution. The mesh is initially uniform and contains a set number of nodes $(N+1)$. The approach is first-order with respect to the singular perturbation parameter ε, and the authors show that there is a mesh that evenly distributes the arc length along the polygo-

nal solution curve. In 2007, N. Kopteva [95] deals with a nonlinear two-point BVP singularly perturbed type over a non-uniform mesh. Through the use of a monitor function and an equidistribution grid, the author achieved a second level of convergence in discrete maximum norm. The author presents numerical findings that corroborate the theoretical conclusion. A 2D seminear SSP of reaction-diffusion type obtained estimates in the maximum norm was introduced by N. Kopteva in 2007 [96]. N. Kopteva et al. examined a 3D semilinear SSP in 2011 and obtained estimates in maximum norm [97]. N. Kopteva et al. examined a semilinear two-point BVP of reaction-diffusion type with many solutions in 2009 [98]. They used an overlapping Schwarz approach to analyse the suggested issue. N. Kopteva discusses singly perturbed BVP of response diffusion in [99] and uses adaptive anisotropic meshes to produce posteriori error estimates in maximum-norm.

The authors of this study built a nonstandard upwind first-order FDM on piecewise uniform meshes and took into account a quasilinear singularly perturbed two-point BVP. In a discrete L-norm, the suggested approach is regarded as parameter uniform.

The authors of [100] took into account nonlinear singularly perturbed IVPs. To address these kinds of issues, the author has developed a closed-form iterative analytical technique. A variant of the iteration strategy based on Lagrange's multiplier makes up the suggested methodology. Theoretical findings are suggested by the authors' consideration of a few issues and numerical data.

A closed-form iterative analytical approach for one-dimensional nonlinear singly perturbed BVP of reaction-diffusion type was developed by the authors in [101]. The variation of iteration method (VIM) is based on a Lagrange multiplier assessed by Liouville-Green transformation and variable theory. After doing a comparative study, the authors conclude that the approach is resilient with respect to the singular perturbation parameter ε.

In order to solve nonlinear singularly perturbed two-point BVPs with Robin boundary conditions, SC Rao and M Kumar [102] created a collocation technique based on the B-spline. Prior to implementing the suggested approach and piecewise uniform mesh over the linearised issue, the authors first linearised the original problem using the quasilinearization methodology. The suggested technique's convergence and stability are determined.

The authors of [103] provide a neural-evolutionary artificial neural network (ANN) approach for approximating singularly perturbed BVPs of both linear and nonlin-

ear forms. The suggested approach combines genetic algorithms, feed-forward artificial neural networks, and sequential quadratic programming (SQP) approaches. The suggested design scheme's performance is evaluated by the authors using six linear and nonlinear BVPs of SSP, and the approach is determined to be reliable and efficient.

M. Kumar et al. presented linear and nonlinear SPPs on a domain [p, q] in [104] and suggested an initial value method to address these kinds of issues. The initial value approach has been used directly to linear issues by the authors, while the quasi-linearization methodology has been used to linearise nonlinear problems. The suggested techniques are then used to tackle the reduced challenges.

A comparison study is conducted for singularly perturbed nonlinear BVPs using an adaptive mesh that was built by the author in the [105] publication. For the suggested problem, the author has performed an a posteriori error analysis. Using the numerical methods that are currently available in the literature, a comparative study is conducted.

A hybrid FDM over a Bakhvalov-Shishkin mesh to a quasilinear singly perturbed BVPs was proposed by Q. Zheng et al. [106]. The approach is shown to be uniformly convergent with respect to the singular perturbation parameter once the convergence study is completed.

A collocation approach based on an orthogonal spline on piece-wise uniform mesh (Shishkin Mesh) was presented by Pankaj Mishra et al. [107] in 2019 after they examined nonlinear singularly perturbed reaction-diffusion problems. The authors employed splines of degree ≥ 3 to perform the convergence study. The findings of the numerical tests validate the theoretical conclusions of the study, and the authors have also demonstrated error estimates in additional standards for which research is still pending.

The Newton-Galerkin method is an adaptive numerical technique for numerically approximating semilinear parabolic SPP that was proposed by Mario Amrein and Thomas P. Wihler in [108]. The backward Euler method in the temporal direction, FEM for adaptive discretisation in spatial variables, and Newton's approach for linearisation make up the suggested methodology. The authors derive an a posteriori error analysis.

A parameter uniform numerical approach for numerically approximating a semilinear system of one-dimensional parabolic singularly perturbed reaction-diffusion IVP was devised and examined by Clavero et al. in [109]. The implicit Euler tech-

nique is used in time, while central FDM is used to discretise in space. It is demonstrated that the suggested approach is first-order in time and second-order in space.

In [110], the authors examined a system of nonlinear first-order SSPs and suggested a numerical technique using an adaptive grid that was based on the backward-Euler approach. The findings of the convergence study show that the suggested approach is first-order convergent.

A numerical technique for such problems was devised by the authors [111] after taking into consideration a system of coupled semilinear singly perturbed reaction-diffusion BVPs inner layers. The boundary layer phenomena has been captured by the authors using the Shishkin mesh. It is shown that the suggested approach has a nearly second order convergence rate and is resilient and convergent.

For generic nonlinear singularly perturbed reaction-diffusion problems with a stable reduced solution, J. Quinn [112] suggested parameter-uniform numerical techniques. Parameter uniform numerical techniques for linear and nonlinear singularly perturbed convection-diffusion boundary turning point problems were proposed by E. O'Riordan and J. Quinn [113].

In [114], Igor Boglaev created and applied a discrete monotone iterative method to approximate the reaction-diffusion type nonlinear parabolic singularly perturbed. To create a non-linear difference scheme, the author first applies upper and lower solution strategies. The author then used a monotone domain decomposition technique based on the Schwartz method to solve the nonlinear difference scheme. Every iteration of the approach solves the linear system. Igor Boglaev discusses semilinear SPPs of the elliptic and parabolic forms in this work [115]. For these kinds of issues, the author has used monotone iterative approaches, and the suggested approach has been shown to be uniformly convergent. For the purpose of solving nonlinear parabolic SPPs numerically, Igor Boglaev developed a monotone alternating direction approach (ADI) in article [116]. Using the upper and lower solution approach of this strategy, the author has produced a monotone sequence. This sequence aids in the development of a nonlinear difference scheme that approximates the nonlinear parabolic issue. It is discovered that monotone sequences have a quadratic rate of convergence.

Chein-Shan Liu et al. create and examine a numerical technique for numerically solving nonlinear singly perturbed BVPs in [117] that is based on a modi-

fied asymptotic approach. A few numerical tests conducted by the authors have shown that the approach is reliable.

A nonlinear singularly perturbed BVP with integral and multi-point integral boundary conditions is presented by the authors in article [118]. In order to create a multi-resolution Nonlinear singularly perturbed BVPs with integral and multi-point integral boundary conditions may be approximated using the Haar wavelet collocation approach. The quasilinearization approach is used to linearise a nonlinear problem. Numerical findings demonstrate the suggested method's resilience and efficacy. The projected theory is supported by numerical experiments and consideration of a few test issues.

1.4 Operator-Based Approximation Methods

In the early 21st century, attention turned toward operator-theoretic frameworks, inspired by approximation theory. The idea was to replace mesh-based discretisation with continuous operator approximations that maintain stability and smoothness. The study of singularly perturbed differential equations (SPDEs) has undergone extensive development, especially in the search for numerically stable, parameter-uniform, and computationally efficient methods. While traditional numerical methods—finite difference, finite element, spline, and collocation techniques have achieved significant success, they often face challenges in capturing the sharp gradients that appear within boundary or interior layers. To overcome these limitations, researchers have turned to operator-based approximation methods, which leverage the theoretical foundations of positive linear operators to construct non-oscillatory, uniformly convergent numerical schemes. The origins of operator-based approximation in numerical analysis trace back to Bernstein (1912) and Chlodowsky (1937) [119, 120]. Their polynomial operators served as the first examples of positive linear operators that approximate functions uniformly on bounded intervals. During the 1940s–1950s, Szász (1950) and Mirakjan (1941) introduced exponential-type operators to handle functions defined on unbounded domains $[0, \infty)$. Their kernels, based on the Poisson distribution, provided natural exponential decay, making them ideal for modelling physical processes that diminish with distance or time , a characteristic of sin-

gular perturbation layers. Major developments includes Bernstein Polynomials applied to differential equations for their positivity and shape- preserving properties and Szász–Mirakyan and Szász–Mirakyan–Kantorovich (SMK) operators for unbounded domains (Mirakjan [1941]; Szász [1950]; Kantorovich [1958])[121] whereas Chlodowsky-type generalizations to handle growing functions and semi-infinite intervals, authors of thesis extended SMK and Bernstein–Chlodowsky operators to singularly perturbed problems, establishing maximum norm convergence and superior numerical accuracy. The methodology of these Operator based approximation methods is discussed in later part of this thesis in detail. These operators bridge classical numerical analysis and functional approximation theory, forming the theoretical backbone of this thesis.

Operator-based methods are inspired by the fundamental property that linear positive operators can approximate any continuous function uniformly under mild regularity conditions (Korovkin's theorem). When applied to differential equations, this property translates into smooth, stable approximations of solutions, especially for problems defined on semi-infinite or unbounded domains.

Recent years have witnessed an emerging synthesis between numerical mathematics and machine learning (ML). Techniques like physics-informed neural networks (PINNs) and operator learning extend the classical notion of numerical operators into data-driven contexts. In the context of singular perturbation, hybrid frameworks combine Operator-based interpolation (e.g., Szász–Mirakyan) for data reconstruction and smoothing, and Machine learning algorithms (e.g., XGBoost, ANN) for parameter prediction and function regression,and Analytical SPDE-based models for physical interpretability. This hybridisation was successfully demonstrated by authors in cyclone energy prediction, illustrating that operator-assisted ML frameworks improve both stability and predictive accuracy.

1.5 Application to Atmospheric Phenomena

This segment delves into the practical uses of the Bernstein related operator in addressing challenges in atmospheric science. Beyond theoretical error assessments, this section emphasizes the operator's application in real-world situations, especially in cyclone dynamics, boundary layer studies, and advanced atmospheric modeling. The Bernstein-Chlodowsky operator is particularly effec-

tive for capturing abrupt transitions and boundary layers in atmospheric events, essential for precise weather forecasting and climate simulations.

1.5.1 Cyclone Dynamics

Cyclones pose a complex challenge for numerical weather prediction due to their intricate multiscale dynamics. Particularly challenging are the steep gradients in wind speed, pressure, and temperature around the cyclone core or eye wall, which are critical for accurately modeling the intensity and path of cyclones. Predictions of cyclones are frequently inaccurate due to conventional numerical methods' inability to accurately capture these rapid changes.

The Bernstein-Chlodowsky operator overcomes these difficulties by more accurately depicting the sharp gradients and boundary layers near the cyclone center. It effectively manages the convection-dominated aspects of cyclones, where large-scale atmospheric movements and small-scale turbulent effects converge. The operator makes sure that fluctuations in wind speed and pressure are accurately recorded, which is crucial for forecasting cyclone intensification and migration, by directing computing resources to locations with substantial transitions.

For instance, cyclone intensification involves the interaction between warm, humid air ascending from the sea surface and the cooler air above. In the vicinity of the cyclone's center, these interactions result in abrupt temperature and pressure gradients. The capacity of the Bernstein-Chlodowsky operator to resolve these gradients improves models of the eye wall dynamics and, consequently, improves storm strength projections over time.

Moreover, the efficiency of the operator enables quicker simulations with reduced computational demands, making it highly suitable for real-time forecasting systems where timely and accurate predictions of cyclones are essential for effective disaster response.

1.5.2 Boundary Layer Modeling

The atmospheric boundary layer (ABL) is a crucial focus for weather prediction models. This narrow zone near the Earth's surface is where most atmospheric interactions, such as the transfer of heat, moisture, and momentum, occur, influencing the development of storms, cyclones, and other severe weather events, as

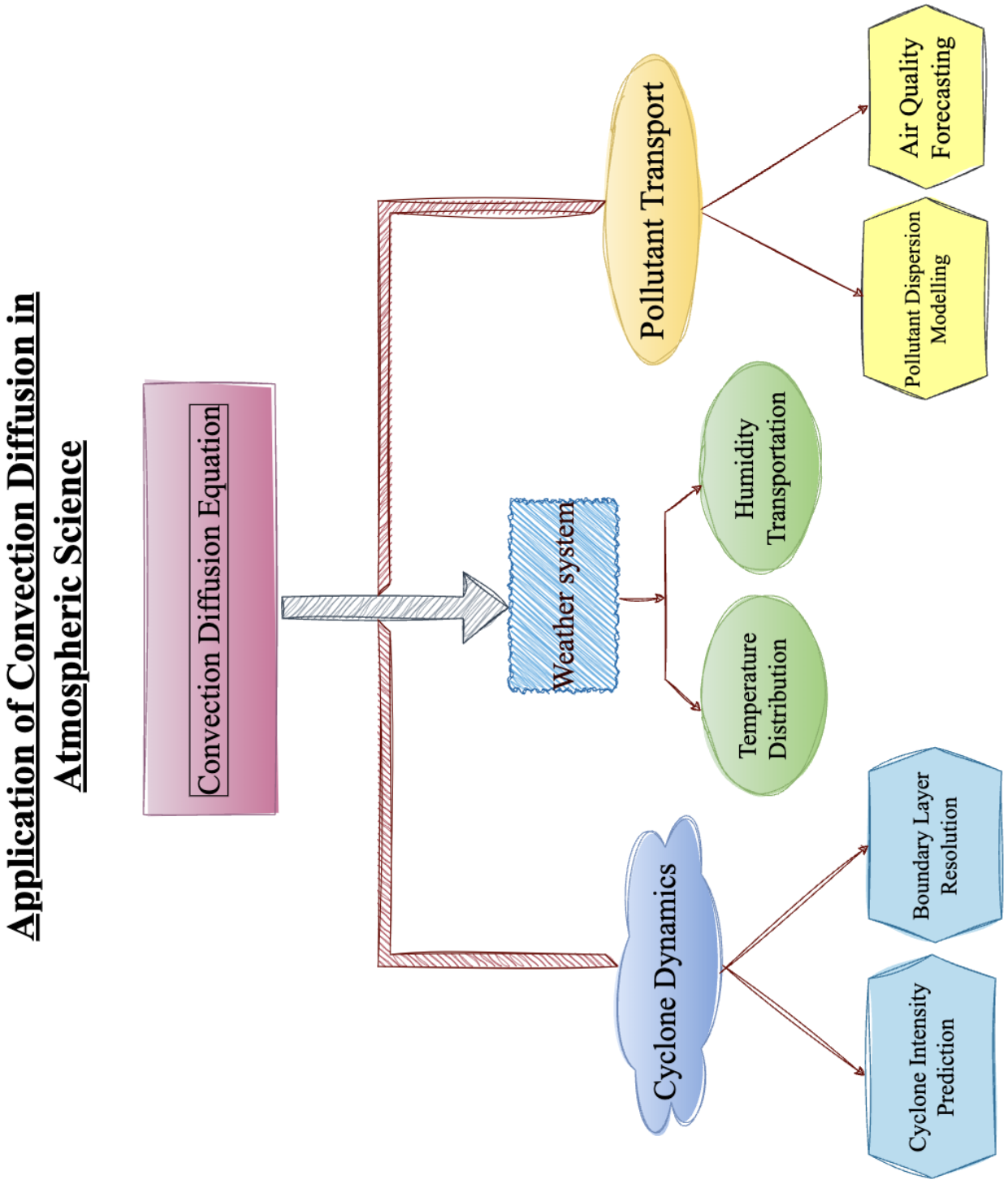

Figure 1.1: Flowchart showing the application of Convection-Diffusion type equations in Atmospheric Science and related fields.

well as affecting pollutant spread and temperature control.

For the purpose of forecasting ground-level meteorological conditions, such as wind speeds, temperature distributions, and humidity levels, accurate modeling of the ABL is essential. Significant modeling issues arise from the dramatic fluctuations in these variables inside the ABL, particularly near the surface. These high gradients are difficult for traditional numerical methods to resolve without the use of extremely small meshes, which can significantly increase computing costs and time.

The Bernstein-Chlodowsky operator addresses these challenges by effectively capturing the steep transitions within the ABL, eliminating the need for excessively fine meshes. This operator is particularly adept at adjusting to the rapid changes in temperature, wind speed, and pollutant levels that occur close to the ground, ensuring that weather models can accurately predict phenomena like ground-level winds, thermal inversions, and air quality.

For example, in areas with swift changes in pollutant levels due to surface emissions or atmospheric conditions, the Bernstein-Chlodowsky operator ensures accurate modeling of these transitions. This leads to more reliable forecasts of pollutant dispersion, which are crucial for environmental monitoring and public health initiatives.

Furthermore, the operator's ability to model thermal gradients assists in accurately forecasting cloud formation and precipitation, enhancing the reliability of short-term weather predictions.

1.5.3 Pollutant Transport Models:

The operator might be used to model long-range pollution transport in future air quality forecasting systems, making sure that quick variations in concentration brought on by shifting wind patterns or atmospheric mixing are appropriately recorded. This would be particularly helpful for tracking the spread of dangerous chemicals after natural catastrophes like volcanic eruptions or wildfires. The operator is a viable instrument for addressing these upcoming issues in atmospheric modeling because of its computing efficiency and capacity to manage abrupt shifts.

Therefore, by applying the Bernstein-Chlodowsky operator to solve real-world atmospheric problems, this study demonstrates its versatility and effectiveness

in addressing the challenges posed by sharp transitions and boundary layers in cyclone dynamics and weather prediction models. The operator's ability to model steep gradients with high accuracy and efficiency makes it a valuable tool for both current and future applications in atmospheric science, from cyclone intensity forecasting to boundary layer simulations and pollutant transport modeling.

1.6 Overview of thesis

This thesis includes six chapters, followed by a conclusion, a future scope, and references. The bibliography and list of publications are given at the end of the thesis. The abstract at the beginning of each chapter gives a brief outline of the work presented in that chapter. The reported work is organized as follows:

Chapter 1, is introductory in nature which gives a brief review of SPPs and survey on numerical analysis of SPDDEs and numerical techniques. Objectives, Literature survey and a brief summary of the present work is also included in this chapter.

Chapter 2, is about the numerical collocation methods based on Bernstein collocation method using equispaced nodes and Chebyshev-Gauss-Lobatto Nodes for solving linear and non linear singularly perturbed differntial equations, and results are then compared with traditional methods and error analysis is carried out.

In *chapter 3*, is devoted to Szasz Mirakyan operator . In this chapter we solved both linear and non linear singularly perturbed differntial equations and compared with traditional Methods Stability Analysis and error analysis is carried.

In *chapter 4*, This chapter presents a novel framework combining the Bernstein-Chlodowsky operator with neural networks termed as Bernstein-Chlodowsky Neural Network (BNN) and Bernstein-Chlodowsky collocation method (CCM) for solving singularly perturbed differential equations (SPDEs) in the context of atmospheric science and cyclone modeling. We solve linear and nonlinear SPDEs using the Bernstein-Chlodowsky collocation method and BNN, emphasizing how well these methods captures the convection dominated processes observed in cyclonic systems. The operator's superior convergence and boundary layer resolution make it an effective tool for cyclone modeling.

Chapter 5, This chapter focuses on predicting the Accumulated Cyclone Energy (ACE) in the NIO during monsoon using an optimized Artificial Neural Network

(ANN) model. The permutation feature is essential in finding the most influential features to improve model performance

Chapter 6, This chapter aims to forecast, using yearly cyclone data, the Accumulated Cyclone Energy (ACE) values for the North Indian Ocean (NIO) area. We study a predictive framework for estimating Accumulated Cyclone Energy (ACE) in the North Indian Ocean (NIO) using historical cyclone data from 1982 to 2023, en- compassing the Arabian Sea (AS) and Bay of Bengal (BOB) basins. Interpolation was performed using the Szász-Mirakyan operator, which preserves the statistical properties of the underlying distribution while reconstructing missing and zero values more effectively than conventional methods. XGBoost and neural networks are two machine learning methods compared in the study.

Chapter 7, Finally, this Chapter is devoted to conclusion of the study and discussion on some future directions of the current research work.

2 Finally, the bibliography and list of author's publications have been given at the end of the thesis.

Chapter 2

Optimizing the Bernstein Collocation Approach: Chebyshev-Gauss-Lobatto Nodes in Singular Perturbation

This chapter provides a numerical comparison of the performance of the variational method and the Bernstein collocation method (BCM) using equispaced nodes and Chebyshev-Gauss-Lobatto Nodes with respect to solving singularly perturbed equations that involve both linear and nonlinear problems. These problems provide major numerical approximation challenges because of their boundary layers and steep gradients. The BCM with Chebyshev nodes was found to perform more accurately than the variational method and the equispaced node configuration through a thorough error assessment that takes into account both maximum absolute error and root mean square error. For instance, for a perturbation parameter $\epsilon = 0.0001$, the BCM with chebyshev nodes shows maximum errors as 2.803×10^{-11}, compared to 7.862×10^{-8} for equispaced nodes and 5.267×10^{-6} for variational method. Additionally, the condition number of the matrices in the BCM with Chebyshev nodes is consistently smaller, demonstrating improved numerical stability. This makes the BCM with Chebyshev nodes an extremely useful tool for handling the complexity of singular perturbations in terms of providing substantial improvements in accuracy and computational reliability over traditional methods.

2.1 Introduction

Singularly perturbed boundary value problems are prevalent in applied research and engineering; reaction-diffusion equations and covection equations are two prominent examples [122, 123]. These formulas are very important for studying convection-diffusion processes, which are common in environmental engineering, chemical engineering, fluid dynamics, and heat transfer. In such contexts, singular perturbations often give rise to boundary layers, challenging the robustness and accuracy of numerical methods. Within singular perturbation analysis, a central goal is to construct asymptotic approximations that accurately model the actual solution, irrespective of the parameter's value [124, 125]. Solving these problems numerically using conventional methods presents challenges; the perturbation parameters can prevent uniform convergence. The root cause of this is the existence of boundary layers [126]. For chemical engineers and chemists, the 1D linear convection-diffusion equation is a useful tool despite its simplicity. Diffusion and convection both have an impact on chemical system behaviour, which it helps to understand and forecast. Its usefulness in the chemical sciences is demonstrated by applications like regulating reaction rates, constructing electrochemical systems, and optimising separation processes.

Bernstein polynomials hold significant practical value in computer-aided geometric design [127, 128] and various other branches of mathematics due to their abundance useful characteristics. Computer-aided design (CAD) is a field that uses mathematical techniques to build free-form objects. Its inception occurred somewhat after that of computer-aided engineering (CAE). Actually, computer-aided design [129], or CAD, is the use of technology to the development, editing, analysis, and optimization of geometric models and drawings. The Bézier curve, so named after its creator, Dr. Pierre Bézier, was the first technique to create free-form curves and surfaces. In 1966, Bézier, an engineer with the Renault automobile manufacturer, created this technique. The identical technique was actually created a few years earlier by Paul de Casteljau, another French engineer who worked at Citroën. B-splines, a further advancement of Bézier's technique, offer greater modeling freedom for free-form surfaces and curves. The bernstein polynomials are used to solve partial differential equations [119, 120], inetegral equation, etc. These polynomials plays important role in approximation theory

and gives the proof of Weierstrass approximation theorem [130]. The Bernstein polynomials has wide range of application in the filed of control theory [131] and chemical reactions [132]. The property that lacks in bernstein polynomials is that these polynomials does not possess orthogonality [119] which makes method like finite difference , finite element, and least square methods easier to use. Other families of orthogonal polynomials, including as Legendre, Chebyshev, and Jacobi polynomials, typically provide more efficient solutions for these particular applications. [133] presents a software suite of 17 MATLAB functions for solving differential equations by the spectral collocation method [134, 135]. This includes functions for computing derivatives of arbitrary order corresponding to Chebyshev, Hermite, Laguerre, Fourier, and sinc interpolants. Bernstein collocation method is also spectral collocation method based on bernstein polynomial. This chapter presents numerical methods for solving singularly perturbed equations in which the dominant processes are convection-diffusion or reaction-diffusion. Because of the difficulties arising from sudden modifications in boundary layers, we focus on the Bernstein collocation approach as a computationally promising technique. This approach differs in that it models solutions using Bernstein polynomials. This method works especially effectively for resolving the abrupt changes typical of boundary layers in singularly perturbed issues. During implementation, an equispaced collocation approach based on Bernstein polynomials was used [136]. Apart from the collocation technique, the use of the variational method, which forms the foundation of the Galerkin approach [137], is well known for producing approximations of solutions that are perpendicular to the subspace that the basis functions cover. This variational property ensures that the residual of the approximation, when integrated against any of the basis functions, vanishes, leading to a systematic minimization of the error.

$$-\varepsilon u''(x) + r(x)u'(x) + s(x)u(x) = f(x), \quad \text{for} \quad x \in (a, b), \tag{2.1}$$

accompanied by the dirichlet boundary conditions:

$$u(a) = \alpha, \quad u(b) = \beta, \tag{2.2}$$

with α and β being known values at the respective boundaries of the domain,

and ε is as small parameter. In above equation, the term $\varepsilon u''(x)$ represents the diffusion effect. The boundary layer gets thinner and steeper as ε decreases, making it harder for numerical approaches to resolve precisely. Whereas $r(x)u'(x)$ represent advection effect which shows the asymmetry and directionality of the solution and $s(x)u(x)$ represent reaction or decay/ growth behaviour of solution.

The core challenge addressed in this chapter is the numerical approximation of the solution to SPDEs, particularly where traditional methods struggle due to the small magnitude of ε and the resulting boundary layer effects. [122] primarily focuses on finite difference and fitted mesh methods, which are effective for certain boundary layer problems but often lack the flexibility and high accuracy provided by spectral methods and [123] emphasizes variational techniques [138] and their advantages in minimizing residuals. By addressing the limitations of earlier methods [122, 123] specifically their challenges in stability, accuracy, and applicability to nonlinear problems our approach not only bridges these gaps but also establishes a novel and effective methodology for singular perturbation problems. We assess the Bernstein Collocation Method's efficiency with two types of nodal distributions: equispaced and Chebyshev nodes [139], and compare the results to those obtained via variational methods. The aim is to highlight the advantages of the BCM in terms of accuracy and convergence when confronting the complexities introduced by singular perturbations. Furthermore, the improved matrix conditioning enhances computational stability, marking a significant advancement over traditional methods. This work demonstrates the efficacy of the proposed method across linear and nonlinear sPDEs, setting a new benchmark for accuracy and stability in numerical approximations.

2.2 Definitions

2.2.1 Bernstein polynomial

Bernstein polynomials represent a specific group of polynomials with significant roles in approximation theory and in the field of computer graphics.

A Bernstein polynomial of degree n is defined for $k = 0, 1, 2, ..., n$ as :

$$B_{k,n}(t) = \binom{n}{k} t^k (1-t)^{n-k} \tag{2.3}$$

where

- $B_{k,n}(t)$ is k^{th} Bernstein polynomial of degree n.
- $\binom{n}{k}$ is a binomial coefficient, calculated as $\binom{n}{k} = \frac{n!}{k!(n-k)!}$.
- t is variable, within the interval $[0, 1]$.

Some properties of bernstein polynomials:

1. $B_{k,n}(t)$ is non-negative within the interval $[0, 1]$.
2. $B_{k,n}(t)$ is continuous function on $[0, 1]$.
3. The sum of Bernstein polynomials of degree n is 1 for every $t \in [0, 1]$:

$$\sum_{k=0}^{n} B_{k,n}(t) = 1.$$

4. Bernstein polynomials are symmetric in the sense that $B_{k,n}(t) = B_{n-k,n}(1-t)$.
5. $B_{k,n}(t)$ can be written in the form of recursive relation:

$$B_{k,n}(t) = (1-t)B_{k,n-1}(t) + tB_{k-1,n-1}(t).$$

6. Asymptotic Error Bound: For a sufficiently smooth function $u(x)$, the Bernstein polynomial approximation [140] satisfies the uniform convergence property:

$$||u(x) - B_n|| \leq C.\frac{L(u, 1/n)}{\sqrt{n}}$$

where $L(u, 1/n)$ is modulus of continuity of $u(x)$. This bound ensures that the error decreases as the degree n increases, particularly in smooth regions of the solution.

The condition number of this matrix, defined as:

$$K(A) = ||A||.||A^{-1}||$$

For ill-conditioned matrices, $K(A)$ is large, leading to instability and inaccurate solutions. The lack of orthogonality in Bernstein polynomials exacerbates this issue because the basis functions are highly correlated, particularly for large n. Few moments of Bernstein (values of the Bernstein polynomials on the power functions) [141] operators are:

$$\sum_{k=0}^{n} B_{k,n}(t) = 1, \tag{2.4}$$

$$\sum_{k=0}^{n} \left(\frac{k}{n}\right) B_{k,n}(t) = t, \tag{2.5}$$

$$\sum_{k=0}^{n} \left(\frac{k}{n}\right)^2 B_{k,n}(t) = \frac{n-1}{n}t^2 + \frac{t}{n}. \tag{2.6}$$

2.2.2 Function Approximation

A square-integrable function $f(x)$ defined on the interval $(0, 1)$ can be represented as a linear combination of Bernstein basis polynomials [142] can be written as:

$$f(x) \approx \hat{f}_n(x) = \sum_{i=0}^{n} a_i B_{k,n}(x) = \mathbf{a}^\top \mathbf{B}(x), \tag{2.7}$$

where the coefficient vector is

$$\mathbf{a} = [a_0, a_1, \ldots, a_n], \tag{2.8}$$

and the vector of Bernstein basis polynomials is

$$\mathbf{B}(x) = [B_{0,n}(x), B_{1,n}(x), \ldots, B_{n,n}(x)]^\top. \tag{2.9}$$

The Bernstein basis polynomial $B_{k,n}(x)$ is defined by

29

$$B_{k,n}(x) = \binom{n}{k} x^k (1-x)^{n-k} = \sum_{j=0}^{n-k} (-1)^j \binom{n}{k} \binom{n-k}{j} x^{k+j}. \tag{2.10}$$

The approximation $\hat{f}_n(x)$ can be expressed in matrix form by incorporating the expression above as

$$\hat{f}_n(x) = \mathbf{a}^\top \mathbf{D} \varphi_{\mathbf{n}}(x), \tag{2.11}$$

where the matrix $\mathbf{D}$ is defined by

$$\mathbf{D} = \begin{bmatrix} (-1)^0 \binom{n}{0} & (-1)^1 \binom{n}{0}\binom{n-1}{1} & \cdots & (-1)^{n-0} \binom{n}{0}\binom{n-0}{n-0} \\ 0 & (-1)^0 \binom{n}{1} & \cdots & (-1)^{n-1} \binom{n}{1}\binom{n-1}{n-1} \\ \vdots & \vdots & \ddots & \vdots \\ 0 & 0 & \cdots & (-1)^0 \binom{n}{n} \end{bmatrix}, \tag{2.12}$$

and the vector $\varphi_{\mathbf{n}}(x)$ is given by

$$\varphi_{\mathbf{n}}(x) = [1, x, \ldots, x^n]^\top. \tag{2.13}$$

2.3 Methodologyy

In this section detailed methodology to solve Equation 2.1 using variational method , BCM with equispaced nodes and BCM with Chebyshev-Gauss-Lobatto Nodes are discussed:

2.3.1 Variational Method

The variational method [138, 143], often used in the calculus of variations, involves finding a function that minimizes (or maximizes) a functional, which is typically an integral of a function and its derivatives. When applied to differential equations, the method transforms the differential equation into a weak formulation [137], which seeks a function in a function space that minimizes the residual in a weighted average sense over the domain.

Consider the singularly perturbed differential equation with boundary conditions as defined in Equation 2.1 and when Bernstein polynomials are used with the

variational method, the solution to the differential equation is approximated by a linear combination of Bernstein polynomials:

$$u_n(x) = \sum_{i=0}^{n} c_k B_{k,n}(x) \tag{2.14}$$

where c_k are the coefficients to be determined and $u(x)$ is the solution of differential equation. As Bernstein polynomial is differentiable, therefore,

$$u_n'(x) = \sum c_k B_{k,n}'(x) \tag{2.15}$$

$$u_n''(x) = \sum c_k B_{k,n}''(x) \tag{2.16}$$

Integrating the equation 2.1 over the interval $[0, 1]$,

$$\int_0^1 \left[-\varepsilon u_n''(x) + r(x)u_n'(x) + s(x)u_n(x)\right] dx = \int_0^1 f(x)dx. \tag{2.17}$$

Choose test function $v(x) = B_{j,n}(x)$ that is sufficiently smooth and vanishes at boundaries at $x = 0$ and $x = 1$

$$\int_0^1 \left[-\varepsilon u_n''(x) + r(x)u_n'(x) + s(x)u_n(x)\right] v(x)dx = \int_0^1 f(x)v(x)dx. \tag{2.18}$$

Now using integrating by parts

$$\int_0^1 u''vdx = (u'v)_0^1 - \int_0^1 u'v'.$$

As $v(0) = v(1) = 0$ and for the mesh points $x_i, i = 0, 1, 2, \ldots, n$, the equation 2.18 becomes,

$$\int_0^1 \left[\varepsilon u_n'(x_i)v'(x_i) + r(x_i)u_n'(x_i)v(x_i) + s(x_i)u_n(x_i)v(x_i)\right] dx = \int_0^1 f(x_i)v(x_i)dx. \tag{2.19}$$

As test function $v(x) = B_{j,n}(x)$, $j = 0, 1, \ldots, n$ within $[0, 1]$ and approximate solution is given in equation 2.14. Therefore the equation 2.19 becomes,

$$\sum_{k=0}^{n} \left\{ \int_0^1 [\varepsilon B_{k,n}'(x_i)B_{j,n}'(x_i) + r(x_i)B_{k,n}'(x_i)B_{j,n}(x_i) + s(x_i)B_{k,n}(x_i)B_{j,n}(x_i)]dx \right\} c_k = \int_0^1 f(x_i)B_{j,n}(x_i)dx \tag{2.20}$$

and $A_{k,j}$ is

$$A_{k,j} = \int_0^1 [\varepsilon B'_{k,n}(x_i)B'_{j,n}(x_i) + r(x_i)B'_{k,n}(x_i)B_{j,n}(x_i) + s(x_i)B_{k,n}(x_i)B_{j,n}(x_i)]dx$$

and column matrix b is given as

$$b_j = \int_0^1 f(x_i)B_{j,n}(x_i)dx$$

these conditions yield a system of $(n+1)$ simultaneous equations i.e $(n+1)$ by $(n+1)$ linear system of equations. The integral involving the product of the basis function and the test function constitutes the elements of the system matrix A, and the integral of any forcing function (if present) with the test function constitutes the elements of the right-hand side vector b. Incorporating the given boundary conditions, the matrix equation **AX = b** is resolved by adapting the original matrix. This adaptation involves the removal of the first row and column as well as the last row and column, aligning the matrix structure with the imposed boundary conditions. Solving this system provides the constants $c_0, c_1, \ldots, c_n$, which can be used to construct the improved solution $\tilde{u}(x)$.

2.3.2 Bernstein Collocation Method with Equispaced Nodes

BCM is based on the idea of approximating the solution of a differential equation as a sum of certain basis functions. In this case, Bernstein polynomials are often chosen as the basis due to their beneficial properties, such as non-negativity and forming a partition of unity. Equispaced nodes are a set of equally spaced points in the interval of interest, typically $[0, 1]$. For n nodes, they are defined as:

$$x_j = \frac{j}{n-1} \quad \text{for} \quad j = 0, 1, \ldots, n-1 \tag{2.21}$$

Let the approximate solution $u_n(x)$ to the Equation 2.1 is represented as a linear combination of the Bernstein basis functions defined in Equation 2.14. The collocation method involves enforcing the differential equation to be satisfied exactly at the equispaced collocation nodes. This leads to a system of equations for the unknown coefficients c_k.

36 The equation 2.14 can be written as :

$$u(x) = \sum_{i=0}^{n} c_k B_{k,n}(x) = A^T \mathbf{B}(x) \tag{2.22}$$

where $A = [c_0, c_1, ..., c_n]$ and **B**(x) is defined in equation 2.9. Therefore, $\mathbf{B}(x) = D\varphi_n(x)$ where $\varphi_n(x)$ is defined in 2.13.

$$u(x) = \varphi_n^T(x) D^T A \tag{2.23}$$

$$\frac{d}{dx}\varphi_n(x) \approx I\varphi_n(x) \tag{2.24}$$

where,

$$I = \begin{bmatrix} 0 & 0 & \cdots & 0 \\ 1 & 0 & \cdots & 0 \\ 0 & 2 & \cdots & 0 \\ \vdots & \vdots & \ddots & \vdots \\ 0 & 0 & \cdots & n \end{bmatrix}$$

Therefore,

$$u_n^k(x) \approx \varphi_n^T(x)(I^k)^T D^T A \tag{2.25}$$

Inserting the approximate solution into the differential equation 2.1 and the matrix form of equation 2.1 is given as

$$-\varepsilon\varphi_n^T(I^2)^T D^T A + r(x)\varphi_n^T I^T D^T A + s(x)\varphi_n^T D^T A = f(x) \tag{2.26}$$

$$(X(a))^T D^T A - \alpha = 0$$

$$(X(b))^T D^T A - \beta = 0$$

For the collocation points x_j, above equation give rise to the algebraic system of equation defined as

$$-\varepsilon\overline{\varphi}(I^2)^T D^T A + R\overline{\varphi} I^T D^T A + S\overline{\varphi} D^T A = F \tag{2.27}$$

$$\left(-\varepsilon\overline{\varphi}(I^2)^T D^T + R\overline{\varphi}I^T D^T + S\overline{\varphi}D^T\right) A = F \tag{2.28}$$

$$WA = F \tag{2.29}$$

where $W = -\varepsilon\overline{\varphi}(I^2)^T D^T + R\overline{\varphi}I^T D^T + S\overline{\varphi}D^T$.

$$R = \begin{bmatrix} r(x_0) & 0 & \cdots & 0 \\ 0 & r(x_1) & \cdots & 0 \\ \vdots & \vdots & \ddots & \vdots \\ 0 & 0 & \cdots & r(x_n) \end{bmatrix} \text{ and } S = \begin{bmatrix} s(x_0) & 0 & \cdots & 0 \\ 0 & s(x_1) & \cdots & 0 \\ \vdots & \vdots & \ddots & \vdots \\ 0 & 0 & \cdots & s(x_n) \end{bmatrix}$$

$$\overline{\varphi} = \begin{bmatrix} 1 & x_0 & \cdots & x_0^n \\ 1 & x_1 & \cdots & x_1^n \\ 1 & x_2 & \cdots & x_2^n \\ \vdots & \vdots & \ddots & \vdots \\ 1 & x_n & \cdots & x_n^n \end{bmatrix} \text{ and } F = [f(x_0), f(x_1), ..., f(x_n)]$$

Enforcing the differential equation and boundary conditions results in a system of $(n+1)$ equations which upon resolution, reveal the coefficients $c_0, c_1, \ldots, c_n$.

2.3.3 Bernstein collocation method with Chebyshev-Gauss-Lobatto Nodes

The Chebyshev-Gauss-Lobatto nodes are a set of points that are distributed non-uniformly on the interval $[0, 1]$. They cluster more densely near the endpoints of the interval and are derived from the roots of the Chebyshev polynomials of the first kind, which are orthogonal on the interval $[-1, 1]$ with respect to the weight $(1-x^2)^{-1/2}$. The transformation $x = \frac{1+t}{2}$ is used to map these nodes to the interval $[0, 1]$.

The nodes are given by the formula:

$$x_i = \frac{1}{2}\left(1 + \cos\left(\frac{\pi i}{n}\right)\right) \quad \text{for} \quad i = 0, 1, \ldots, n$$

The BCM with Chebyshev-Gauss-Lobatto nodes is particularly well-suited for problems that are known to have boundary layers or sharp gradients, as the

distribution of nodes provides better resolution where it's needed most. This method is part of a family of spectral methods that offer high accuracy for problems with smooth solutions and are often used when high precision is required. This process involves the same steps just instead of equispaced nodes we use Chebyshev-Gauss-Lobatto nodes.

Advantages of Chebyshev-Gauss-Lobatto

- The distribution of Chebyshev nodes, which are denser near the interval's endpoints, is particularly effective for capturing boundary layer behavior in differential equations, a challenge often inadequately addressed by equispaced nodes. Legendre nodes, on the other hand, are more evenly spaced over the interval, which may result in lower resolution for singularly perturbed situations close to borders.

- In numerical computations, Chebyshev-Gauss-Lobatto nodes are known for their stability, especially in the context of spectral methods, where they are often preferred over equispaced nodes. The cosine-based formula for CGL nodes allows straightforward computation. Legendre nodes require solving the roots of Legendre polynomials, which is computationally more expensive, particularly for high-degree polynomials.

- Unlike equispaced nodes, Chebyshev-Gauss-Lobatto nodes significantly mitigate the Runge phenomenon, which is a common problem in polynomial interpolation, especially at higher degrees.

- When dealing with high-degree polynomial approximations, Chebyshev nodes are more efficient and reliable compared to equispaced nodes, where the accuracy can significantly deteriorate.

In summary, the choice of Chebyshev-Gauss-Lobatto nodes over equispaced nodes [143] and traditional variational methods offers substantial improvements in terms of accuracy, stability, and efficiency, particularly in complex numerical and approximation problems. The schematic diagram for BCM with Chebyshev node is shown in Figure 2.1.

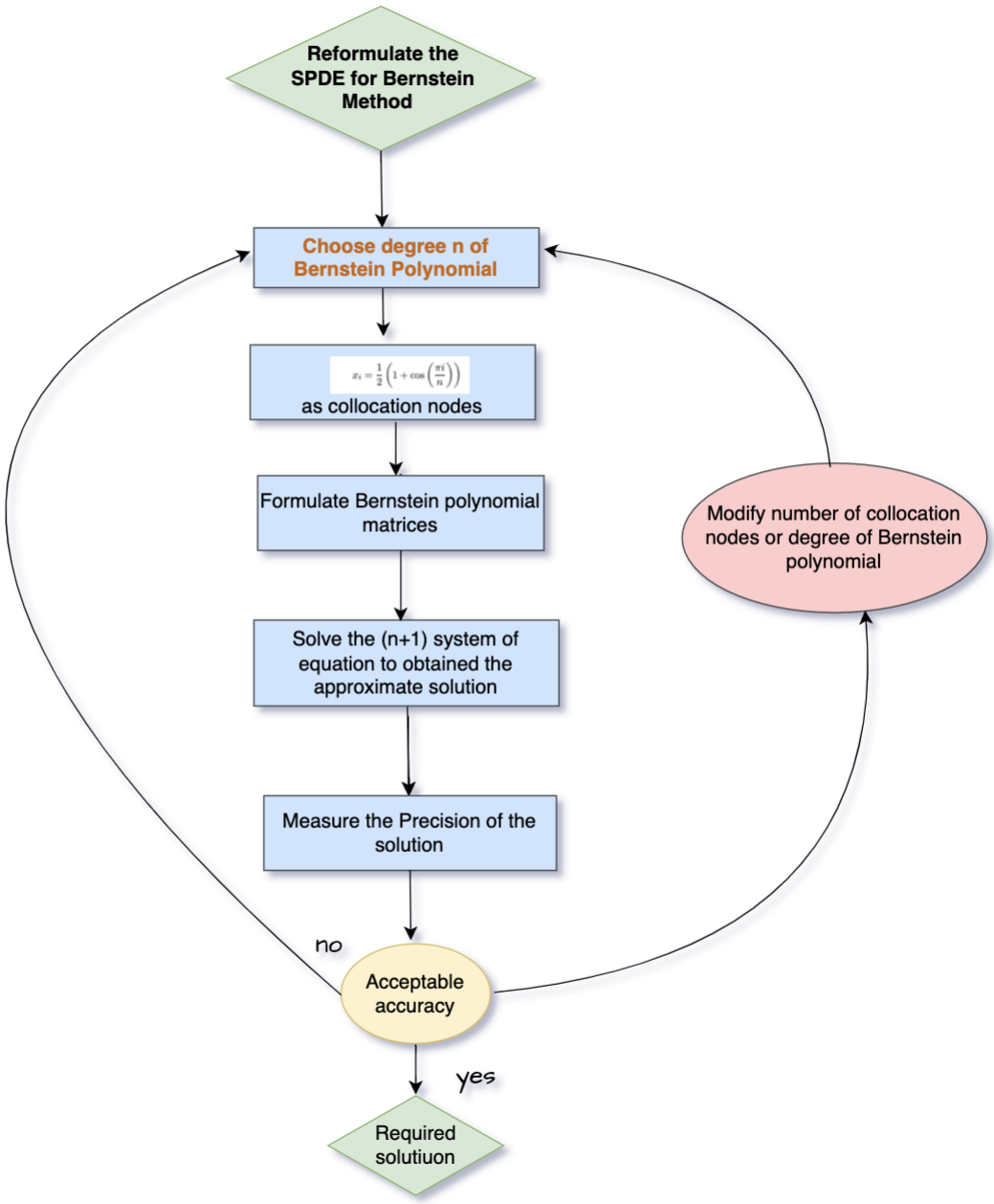

Figure 2.1: Schematic diagram for BCM with Chebyshev node.

2.4 Error Analysis

In this section error analysis is carried out for problem 2.1. Let us define the Chebyshev-Gauss-Lobatto as

$$x_i = \frac{1}{2}\left(1 + \cos\left(\frac{\pi i}{n}\right)\right) \quad \text{for} \quad i = 0, 1, \ldots, n$$

Chebyshev-Gauss-Lobatto nodes are chosen for their non-uniform spacing, clustering more densely at the endpoints of the interval. This is particularly useful for singularly perturbed problems where the solution may have boundary layers. The error analysis [142] would involve estimating the interpolation error, which depends on the smoothness of the true solution u and the distribution of the nodes. Chebyshev nodes can reduce the error due to their distribution, which is optimal in the sense of minimizing the maximum error over the interval.

Suppose $X = C[0, 1]$ be the Banach space equipped with norm defined as

$$||u|| = max_{x\in[0,1]}|u(x)| \tag{2.30}$$

Theorem 1. Let u be a continuous function on the interval $[0, 1]$. For every positive $\xi > 0$, there exists a positive integer M such that for all $t \in [0, 1]$ and for any integer $m \geq M$, the following inequality holds:

$$\|u(t) - B_m(u)(t)\|_\infty < \xi.$$

Moreover, if u belongs to the space $C^k[0, 1]$ for any non-negative integer k, then the k-th derivative of the Bernstein approximation of u, $B_m(u)$, converges to the k-th derivative of u as m approaches infinity:

$$\lim_{m\to\infty} (B_m(u))^{(k)}(t) = u^{(k)}(t).$$

Proof: For detailed proof [140]

Theorem 2. Let u_ξ be the solution to a singularly perturbed differential equation and $u_{n,\xi}$ be the Bernstein variational approximation of degree n. Under appropriate smoothness assumptions on the exact solution and boundary conditions, there exists

a positive constant C, independent of ξ and n, such that [144]

$$\|u_\xi - u_{n,\xi}\| \leq Cn^{-\alpha}$$

for some $\alpha > 0$, where $\|\cdot\|$ denotes an appropriate norm.

Theorem 3. Consider a function F that is bounded and continuous on the closed interval $[0, 1]$. Assume that the second derivative of F, denoted by F'', exists on the same interval. Under these conditions, the deviation of the Bernstein polynomial approximation $B_m(F)$ from the function F can be bounded by

$$\|B_m(F) - F\|_\infty \leq \frac{1}{2m} \max_{x\in[0,1]} x(1-x)\|F''\|_\infty.$$

Proof. A comprehensive proof is available in the referenced literature [145]. □

Theorem 4. If $u(x)$ is sufficiently smooth on $[0, 1]$ and Let $u(x)$ be the exact solution of 2.1 and B_n is the bernstein polynomial of degree n then the Bernstein solution at Chebhyshev Gauss-Lobatto nodes converges to $u(x)$.

Proof: We know that the difference of $B_n(u, x)$ and $u(x)$ is

$$B_n(u,x) - u(x) = \sum_{k=0}^{n} \left(u\left(\frac{k}{n}\right) B_{k,n}(x) - u(x) \right) .1. \tag{2.31}$$

Using the relation 2.4, in the following equation, we have [140]

$$B_n(u,x) - u(x) = \sum_{k=0}^{n} \left(u\left(\frac{k}{n}\right) - u(x) \right) B_{k,n}(x), \tag{2.32}$$

so

$$|B_n(u,x) - u(x)| \leq \sum_{k=0}^{n} \left| u\left(\frac{k}{n}\right) - u(x) \right| B_{k,n}(x). \tag{2.33}$$

As $u(x)$ is uniformly continuous on $[0, 1]$, therefore, $\exists$ a real number $\delta > 0$ for a given real number $\xi > 0$, such that

$$\text{for } |x_1 - x_2| < \delta \quad \text{we have , } |u(x_1) - u(x_2)| < \xi. \tag{2.34}$$

For $\delta_1 > 0$, $\delta_2 > 0$ and $x \in [0,1]$, divide the set of chebyshev nodes into three sets

$$A = \{x_i : 0 \leq |x_i - x| < \delta_1\}$$
$$B = \{x_i : \delta_1 \leq |x_i - x| < \delta_2\} \text{ and}$$
$$C = \{x_i : \delta_2 < |x_i - x| \leq 1\}$$

where

$$x_i = \frac{1}{2}\left(1 + \cos\left(\frac{\pi i}{n}\right)\right) \quad \text{for} \quad i = 0, 1, \ldots, n$$

A and C gives the nodes at boundary layers and both have same number of points whereas B gives the nodes at interior layer and thus the series on the right-hand side of the inequality (4.4) can be divided into two series given as :

$$|B_n(u,x) - u(x)| \leq \sum_{\substack{i=0 \\ (x_i \in A \text{ or} C)}}^{n} |u(x_i) - u(x)|\, B_{k,n}(x) + \sum_{\substack{i=0 \\ (x_i \in B)}}^{n} |u(x_i) - u(x)|\, B_{k,n}(x). \tag{2.35}$$

$$|B_n(u,x) - u(x)| \leq I_1(x_i \in A) + I_2(x_i \in B). \tag{2.36}$$

For the case I_1, let $\xi > 0$ then, $\exists$ real number δ_1 such that

$$|u(x_i) - u(x)| < \frac{\xi}{2} \text{ for } |x_i - x| < \delta_1. \tag{2.37}$$

Now, for the case I_2, $|x_i - x| < \delta_2$ this is trivial and we have $|x_i - x| \geq \delta_1$, therefore,

$$1 \leq \frac{(x_i - x)^2}{\delta_1^2} \leq \frac{\phi}{\delta_1^2}.$$

Let $|f(x)| \leq M$, and assuming that $x_i \in B$, then the above inequality can be written as

$$\frac{2M\phi}{\delta_1^2} \geq 2M$$
$$2M < \frac{2M\phi}{\delta_1^2} + \xi$$
$$-\xi - \frac{2M\phi}{\delta_1^2} < -2M \tag{2.38}$$

The inequality

$$-\xi - \frac{2M\phi}{\delta_1^2} < -2M < (u(x_i) - u(x)) < 2M < \frac{2M\phi}{\delta_2^2} + \xi \tag{2.39}$$

will hold in this subinterval. Choose $\delta = \min\{\delta_1, \delta_2\}$. Therefore,

$$\sum_{i=0}^{n} |u(x_i) - u(x)| B_{k,n}(x) \leq \frac{1}{\delta^2} \sum_{i=0}^{n} (x_i - x)^2 |u(x_i) - u(x)| B_{k,n}(x),$$

where $(x_i - x)^2 = \left(\frac{1}{2}\left(1 + \cos\left(\frac{\pi i}{n}\right)\right) - x\right)^2 = \phi > 0$ and using theorem 3 and Korovkin second theorem [146] this function is bounded and for $\xi > 0$ right side of inequality (above equation) converges to ξ and left side to $-\xi$, we have,

$$\sum_{\substack{i=0 \\ (x_i \in B)}}^{n} |u(x_i) - u(x)| B_{k,n}(x) < \frac{2M}{4n\delta^2}.$$

collecting the estimates of 2.36

$$|B_n(u, x) - u(x)| < \frac{\xi}{2} + \frac{M}{2n\delta^2} \tag{2.40}$$

For a positive real number $\xi > 0$, there exists a number $N(\xi)$ such that for all $n \geq N(\xi)$, choose n to be so large that $\frac{M}{2n\delta^2} < \xi$ then

$$|B_n(u, x) - u(x)| < \xi \tag{2.41}$$

Hence Proved.

2.5 Numerical Results

Example 2.5.1. *Consider 1D linear convection–diffusion problem [147].*

$$-\varepsilon u'' - 2u' = 0; \quad x \in (0, 1), \quad 0 < \varepsilon \ll 1,$$

with boundary conditions

$$u(0) = 1 \quad and \quad u(1) = 0;$$

This equation can be used in electrochemical process, kinetics of chemical reactions and chromatography. The exact solution is

$$u = \frac{\exp(-2x/\varepsilon) - \exp(-2/\varepsilon)}{1 - \exp(-2/\varepsilon)}.$$

Maximum error for Example 2.5.1

ε	$N = 16$	$N = 32$	$N = 64$
0.1	VM = 1.117347e-06 ES = 5.051608e-04 CN = 3.916684e-09	VM = 4.44e-09 ES = 2.07e-09 CN = 4.09e-10	VM = 1.77383e-04 ES = 9.40241e-06 CN = 6.55867e-11
0.01	VM = 1.657810e-01 ES = 4.529805e-01 CN = 1.477967e-05	VM = 3.59e-03 ES = 0.184 CN = 1.36e-03	VM = 1.66931e-04 ES = 1.05495e-02 CN = 1.12216e-06
0.001	VM = 4.678486e+00 ES = 8.787602e-01 CN = 7.077139e-03	VM = 0.83 ES = 0.75 CN = 0.37	VM = 2.77650e-01 ES = 6.25523e-01 CN = 6.82858e-05
0.0001	VM = 5.111890e+01 ES = 9.471194e-01 CN = 8.379225e-03	VM = 43.27 ES = 0.88 CN = 0.45	VM = 8.42262e-01 ES = 7.54439e-01 CN = 7.83557e-03
1e-05	VM = 5.156183e+02 ES = 9.471019e-01 CN = 8.374311e-02	VM = 35.87 ES = 0.88 CN = 0.44	VM = 2.40243e+01 ES = 7.55436e-01 CN = 6.54886e-03

Table 2.1: Maximum Error for different values of ε using methods for $N = 16, 32, 64$ for Example 2.5.1.

The variational method shows significant errors as ε decreases, indicating that it may not handle thin boundary layers well with a lower degree of polynomials. The errors and RMSE values continue to grow as ε becomes smaller. This suggests that while increasing N improves the resolution of the method, it may still not be sufficiently robust for very thin boundary layers without further refinement. The BCM with Chebyshev-Gauss-Lobatto nodes consistently outperforms the other methods across different values of N and ε, making it the most reliable for this problem, especially as the boundary layer becomes thinner. The variational method demonstrates the fastest computation times across all tested values of N, due to its relatively simple matrix assembly and solution process. However, its accuracy is significantly lower, particularly for small values of ε. The BCM with equispaced nodes requires slightly more computation time, as the matrix conditioning is more demanding. Finally, the BCM with Chebyshev-Gauss-Lobatto nodes shows the highest computation times, reflecting the added complexity of node clustering and matrix assembly. Despite this, the Chebyshev-based BCM provides superior accuracy, particularly for problems with sharp boundary layers. Increasing the degree of polynomials (N) generally leads to better accuracy for the Galerkin method and BCM with Chebyshev-

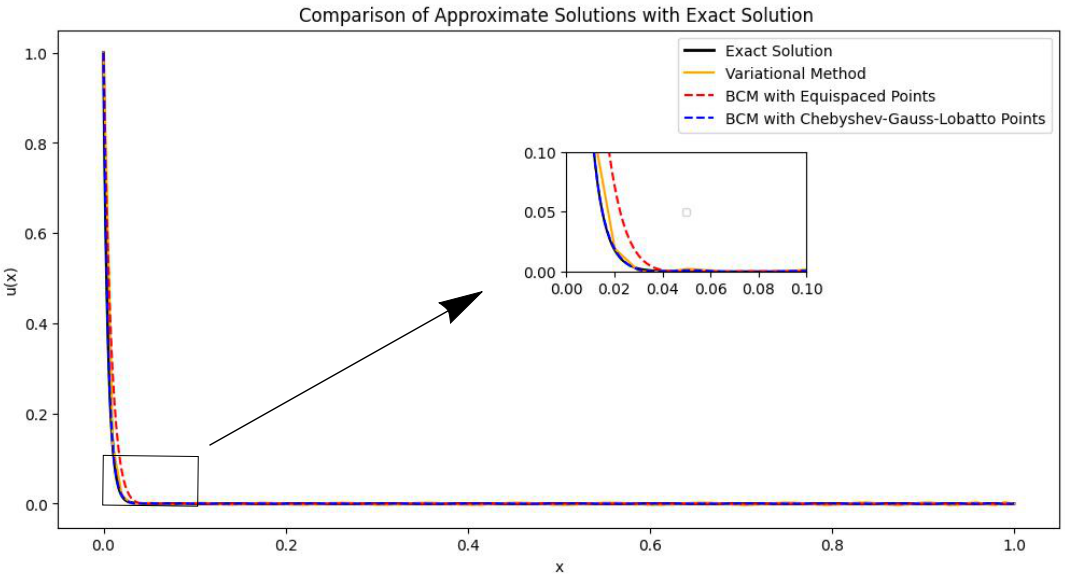

Figure 2.2: Comparison of exact solution with approximate solution for $\epsilon = 0.001$ and $N = 32$ for Example 2.5.1.

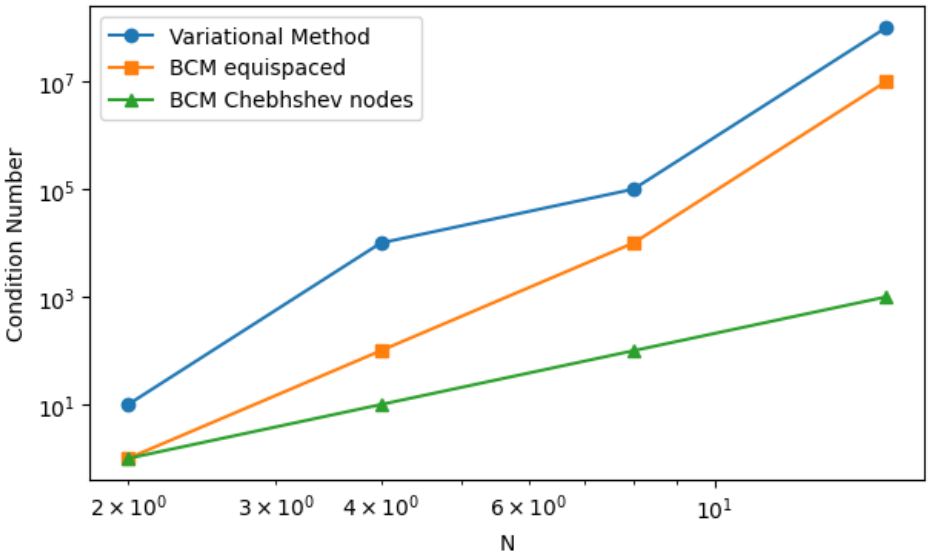

Figure 2.3: Condition number for different value of N for Example 2.5.1.

Root Mean Square error for Example 2.5.1

ε	$N = 16$	$N = 32$	$N = 64$
0.1	VM = 7.274071e-07 ES = 1.140505e-04 CN = 8.992726e-10	VM= 2.74e-09 ES = 2.02e-09 CN = 2.30e-10	VM = 8.73292e-05 ES = 1.69395e-06 CN = 1.00017e-11
0.01	VM = 8.372477e-02 ES = 6.017927e-02 CN = 1.965103e-05	VM = 1.82e-03 ES = 0.0191 CN = 3.02e-04	VM = 7.70160e-05 ES = 8.96528e-04 CN = 1.74317e-07
0.001	VM = 3.260324e+00 ES = 8.861036e-02 CN = 5.689023e-02	VM = 0.51 ES = 0.0543 CN = 0.0215	VM = 1.52587e-01 ES = 3.31751e-02 CN = 2.53904e-06
0.0001	VM = 3.680886e+01 ES = 8.996845e-02 CN = 6.033428e-03	VM = 28.66 ES = 0.0563 CN = 0.028	VM = 5.88546e-01 ES = 3.55288e-02 CN = 2.68647e-03
1e-05	VM = 3.724963e+02 ES = 8.995084e-02 CN = 6.048782e-03	VM = 24.0 ES = 0.0563 CN = 0.0285	VM = 1.70211e+01 ES = 3.56273e-02 CN = 2.99289e-03

Table 2.2: Root Mean Square Error for different values of ε using methods for $N = 16, 32, 64$ for Example 2.5.1.

Gauss-Lobatto nodes, but it also increases computational complexity. The benefits of increasing N are more pronounced for the BCM with Chebyshev-Gauss-Lobatto nodes. The variational method exhibits the largest error, particularly in the boundary layer regions, due to its limited ability to capture steep gradients effectively. The BCM with equispaced nodes performs better but still struggles near the boundaries, as equispaced nodes do not provide sufficient resolution in these critical regions. In contrast, the BCM with Chebyshev-Gauss-Lobatto nodes shows significantly smaller discrepancies, especially in the boundary layers, due to the clustering of nodes near the endpoints. The maximum error and root mean square error for $N = 16, 32, 64$ for different values of ε are shown in Table 2.1, 2.2 where VM, ES, CN denotes the variational method, BCM with equispaced nodes and BCM with Chebyshev-Gauss-Lobatto nodes, respectively and comparison of exact solution with variational method, BCM at equispaced nodes and chebyshev nodes is shown in Figure 2.2 for $N = 32$ and $\varepsilon = 0.001$. To verify the statistical significance of the differences in accuracy between the variational method and BCM with Chebyshev-Gauss-Lobatto nodes, we conducted a paired t-test for the maximum errors and RMSE values at different node counts ($N = 16, 32, 64$). The p-values for all cases were below 0.001, indicating statistically significant improvements in accuracy using the BCM with Chebyshev nodes. This analysis confirms that the observed differences are not due to random variation but are a result of the superior numerical properties of the

proposed method. Figure 2.3 provide an insightful analysis of the condition numbers for different numerical methods. Lower condition numbers are directly linked to improved numerical stability and reduced sensitivity to rounding errors in computations. The lower condition numbers achieved by BCM with CGL nodes lead to more accurate and reliable solutions, even for small perturbation parameters ε. This justifies the preference for methods that prioritize numerical stability through well-conditioned system matrices.

Example 2.5.2. *We consider 1D linear convection–diffusion problem with turning point as*

$$-\varepsilon u'' + 2(2x-1)u' + 4u = 0; \quad x \in (0,1), \quad 0 < \varepsilon \ll 1, \tag{2.42}$$

with boundary conditions

$$u(0) = 1 \quad \textit{and} \quad u(1) = 1; \tag{2.43}$$

Turning points in physical models are critical as they signify locations where the dominant behavior of the system changes, such as transitions between diffusion- and convection-dominated regimes. In the context of catalytic reactors, turning points can represent zones where the reaction kinetics change significantly, influencing the overall efficiency of the reactor. There are several uses for the provided 1D linear convection-diffusion equation with a turning point in various chemical contexts. It clarifies how chemical species migrate in reaction-diffusion systems which include catalytic reactors where diffusion and convection play important roles. It reflects the movement of ions in the presence of electric fields and concentration gradients inside electrochemical systems, such as batteries. It also helps with environmental chemistry to predict the dispersion of pollutants and pharmacokinetics to develop drug delivery systems, all of which are aspects of chemical reactor engineering. This formula is a useful tool for studying complex transport phenomena, which are necessary for building efficient systems and optimizing chemical processes in a variety of chemical applications [148]. The exact solution is

$$u = \exp\left(\frac{-2x(1-x)}{\varepsilon}\right). \tag{2.44}$$

The variational method, while performing reasonably well at higher values of ε shows a significant increase in error as ε decreases. This indicates its limitations in

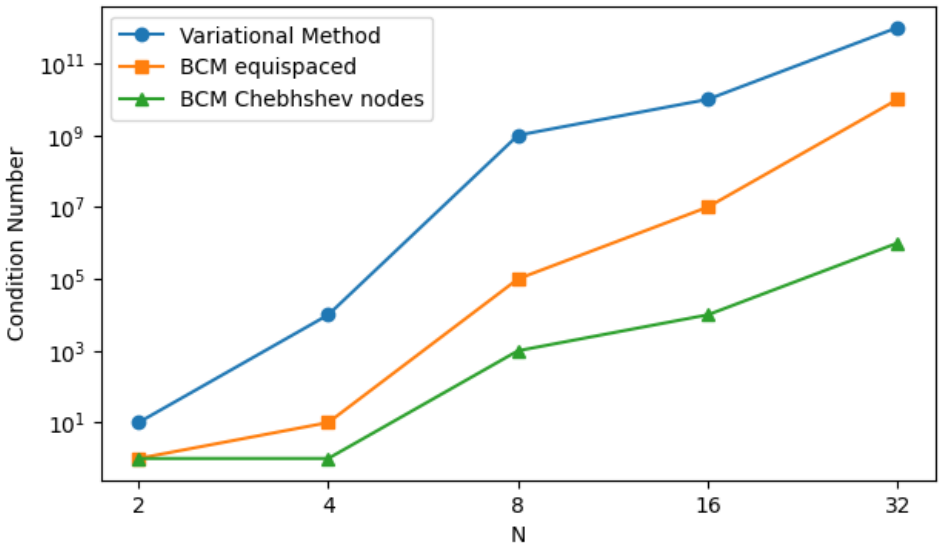

Figure 2.4: Condition number for different value of N for Example 2.5.2.

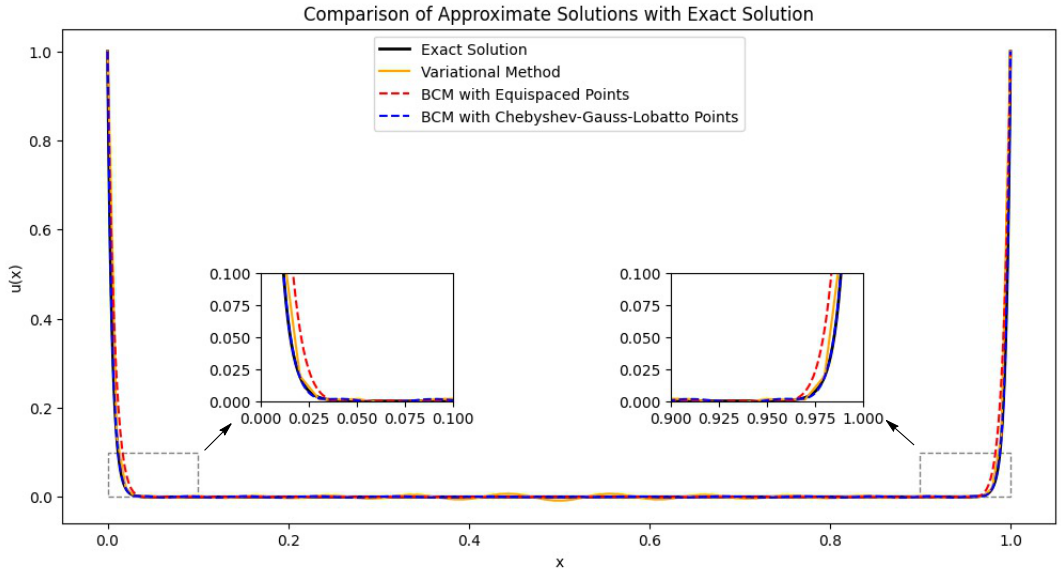

Figure 2.5: Comparison of exact solution with approximate solution for $\varepsilon = 0.001$ and $N = 32$ for Example 2.5.2

Maximum error for Example 2.5.2

ε	$N = 16$	$N = 32$	$N = 64$
0.1	VM = 6.644114e-06 ES = 1.207679e-03 CN = 9.548789e-09	VM = 7.949558e-10 ES = 4.284569e-09 CN = 4.934941e-14	VM = 1.619138e-06 ES = 1.158580e-05 CN = 9.471110e-11
0.01	VM = 3.080556e-01 ES = 4.106389e-01 CN = 1.353148e-05	VM = 8.467670e-03 ES = 1.577407e-01 CN = 1.619785e-03	VM = 4.930264e-03 ES = 1.071865e-02 CN = 3.260011e-05
0.001	VM = 2.594427e+00 ES = 8.627769e-01 CN = 8.293174e-03	VM = 1.893492e+00 ES = 7.294452e-01 CN = 4.156890e-01	VM = 3.114037e+00 ES = 6.275232e-01 CN = 9.994005e-02
0.0001	VM = 3.254832e+00 ES = 9.386752e-01 CN = 1.035094e-03	VM = 4.020975e+00 ES = 8.636396e-01 CN = 2.605251e-01	VM = 1.122746e+01 ES = 7.297220e-01 CN = 9.616380e-02
1e-05	VM = 3.329855e+00 ES = 9.386425e-01 CN = 1.059015e-03	VM = 2.939761e+00 ES = 8.635301e-01 CN = 1.051880e-01	VM = 1.158473e+01 ES = 7.283668e-01 CN = 9.800913e-02

Table 2.3: Maximum Error for different values of ε using methods for $N = 16, 32, 64$ for Example 2.5.2.

accurately resolving problems with steeper gradients ε. The BCM with equispaced nodes shows a moderate level of performance. It generally performs better than the variational method but is not as effective as the BCM with Chebyshev nodes, particularly at lower values of ε. Furthermore, increasing the number of nodes (N) tends to enhance the precision of all methods, with the BCM Chebyshev method benefiting the most. This improvement is particularly noticeable at higher node counts, reinforcing the method's efficiency. The maximum error and root mean square error for $N = 16, 32, 64$ for different values of ε are shown in Table 2.3, 2.4 and comparison of exact solution with variational method, BCM at equispaced nodes and chebyshev nodes is shown in Figure 2.5 for $N = 32$ and $\varepsilon = 0.001$. The condition number of matrices in different methods is shown in Figure 2.4. The condition numbers of the matrices obtained using VM, ES and CN are compared and BCM with chebyshev nodes exhibits smaller condition number, this shows that this method is well conditioned.

Example 2.5.3. *Consider [149]*

$$\begin{cases} -\varepsilon v'' + v + v^2 = e^{-\frac{2x}{\sqrt{\varepsilon}}} \\ v(0) = 1, \quad v(1) = e^{-\frac{1}{\sqrt{\varepsilon}}} \end{cases} \tag{2.45}$$

The provided equtaion can be used in electrochemistry, modelling of chemical

Root Mean Square error for Example 2.5.2

ε	$N = 16$	$N = 32$	$N = 64$
0.1	VM = 3.982554e-06 ES = 3.799520e-04 CN = 5.242839e-10	VM = 4.496978e-10 ES = 1.195994e-09 CN = 2.578613e-14	VM = 6.857614e-07 ES = 2.149261e-06 CN = 2.822902e-11
0.01	VM = 1.015438e-01 ES = 7.339804e-02 CN = 9.372317e-07	VM = 3.161594e-03 ES = 2.240382e-02 CN = 9.705808e-04	VM = 2.607819e-04 ES = 1.187935e-03 CN = 6.795407e-05
0.001	VM = 7.769301e-01 ES = 1.146439e-01 CN = 5.548606e-04	VM = 4.258808e-01 ES = 7.129443e-02 CN = 2.897101e-02	VM = 6.134371e-01 ES = 4.394416e-02 CN = 4.479926e-03
0.0001	VM = 9.740591e-01 ES = 1.166156e-01 CN = 6.860670e-02	VM = 8.962176e-01 ES = 7.424585e-02 CN = 6.392219e-02	VM = 2.056816e+00 ES = 4.444844e-02 CN = 4.088883e-03
1e-05	VM = 9.965203e-01 ES = 1.165781e-01 CN = 7.013232e-02	VM = 6.571314e-01 ES = 7.420531e-02 CN = 6.986647e-02	VM = 2.123071e+00 ES = 4.418532e-02 CN = 4.556164e-03

Table 2.4: Root Mean Square Error for different values of ε using methods for $N = 16, 32, 64$ for Example (2.5.2).

reactions and catalysis, where v^2 describes the catalytic activity [169] and source term described the influence of reactant on catalytic surface. The exact solution of the above problem is given as:

$$v(x) = e^{-\frac{x}{\sqrt{\varepsilon}}}. \tag{2.46}$$

The maximum error and root mean square error for $N = 16, 32, 64$ for different values of ε are shown in Table 2.5, 2.6 and comparison of exact solution with variational method, BCM at equispaced nodes and chebyshev nodes is shown in Figure 2.6 for $N = 32$ and $\varepsilon = 0.001$. And it is observed that for non-linear problem also BCM with chebyshev nodes is more effective as compared to variational and BCM with equispaced collocation points in terms of accuracy. It is clearly visible in this case also, BCM with chebyshev nodes outperforms the other methods for diferent values of N and ε. The Bernstein Collocation Method (BCM) with Chebyshev-Gauss-Lobatto (CGL) nodes maintains significantly lower condition numbers compared to equispaced nodes or the variational method, as shown in Figure 2.7 This reduction in condition numbers is due to the clustering of CGL nodes near boundaries, which minimizes matrix correlation and ensures stable matrix inversion. Consequently, the lower condition numbers achieved by BCM with CGL nodes lead to more accurate and reliable solutions, even for small perturbation parameters ε. This justifies the preference for methods that prioritize numerical stability through well-conditioned

system matrices.

Maximum error for Example 2.5.3

ε	$N = 16$	$N = 32$	$N = 64$
0.1	VM = 1.64910e-03 ES = 4.62391e-12 CN = 9.16192e-14	VM = 1.33020e-03 ES = 4.31866e-10 CN = 9.92237e-13	VM = 1.20225e-03 ES = 1.73116e-03 CN = 3.216918e-09
0.01	VM = 2.12543e-08 ES = 1.21087e-07 CN = 6.73345e-10	VM = 3.03157e-07 ES = 2.29105e-11 CN = 1.55536e-11	VM = 1.086582e-07 ES = 4.323502e-05 CN = 8.286448e-10
0.001	VM = 5.69641e-04 ES = 6.20911e-03 CN = 8.56708e-07	VM = 1.46381e-10 ES = 9.97072e-09 CN = 1.74060e-13	VM = 5.267206e-06 ES = 7.862639e-08 CN = 2.803281e-11
0.0001	VM = 1.79363e-01 ES = 2.24420e-01 CN = 2.61915e-03	VM = 2.75320e-05 ES = 1.80779e-02 CN = 7.83544e-06	VM = 3.986359e-04 ES = 2.236386e-04 CN = 7.153543e-06
1e-05	VM = 1.06099e-01 ES = 5.27390e-01 CN = 1.61054e-03	VM = 2.02394e-02 ES = 2.14715e-01 CN = 1.02811e-02	VM = 1.260625e-03 ES = 3.059913e-02 CN = 4.082013e-03

Table 2.5: Maximum Error for different values of ε using methods for $N = 16, 32, 64$ for Example 2.5.3.

Example 2.5.4. *We consider 1D linear reaction-diffusion problem as [147]*

$$-\varepsilon u''(x,\varepsilon) + u(x,\varepsilon) = -\cos^2(\pi x) - 2\varepsilon\pi\cos(2\pi x), \quad x \in (0,1), \quad 0 < \varepsilon \ll 1, \tag{2.47}$$

with boundary conditions

$$u(0,\varepsilon) = 0, \quad u(1,\varepsilon) = 0. \tag{2.48}$$

63

The exact solution is

$$u(x,\varepsilon) = \frac{\exp\left(-\frac{(1-x)}{\sqrt{\varepsilon}}\right) + \exp\left(-\frac{x}{\sqrt{\varepsilon}}\right)}{1 + \exp\left(-\frac{1}{\sqrt{\varepsilon}}\right)} - \cos^2(\pi x). \tag{2.49}$$

The maximum error and root mean square error for $N = 16, 32, 64$ for different values of ε are shown in Table 2.7, 2.8 and comparison of exact solution with variational method , BCM at equispaced nodes and chebyshev nodes is shown in Figure2.9 for $N = 32$ and $\varepsilon = 0.001$. The condition number of matrices in different methods is shown in Figure 2.8.

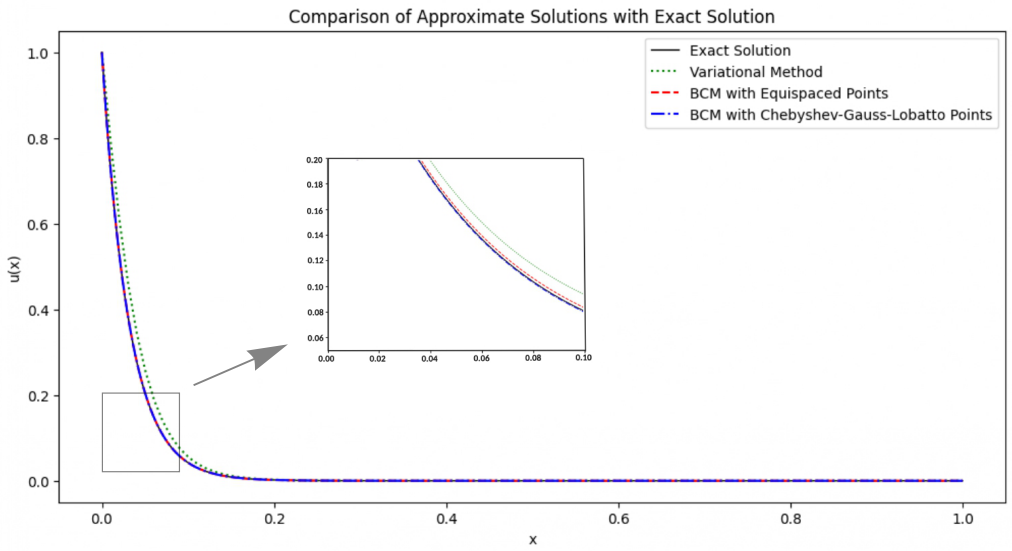

Figure 2.6: Comparison of exact solution with approximate solution for $\varepsilon = 0.001$ and $N = 32$ Example 2.5.3

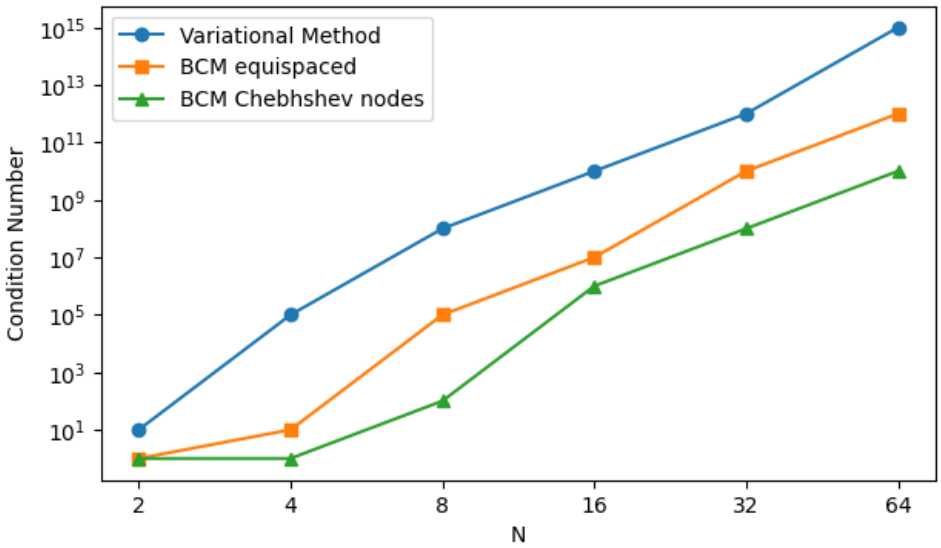

Figure 2.7: Condition number for different value of N for Example 2.5.3.

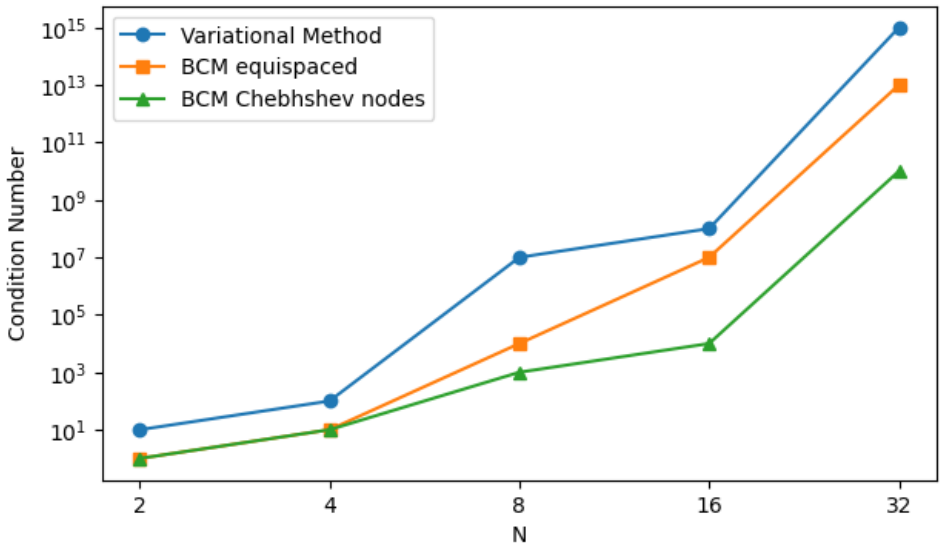

Figure 2.8: Condition number for different value of N for Example 2.5.4.

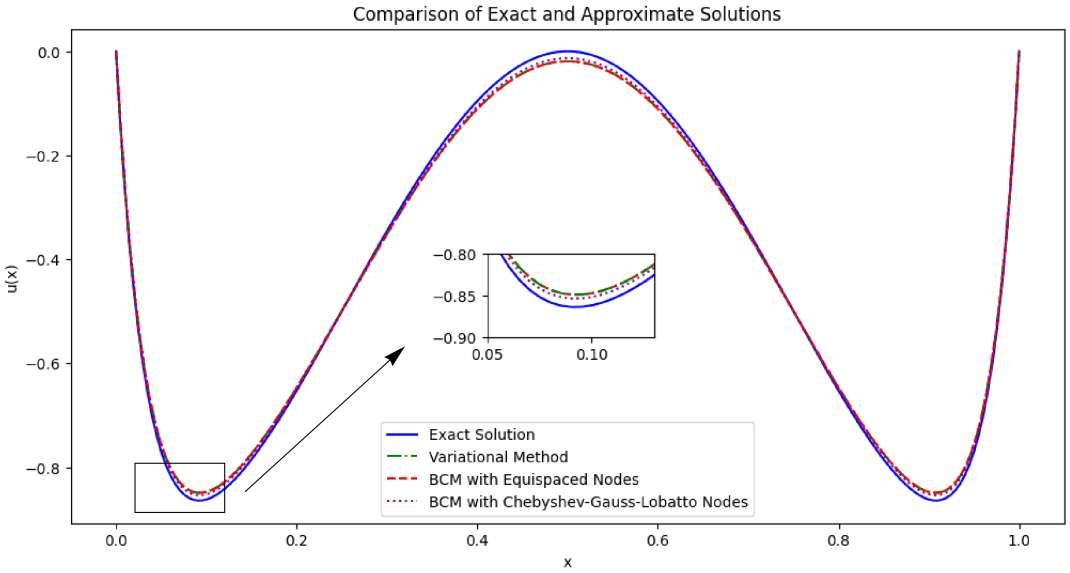

Figure 2.9: Comparison of exact solution with approximate solution for $\varepsilon = 0.001$ and $N = 32$ for Example 2.5.4.

Root Mean Square error for Example 2.5.3

ε	$N = 16$	$N = 32$	$N = 64$
0.1	VM = 1.23146e-03 ES = 2.34308e-12 CN = 5.55654e-14	VM = 9.93328e-04 ES = 2.38603e-10 CN = 6.21164e-11	VM = 8.954013e-04 ES = 8.204405e-04 CN = 1.869762e-09
0.01	VM = 1.76000e-08 ES = 3.64733e-08 CN = 3.81823e-10	VM = 1.93027e-07 ES = 7.69033e-12 CN = 1.05052e-11	VM = 5.410542e-08 ES = 8.738543e-06 CN = 1.831973e-10
0.001	VM = 3.08690e-05 ES = 1.17525e-03 CN = 4.31797e-10	VM = 7.43776e-11 ES = 1.68184e-09 CN = 9.60304e-14	VM = 2.966897e-06 ES = 1.076134e-08 CN = 8.446761e-12
0.0001	VM = 5.42590e-03 ES = 3.37515e-02 CN = 8.19378e-05	VM = 1.06784e-05 ES = 2.08333e-03 CN = 3.38126e-06	VM = 1.400651e-04 ES = 2.399477e-05 CN = 2.167820e-06
1e-05	VM = 2.19997e-01 ES = 6.32235e-02 CN = 3.32439e-02	VM = 4.93369e-03 ES = 2.20110e-02 CN = 2.64540e-03	VM = 2.588136e-04 ES = 3.567295e-03 CN = 4.259700e-05

Table 2.6: Root Mean Square Error for different values of ε using methods for $N = 16, 32, 64$ for Example 2.5.3.

2.6 Conclusion

In this chapter, different methods for solving singularly perturbed differential equations were compared. These equations are characterized by their steep gradients and boundary layers. The Bernstein collocation method (BCM) using both evenly spaced and Chebyshev nodes, alongside the variational method, were the focal points of this comparison. Various types of equations, both linear and nonlinear, were included in the tests. Generally, Quasilinearization technique was used to linearize the non linear equation. Instead of this, BCM method directly converts the nonlinear equation into system of equation.

The results shows that BCM with Chebyshev nodes are more effective than when using equispaced nodes or the variational method. Calculated error tables shows the lower RMSE and maximum error at BCM with chebyshev nodes, especially when perturbation paramter ε becomes smaller. And BCM with chebyshev nodes exhibits smaller condition number which shows this is well conditioned.

In conclusion, the application of Chebyshev nodes in BCM represents a robust approach for accurately solving differential equations. Compared to alternative nodal distributions and conventional variational techniques, the Bernstein collocation method incorporating Chebyshev-Gauss-Lobatto nodes provides notable

Maximum error for Example 2.5.4

ε	$N = 16$	$N = 32$	$N = 64$
0.1	VM = 1.308038e+00 ES = 3.791951e-04 CN = 3.591951e-09	VM = 1.357994e+00 ES = 3.791951e-01 CN = 3.821765e-02	VM = 1.373948e+00 ES = 3.791920e-01 CN = 3.791951e-01
0.01	VM = 1.003223e+00 ES = 9.772697e-02 CN = 9.211698e-05	VM = 1.043844e+00 ES = 9.772698e-02 CN = 8.371421e-03	VM = 1.056817e+00 ES = 9.771244e-02 CN = 9.772698e-02
0.001	VM = 9.526521e-01 ES = 1.325215e-02 CN = 1.294389e-03	VM = 9.897203e-01 ES = 1.293846e-02 CN = 2.125832e-03	VM = 1.001458e+00 ES = 1.433917e-02 CN = 1.698852e-03
0.0001	VM = 9.420876e-01 ES = 2.199610e-01 CN = 1.441857e-02	VM = 9.842365e-01 ES = 2.320124e-02 CN = 1.339782e-03	VM = 9.963909e-01 ES = 1.334713e-02 CN = 1.339636e-03
1e-05	VM = 9.298811e-01 ES = 5.217184e-01 CN = 1.550446e-01	VM = 9.771065e-01 ES = 2.221473e-01 CN = 9.771761e-03	VM = 9.953340e-01 ES = 3.656593e-02 CN = 4.184092e-04

Table 2.7: Maximum Error for different values of ε using methods for $N = 16, 32, 64$ for Example 2.5.4.

Root Mean Square error for Example 2.5.4

ε	$N = 16$	$N = 32$	$N = 64$
0.1	VM = 8.335144e-01 ES = 2.153870e-01 CN = 2.153870e-02	VM = 8.701415e-01 ES = 2.153870e-01 CN = 1.243370e-01	VM = 8.818507e-01 ES = 2.153840e-01 CN = 1.153870e-02
0.01	VM = 6.120033e-01 ES = 5.373098e-02 CN = 5.133028e-02	VM = 6.437250e-01 ES = 5.373097e-02 CN = 3.143037e-02	VM = 6.539100e-01 ES = 5.381575e-02 CN = 3.273097e-02
0.001	VM = 5.716206e-01 ES = 8.953939e-03 CN = 8.246211e-03	VM = 6.011957e-01 ES = 8.246578e-03 CN = 5.135607e-03	VM = 6.107631e-01 ES = 8.287782e-03 CN = 5.126577e-03
0.0001	VM = 5.677016e-01 ES = 4.668220e-02 CN = 8.713072e-03	VM = 5.967715e-01 ES = 3.980828e-03 CN = 9.142636e-04	VM = 6.062166e-01 ES = 9.139604e-04 CN = 3.142636e-04
1e-05	VM = 5.679366e-01 ES = 8.810849e-02 CN = 3.889673e-02	VM = 5.963914e-01 ES = 3.213089e-02 CN = 2.945052e-03	VM = 6.057624e-01 ES = 5.122987e-03 CN = 2.564636e-04

Table 2.8: Root Mean Square Error for different values of ε using methods for $N = 16, 32, 64$ for Example 2.5.4.

advantages in terms of accuracy, stability, and efficiency for solving singularly perturbed differential equations. The method's ability to address the steep boundary layers typical of these complex problems is enhanced by the optimum clustering of the Chebyshev-Gauss-Lobatto nodes.This study has great importance for the progression of numerical analysis in the future and provides a useful resource for

experts requiring accurate modelling and problem-solving methods. It was also mentioned that there is need for more research to increase the effectiveness and range of applications of this strategy.

Chapter 3

Numerical Solution of Singularly Perturbed Equations using Szász-Mirakyan-Kantorovich Operator

This chapter introduces an numerical technique for solving singularly perturbed differential equations using Szász-Mirakyan-Kantorovich (SMK) operators. The solution of such kind of problems shows boundary and interior layers due to presence of small parameter ε. Additionally, the suggested problem's convergence analysis is done using the maximum norm. Linear and nonlinear problems have been considered, and a comparison study with other current methods has been conducted to demonstrate the effectiveness of the SMK method. The approximated result from the proposed technique (SMK) appears to be better than the existing approach. The numerical results consistently showcase the SMK method's outperformance of traditional techniques.

3.1 Introduction

In applied research and engineering, singularly perturbed boundary value problems are common; reaction-diffusion equations and covection equations are two well-known examples [122, 123]. Convection-diffusion processes are often studied in environmental engineering, chemical engineering, fluid dynamics, and heat transfer. These formulae are crucial for understanding these processes. Singular perturbations in these situations frequently result in boundary layers, which puts numerical techniques' accuracy and resilience to the test. One of the main objectives of singular perturbation analysis is to build asymptotic approximations that, for any given parameter value, faithfully reflect the real solution [124, 125]. It is difficult to solve these issues numerically using standard techniques because the perturbation parameters may make uniform convergence impossible. Boundary layer existence is the primary reason of this [126]. The most basic mathematical representation of a convection-diffusion issue is a boundary value problem with two points is given in Equation 2.1. Convection is represented by the word u', while the roles of a source and driving term, respectively, are played by u and f. Diffusion and convection should be modeled using second-order and first-order derivatives, respectively.

Because they have so many beneficial properties, Bernstein polynomials are very helpful in computer-aided geometric design [127, 128] and many other areas of mathematics. In the discipline of computer-aided design (CAD), free-form objects are constructed using mathematical methods. It was founded a little later than computer-aided engineering (CAE). In actuality, computer-aided design, or CAD [129], is the use of technology to geometric model and drawing creation, modification, analysis, and optimization. The first method for producing free-form curves and surfaces was the Bézier curve, named for its inventor, Dr. Pierre Bézier. This method was developed in 1966 by Bézier, an engineer for the car company Renault. Many publications have focused on these operators. In this regard, Bernstein's seminal work on Bernstein polynomials maintains its long-standing leadership in approximation theory. Shortly after, literature has started to often extend it to an indefinite interval [121]. The Szász-Mirakyan operators (sometimes called "Mirakian" and "Mirakjan") [150] are extensions of Bernstein polynomials to infinite intervals, first introduced by Otto Szász in 1950 and G. M.

Mirakjan in 1941.. Numerous methods have been proposed in the literature to improve Szász-Mirakyan operators [151], and it has been demonstrated that these new operators have approximation features that are comparable to those of their classical counterparts. In addition to approximating a function, Szász-Mirakyan operators can be used to solve differential and integral equations and compute numerical integration, also known as the quadrature formula and evenly spaced mesh to approximate improper integrals. Motivated by Maleknejad et al. [152], we present a numerical technique in this work based on the Szász-Mirakyan approximation method to solve the linear and nonlinear singularly perturbed differential equations.

3.2 Definitions

3.2.1 Szasz Mirakyan operator

In the field of approximation theory, the Szász-Mirakyan operators serve as a generalization of Bernstein polynomials applicable to infinite intervals. These operators were introduced by mathematicians Otto Szász in 1950 and G. M. Mirakjan in 1941. The Szasz-Mirakyan operator is defined as [121]:

$$S_{n,k}(x) = (S_n f)(x) = \sum_{k=0}^{\infty} e^{-nx} \frac{(nx)^k}{k!} f\left(\frac{k}{n}\right). \tag{3.1}$$

In this article, partial szasz-Mirakyan operator is used and for $m \in z^+$, it is defined as

$$(S_n f)(x) = \sum_{k=0}^{mn} p_{n,k}(x) f\left(\frac{k}{n}\right), \tag{3.2}$$

where $x \in [0, \infty) \subset$ R and $n \in$ N and

$$p_{n,k}(x) = e^{-nx} \frac{(nx)^k}{k!}. \tag{3.3}$$

Some properties of szasz operator are :

1. **Positivity:** $p_{n,k}(x)$ is non-negative within the interval $[0, \infty]$.
2. **Continuous:** $p_{n,k}(x)$ is continuous function on $[0, \infty]$.
3. **Partition of unity:** The sum of szasz polynomials of degree n is 1 for every

$x \in [0, \infty]$.

4. **Linearity:** $S_n(\alpha f + \beta g; x) = \alpha S_n(f; x) + \beta S_n(g; x)$

5. **Convergence:** $\lim_{n\to\infty} S_n(f; x) = f(x)$.

The moments of the Szasz-Mirakyan operator [141] are obtained by applying the operator to the monomials $f(t) = t^m$ for $m = 0, 1, 2, 3, \ldots$.

Zeroth Moment

For $f(t) = 1 = e_0$:

$$S_n(1; x) = \sum_{k=0}^{\infty} 1 \cdot e^{-(nx)} \frac{(nx)^k}{k!} = e^{-(nx)} \sum_{k=0}^{\infty} \frac{(nx)^k}{k!} = e^{-(nx)} \cdot e^x = 1.$$

So, the zeroth moment is $S_n(e_0, x) = 1$.

First Moment

For $f(t) = t = e_1$:

$$S_n(t; x) = \sum_{k=0}^{\infty} \left(\frac{k}{n}\right) e^{-(nx)} \frac{(nx)^k}{k!} = \frac{1}{n} \sum_{k=0}^{\infty} k e^{-(nx)} \frac{(nx)^k}{k!}.$$

The series $\sum_{k=0}^{\infty} k e^{-(nx)} \frac{(nx)^k}{k!}$ can be simplified by recognizing it as the mean of the Poisson distribution with parameter x, which is nx:

$$\sum_{k=0}^{\infty} k e^{-(nx)} \frac{(nx)^k}{k!} = nx.$$

Thus,

$$S_n(t; x) = x.$$

So, the first moment is $S_n(e_1, x) = x$.

Summary of Moments

$$S_n(e_0, x) = 1, \tag{3.4}$$
$$S_n(e_1, x) = \frac{x}{n}, \tag{3.5}$$
$$S_n(e_2, x) = \frac{x}{n} + x^2, \tag{3.6}$$
$$S_n(e_3, x) = \frac{x}{n^2} + \frac{3x^2}{n} + x^3. \tag{3.7}$$
$$\tag{3.8}$$

where e_0, e_1, e_2, e_3 are $1, x, x^2, x^3$, respectively. Derivative of szasz polynomial is given as :

First Derivative $S_n'(f;x)$

Differentiating the Szasz-Mirakyan operator with respect to x:

$$S_n'(f;x) = \frac{d}{dx}\left(\sum_{k=0}^{\infty} f\left(\frac{k}{n}\right) e^{-nx}\frac{(nx)^k}{k!}\right).$$

Applying the product rule:

$$S_n'(f;x) = \sum_{k=0}^{\infty} f\left(\frac{k}{n}\right)\left(\frac{d}{dx}\left(e^{-nx}\frac{(nx)^k}{k!}\right)\right),$$

The derivative of $e^{-nx}\frac{(nx)^k}{k!}$ is:

$$\frac{d}{dx}\left(e^{-nx}\frac{(nx)^k}{k!}\right) = e^{-nx}\left(\frac{k(nx)^{k-1}.n}{k!} - \frac{n(nx)^k}{k!}\right) = e^{-nx}\frac{n(nx)^{k-1}}{(k-1)!} - e^{-nx}\frac{n(nx)^k}{k!},$$

Thus,

$$S_n'(f;x) = \sum_{k=0}^{\infty} f\left(\frac{k}{n}\right)\left(e^{-nx}\frac{n(nx)^{k-1}}{(k-1)!} - e^{-nx}\frac{n(nx)^k}{k!}\right),$$

Separate the sums:

$$S_n'(f;x) = \sum_{k=0}^{\infty} f\left(\frac{k}{n}\right) e^{-nx} \frac{n(nx)^{k-1}}{(k-1)!} - \sum_{k=0}^{\infty} f\left(\frac{k}{n}\right) e^{-nx} \frac{n(nx)^k}{k!},$$

Adjust the indices in the first sum ($k \to k+1$), then we get

$$S_n'(f;x) = n[S_{n,k-1} - S_{n,k}]. \tag{3.9}$$

Second Derivative $S_n''(f;x)$

To find the second derivative, differentiate $S_n'(f;x)$:

$$S_n''(f;x) = \frac{d}{dx}\left(n \sum_{k=0}^{\infty} f\left(\frac{k+1}{n}\right) e^{-nx} \frac{(nx)^k}{k!} - nS_n(f;x)\right),$$

Differentiate each term separately and implify the derivatives:

$$S_n''(f;x) = \sum_{k=0}^{\infty} f\left(\frac{k+1}{n}\right) n^2 \left(e^{-nx} \frac{(nx)^{k-1}}{(k-1)!} - e^{-nx} \frac{(nx)^k}{k!}\right) - nS_n'(f;x),$$

Adjust the indices in the first sum ($k \to k+1$):

$$S_n''(f;x) = \sum_{k=1}^{\infty} f\left(\frac{k+1}{n}\right) n^2 e^{-nx} \frac{(nx)^{k-1}}{(k-1)!} - \sum_{k=0}^{\infty} f\left(\frac{k+1}{n}\right) n^2 e^{-nx} \frac{(nx)^k}{k!} - nS_n'(f;x),$$

$$S_n''(f;x) = \sum_{k=0}^{\infty} f\left(\frac{k+2}{n}\right) n^2 e^{-nx} \frac{(nx)^k}{k!} - \sum_{k=0}^{\infty} f\left(\frac{k+1}{n}\right) n^2 e^{-nx} \frac{(nx)^k}{k!} - nS_n'(f;x),$$

$$S_n''(f;x) = n^2 \left[S_{n,k-2} - 2S_{n,k-1} + S_{n,k}\right]. \tag{3.10}$$

Remark: SMK can be derived from Bernstein polynomial.

A Bernstein polynomial of degree n is defined for $k = 0, 1, 2, ..., n$ as :

$$B_{k,n}(x) = \binom{n}{k} x^k (1-x)^{n-k}, \tag{3.11}$$

$$B_{k,n}(x) = \binom{n}{k} \left(\frac{x}{1-x}\right)^k (1-x)^n, \tag{3.12}$$

$$= \frac{n(n-1)...(n-k+1)}{k!} \frac{x^k}{(1-x)^k} (1-x)^n, \tag{3.13}$$

$$= e^{-nx} \frac{(nx)^k}{k!}. \tag{3.14}$$

3.3 Methodology

Let us consider a second order singularly perturbed differential equation given in 2.1. The main goal of the proposed approach is to use szasz operator given in 3.1 to estimate the unknown function u(·). So, for this consider an approximate solution given as:

$$u(x) = \sum_{k=0}^{mn} e^{-nx} \frac{(nx)^k}{k!} u\left(\frac{k}{n}\right), \tag{3.15}$$

Substitute the approximate solution into the given SPDE 2.1,for $x \in (a, b)$, we get,

$$\sum_{0}^{mn} u\left(\frac{k}{n}\right) \left[-\varepsilon n^2 (S_{n,k-2} - 2S_{n,k-1} + S_{n,k}) + h(x) * n(S_{n,k-1} - S_{n,k}) + k(x) S_{n,k}\right] = f(x), \tag{3.16}$$

For the collocation points $x_j = \frac{j}{n-1}$, above equation give rise to algebraic system which helps in finding the unknown coefficients.

$$Ux = F, \tag{3.17}$$

where

$$U = \left[-\varepsilon n^2 (S_{n,k-2} - 2S_{n,k-1} + S_{n,k}) + h(x) * n(S_{n,k-1} - S_{n,k}) + k(x) S_{n,k}\right],$$

$$F = [f(x_0), f(x_1), ..., f(x_{mn})]^\top, \quad x = [u(0), u(1/n), ..., u(m)]^\top.$$

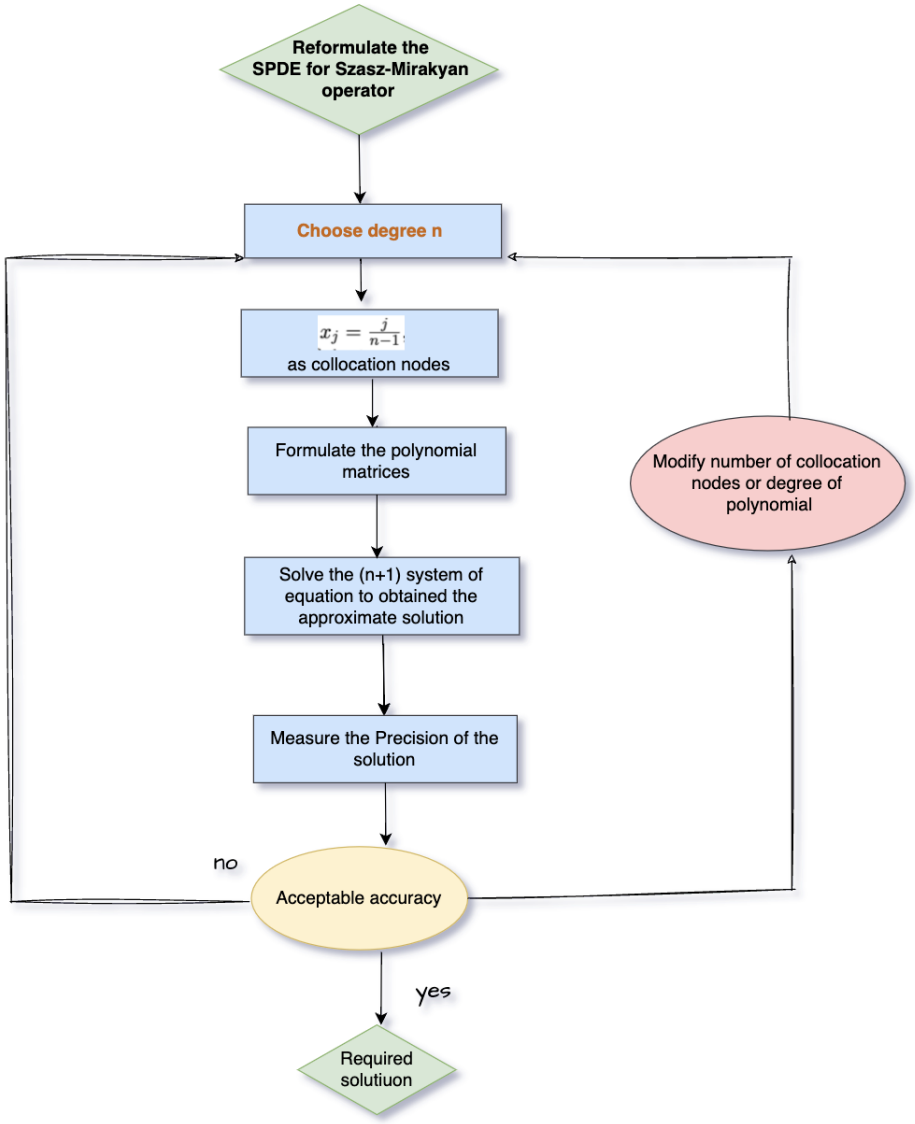

Figure 3.1: Schematic diagram for Szasz operator

here U is $mn \times mn$ matrix of unknown values and F and x are $mn \times 1$ vectors. F is the vector formed by the right-hand side $f(x_i)$ at the discretized points. Hence, the first row and column as well as last row and column are replaced with the imposed boundary conditions. And solving this system of equation, the unknown vector x is determined which can be used to construct approximate solution 3.15

3.3.1 Condition Number

57

The condition number of a matrix or a mathematical problem quantifies the sensitivity of the solution to changes or errors in the input data. It essentially measures how much the output value can change in response to slight alterations in the input. A high condition number indicates that the problem is ill-conditioned,

meaning small input changes can cause large changes in the output, potentially leading to numerical instability. Conversely, a low condition number suggests the problem is well-conditioned, with the output being relatively stable against input variations.

Lemma: Let S_n be the Szasz-Mirakyan operator used to approximate the solution, and A be the matrix derived from the discretization of the differential equation using the operator. If

$$\max_{x\in[a,b]}\left(-\varepsilon n^2\left|\sum_{k=0}^{\infty}(S_{n,k-2}-2S_{n,k-1}+S_{n,k})\right|+\left|h(x)*n\sum_{k=0}^{\infty}(S_{n,k-1}-S_{n,k})\right|+\left|k(x)\sum_{k=0}^{\infty}S_{n,k}\right|\right)=C_1, \tag{3.18}$$

$||\cdot||$ denoted the maximum norm of rows, and I be the identity matrix, then:

$$\text{cond}(A)\leq\frac{C_1}{1-C_2},$$

such that $||A-I||=C_2<1$.

Proof:

To prove the above condition, we have to find an upper bound of cond(U). So, the condition number is defined as

$$cond(U)=||U||\,||U^{-1}||, \tag{3.19}$$

Therefore, we have find the bounds for both $||U||$ and $||U^{-1}||$.

Hence, U is defined in Equation 3.17.

$$U=\left[-\varepsilon n^2(S_{n,k-2}-2S_{n,k-1}+S_{n,k})+h(x)*n(S_{n,k-1}-S_{n,k})+k(x)S_{n,k}\right],$$

Let $||.||$ is the maximum norm of rows, therefore,

$$||U||=\max_i\sum_{k=0}^{mm}\left|-\varepsilon n^2(S_{n,k-2}-2S_{n,k-1}+S_{n,k})+h(x_i)*n(S_{n,k-1}-S_{n,k})+k(x_i)S_{n,k}\right|,$$

Given the bounds on the coefficients $h(x_i)$ and $k(x_i)$, and the Szasz-Mirakyan

operator's exponential terms, we have:

$$||U|| \leq C_1,$$

where C_1 is derived from the i coefficients and the operator terms.

Consider $\Theta = U - I$:

$$||\Theta|| = \max_i \sum_j |U_{ij} - I_{ij}|,$$

If Θ is small enough, we have:

$$||\Theta|| = C_2 < 1,$$

Using the norm, the condition number of U is:

$$||U^{-1}|| \leq \frac{1}{1 - ||\Theta||} = \frac{1}{1 - C_2},$$

Thus, combining the norms:

$$\text{cond}(U) = ||U||\,||U^{-1}|| \leq \frac{C_1}{1 - C_2}.$$

3.4 Error Analysis

Lemma 1: Consider

$$M_s(x) = \sum_{k=0}^{\infty} p_{n,k}(x)(k - nx)^s, \text{ for } s = 0, 1, 2, 3, 4. \tag{3.20}$$

Then the following holds: $M_0(x) = 1$, $M_1(x) = 0$, $M_2(x) = nx$, $M_3(x) = nx$, $M_4(x) = 3n^2x^2$.

Proof: These results can be easily obatined using binomial expansion of $(k-nx)^s$ for $s = 0, 1, .., 4$ and using 3.4.

Lemma 2: For $x \in [0, \infty]$ and suppose δ be small positive number and η be some constant, then the following inequality holds for $\left|\frac{k}{n} - x\right| \geq \delta$:

$$\sum_{k=0}^{\infty} p_{n,k}(x) \leq \frac{\eta x^2}{n^2\delta^2}, \tag{3.21}$$

η is independent of x and n.

Proof: For some arbitrary constant η and using Lemma 1, we have $|M_4(x)| \geq Nn^2x^2$. We have,

$$\left|\frac{k}{n} - x\right| \geq \delta,$$

$$\implies \frac{(k-nx)^4}{n^4\delta^4} \geq 1,$$

for $\left|\frac{k}{n} - x\right| \geq \delta$ and δ is choosen to be very small such that $\delta > 0$ and we have

$$\sum_{k=0}^{\infty} p_{n,k}(x) \leq \frac{1}{n^4\delta^4} \sum_{k=0}^{\infty} p_{n,k}(k-nx)^4 = \frac{1}{n^4\delta^4} M_4(x) \leq \frac{\eta x^2}{n^2\delta^2}.$$

hence proved.

Theorem 5. Let $\mathbf{F}$ be a bounded and continuous on every finite interval then , we have the following error bound

$$\|S_{n,k}(\mathbf{F}) - \mathbf{F}\| \leq \frac{1}{2n} x \|\mathbf{F"}\| \tag{3.22}$$

at fixed point $x > 0$, for which $\mathbf{F}$ is twice differentiable.

Proof: [153]

Using Taylor's expansion,

$$\mathbf{F}(t) - \mathbf{F}(x) = (t-x), \tag{3.23}$$

$$\mathbf{F}(t) - \mathbf{F}(x) = (t-x)\mathbf{F}'(x) + \frac{1}{2}(t-x)^2\mathbf{F}''(x) + \lambda(t-x)(t-x)^2,$$

where $\lambda(z)$ converges to zero with z. Then choose $t = \frac{k}{n}$, we have

$$n\sum_{k=0}^{\infty} p_{n,k}\left[\mathbf{F}\left(\frac{k}{n}\right) - \mathbf{F}(x)\right] = n\sum_{k=0}^{\infty} p_{n,k}\left[\left(\frac{k}{n} - x\right)\mathbf{F}'(x)\right] + \frac{1}{2}n\sum_{k=0}^{\infty} p_{n,k}\left[\left(\frac{k}{n} - x\right)^2\mathbf{F}''(x)\right]$$
$$+n\sum_{k=0}^{\infty} p_{n,k}\left[\lambda\left(\frac{k}{n} - x\right)\left(\frac{k}{n} - x\right)^2\right],$$

$$n\left[S_{n,k}(\mathbf{F};x)-f(x)\right]=T_1(x)\mathbf{F}'(x)+\frac{1}{2n}M_2(x)\mathbf{F}''(x)+n\sum_{k=0}^{\infty}p_{n,k}\lambda\left(\frac{k}{n}-x\right)\left(\frac{k}{n}-x\right)^2,$$

$$n\left[S_{n,k}(\mathbf{F};x)-\mathbf{F}(x)\right]=\frac{x}{2}\mathbf{F}''(x)+n\Lambda_n(x),$$

where

$$\Lambda_n(x)=\sum_{k=0}^{\infty}p_{n,k}\lambda\left(\frac{k}{n}-x\right)\left(\frac{k}{n}-x\right)^2.$$

Now we have to show that

$$lim_{n\to\infty}n\Lambda_n(x)=0. \tag{3.24}$$

$$\Lambda_n(x)=\sum_{\left|\frac{k}{n}-x\right|\le n}p_{n,k}(x)\lambda\left(\frac{k}{n}-x\right)\left(\frac{k}{n}-x\right)^2 \tag{3.25}$$

$$+\sum_{\left|\frac{k}{n}-x\right|\ge n}p_{n,k}(x)\lambda\left(\frac{k}{n}-x\right)\left(\frac{k}{n}-x\right)^2, \tag{3.26}$$

$$=:\Lambda_{n,1}(x)+\Lambda_{n,2}(x). \tag{3.27}$$

According to Lemma 2, we have

$$|\Lambda_{n,1}(x)|\le\frac{\epsilon}{n^2}M_2(x)=\frac{\epsilon}{n^2}(nx),$$

since ϵ is arbitrary, therefore,

$$\lim_{n\to\infty}n\Lambda_{n,1}(x)=0,$$

Now, for $\Lambda_{n,2}(x)$ using Lemma 2, we have

$$|\Lambda_{n,2}(x)|\le\frac{1}{n^2\delta^2}KNx^2,$$

where $K=\sup_{t\in(0,\infty)}\lambda(t-x)(t-x)^2$, which similarly gives,

$$\lim_{n\to\infty} n\Lambda_{n,2}(x) = 0,$$

Theorem 6. If $u(x)$ is sufficiently smooth on $[0, A]$ for $A > 0$ and Let $u(x)$ be the exact solution of 2.1 and S_n is the Szasz-Mirakyan kontorowich operator of degree n then the szasz solution at equispaced nodes converges to $u(x)$.

Proof: We know that the difference of $S_n(u, x)$ and $u(x)$ is

$$S_n(u, x) - u(x) = \sum_{k=0}^{n} \left(u\left(\frac{k}{n}\right) S_{k,n}(x) - u(x) \right), \tag{3.28}$$

Using the relation 3.4, in the following equation, we have

$$S_n(u, x) - u(x) = \sum_{k=0}^{n} \left(u\left(\frac{k}{n}\right) - u(x) \right) S_{k,n}(x), \tag{3.29}$$

so

$$|S_n(u, x) - u(x)| \leq \sum_{k=0}^{n} \left| u\left(\frac{k}{n}\right) - u(x) \right| S_{k,n}(x). \tag{3.30}$$

For $\delta_1 > 0$ and $x \in [0, A]$, divide the set of equispaced nodes into two sets

$$B = \{x_i : 0 \leq |x_i - x| < \delta_1\},$$
$$C = \{x_i : \delta_1 \leq |x_i - x| < A\}.$$

where

$$x_i = \frac{i}{n - i}; \quad i = 0, 1, \ldots, n;$$

B and C gives the nodes at boundary layers, thus the series on the right-hand side of the inequality can be divided into two series given as :

$$|S_n(u, x) - u(x)| \leq \sum_{\substack{i=0 \\ (x_i \in B)}}^{n} |u(x_i) - u(x)| S_{k,n}(x) + \sum_{\substack{i=0 \\ (x_i \in C)}}^{n} |u(x_i) - u(x)| S_{k,n}(x), \tag{3.31}$$

$$|S_n(u, x) - u(x)| \leq \Lambda_1(x_i \in B) + \Lambda_2(x_i \in C). \tag{3.32}$$

For the case Λ_1,

By the uniform convergence of the sequence of polynomials, we have, for any

$\xi > 0, \exists$ **N** $> N$ such that for all $n \geq$ **N** and $x \in [0, A]$, we have

$$|u(x_i) - u(x)| < \frac{\xi}{2(1+A)} \leq \frac{\xi}{2}. \tag{3.33}$$

Now, for the case Λ_2, $|x_i - x| < A$, this is trivial and we have $|x_i - x| \geq \delta_1$, therefore,

$$1 \leq \frac{(x_i - x)^2}{\delta_1^2},$$

Let $|u(x)| \leq M$ and $x_i \in C$ we have,

$$\sum_{i=0}^{n} |u(x_i) - u(x)| S_{k,n}(x) \leq \frac{1}{\delta^2} \sum_{i=0}^{n} (x_i - x)^2 |u(x_i) - u(x)| S_{k,n}(x),$$

where $(x_i - x)^2 = \left(\frac{i}{n-i} - x\right)^2$ and using Weierstrass approximation theorem and relations 3.4 and theorem 5 above equation becomes:

$$\sum_{\substack{i=0 \\ (x_i \in B)}}^{n} |u(x_i) - u(x)| S_{k,n}(x) < \frac{2M}{4\eta\delta^2},$$

collecting the estimates of 3.32

$$|S_n(u,x) - u(x)| < \frac{\xi}{2} + \frac{M}{2\eta\delta^2}, \tag{3.34}$$

For a positive real number $\xi > 0$, there exists a number $N(\xi)$ such that for all $\eta \geq N(\xi)$, choose η to be so large that $\frac{M}{2\eta\delta^2} < \xi$ then

$$|S_n(u,x) - u(x)| < \xi. \tag{3.35}$$

Hence Proved.

3.5 Numerical Results

Example 3.5.1. The 1D linear convection-diffusion equation is a fundamental mathematical model used to describe the transport of a scalar quantity, such as heat, pollutants, or other substances, within a fluid medium. This type of equation combines both convection, the process by which a substance is carried by the bulk motion of the fluid, and diffusion, the process by which a substance spreads due to

molecular motion.

The equation under consideration is [147]

$$-\varepsilon u'' - 2u' = 0; \quad x \in (0,1), \quad 0 < \varepsilon \ll 1,$$

with boundary conditions

$$u(0) = 1 \quad and \quad u(1) = 0;$$

In this equation, ε represents the diffusion coefficient, which is a small positive parameter $(0 < \varepsilon << 1)$. Such problems are characterized by the presence of boundary layers, regions near the boundary where the solution changes rapidly.

The exact solution is

$$u = \frac{\exp(-2x/\varepsilon) - \exp(-2/\varepsilon)}{1 - \exp(-2/\varepsilon)}.$$

This solution highlights the sharp gradients near the boundaries, which are typical in singularly perturbed problems. The presence of the exponential term with the small parameter ε in the denominator indicates a rapid decay away from the boundary at $x = 0$. Convection-diffusion equations are widely used in various scientific and engineering fields.

ε	$N = 16$	$N = 32$	$N = 64$
0.01	1.052445e-05	1.463111e-08	3.922933e-10
0.001	7.263651e-05	6.143491e-08	4.193816e-09
0.0001	8.576937e-05	7.398075e-08	5.558218e-07
0.00001	8.647634e-05	7.498012e-07	5.608763e-05
0.000001	8.631970e-02	7.505850e-03	5.541958e-03

Table 3.1: Maximum Error Table for Example 3.5.1

The results showcase that as the parameter epsilon is reduced and the number of collocation points is increased, the numerical solution converges towards the exact solution, with the maximum error decreasing. This convergence behavior is indicative of the method's ability to produce highly accurate approximations. Furthermore,

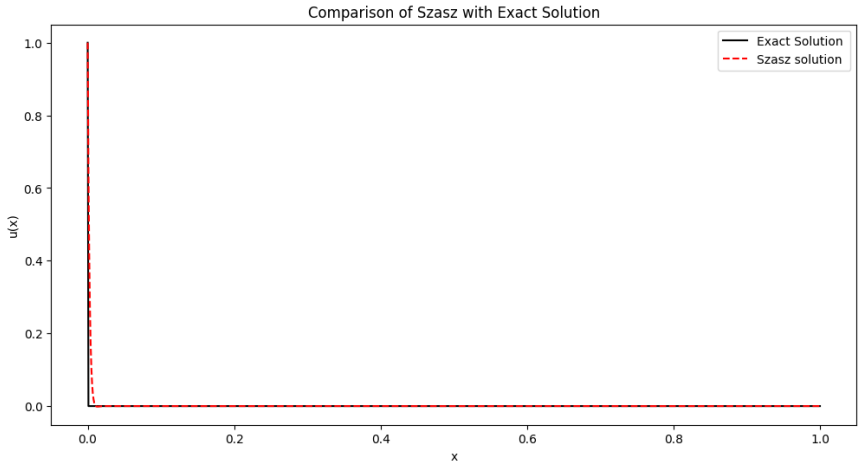

Figure 3.2: Comparison of exact and szasz solution for $N = 90$ and $\varepsilon = 0.000001$ for Example 3.5.1

for each ε, doubling the number of collocation points leads to a significant reduction in the error measures, often by an order of magnitude. This rapid convergence allows the method to achieve impressive accuracy even with a moderate number of collocation points, especially when epsilon is sufficiently small. This system shows the lower condition number which shows that this is well-conditioned. Comparison of exact and Szasz Mirakyan solution is shown in Figure 3.2 and Maximum error is given in Table 3.1.

Example 3.5.2. The given nonlinear singularly perturbed differential equation is a significant model that finds applications in various scientific and engineering disciplines. It is formulated as *[149]:*

$$\begin{cases} -\varepsilon v'' + v + v^2 = e^{-\frac{2x}{\sqrt{\varepsilon}}} \\ v(0) = 1, \quad v(1) = e^{-\frac{1}{\sqrt{\varepsilon}}}. \end{cases} \tag{3.36}$$

The equation combines a second-order differential term, a linear term, and a nonlinear term. The right-hand side, introduces a forcing function that decays rapidly as x increases, which is typical for singularly perturbed problems.

The exact solution,

$$v(x) = e^{-\frac{x}{\sqrt{\varepsilon}}}. \tag{3.37}$$

demonstrates the exponential decay characteristic of such problems. The rapid change near $x = 0$ is indicative of a boundary layer, a common feature in singularly perturbed differential equations.

The numerical results demonstrate that the Szasz method converges to the exact

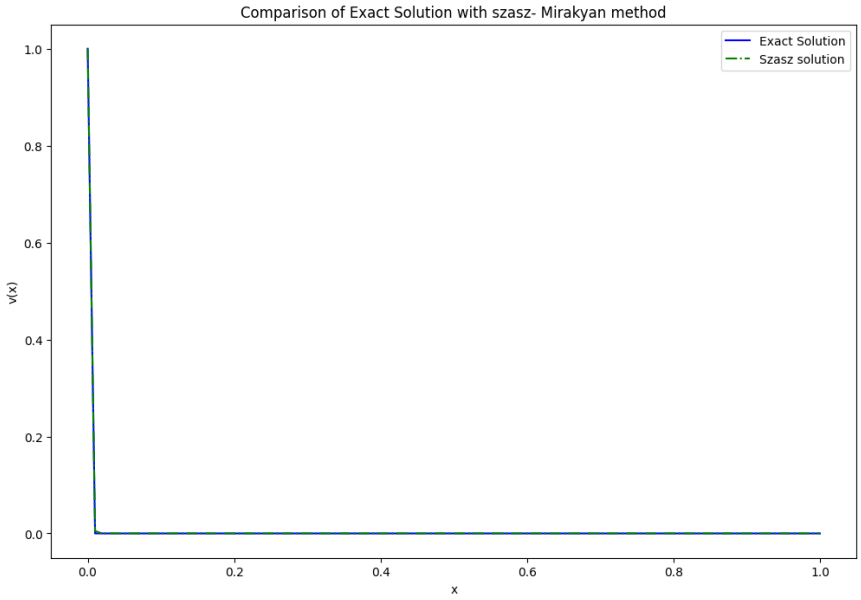

Figure 3.3: Comparison of exact and szasz solution for $N = 90$ and $\varepsilon = 0.000001$ for Example 3.5.2

Maximum error comparison of Szasz-mirakyan solution with spline method in [154].

ε	$N = 16$	$N = 32$	$N = 64$
2^{-4}	2.210537e-04 Method in [154] = 0.39e-02	3.284709e-07 Method in [154] = 0.11e-02	5.635503e-08 Method in [154] = 0.43e-03
2^{-6}	8.416083e-04 Method in [154] = 0.73e-02	9.836043e-07 Method in [154] = 0.23e-02	2.045248e-06 Method in [154] = 0.14e+01
2^{-8}	9.806342e-05 Method in [154] = 0.12e-01	2.305398e-05 Method in [154] = 0.32e-02	4.478301e-05 Method in [154] = 0.14e+01
2^{-10}	1.045478e-03 Method in [154] = 0.11e-01	5.028301e-05 Method in [154] = 0.30e-01	3.136047e-03 Method in [154] = 0.16e+01

Table 3.2: Maximum error table for Example 3.5.2

solution of the singularly perturbed differential equation as both the perturbation parameter epsilon decreases and the number of collocation points N increases. The maximum error consistently decreases for smaller values of epsilon and larger values of N. The approach is effective for obtaining accurate numerical solutions for non-linear singularly perturbed differential equations also. Comparison of exact solution and szasz mirakyan solution is shown in Figure 3.3 and maximum error obtained using szasz method is compared with Spline method [154] as shown in Table 3.2.

Example 3.5.3. The study of singularly perturbed differential equations, particularly those involving both convective and diffusive processes, is essential for modeling various physical phenomena. One such equation is:

$$\epsilon u'' + (1 + x(1-x))u = f(x), \tag{3.38}$$

$$u(0) = 0, \quad u(1) = 0, \tag{3.39}$$

includes a second-order derivative term scaled by the small parameter ε, which represents the diffusion process. The term $(1 + x(1-x))u$ introduces a variable coefficient that modifies the effect of convection depending on the position x. The forcing function $f(x)$ combines polynomial and exponential terms, reflecting the complex external influences on the system.

where

$$f(x) = \left\{ \left[1 + x(1-x) + [2\sqrt{\epsilon} - x^2(1-x)]\, e^{-(1-x)/\sqrt{\epsilon}}\right] + [2\sqrt{\epsilon} - x(1-x^2)]\, e^{-x/\sqrt{\epsilon}} \right. \tag{3.40}$$

The exact solution is

$$u(x) = 1 + (x-1)e^{-x/\sqrt{\epsilon}} - xe^{-(1-x)/\sqrt{\epsilon}}. \tag{3.41}$$

demonstrates the interplay between boundary layers and the internal behavior of the solution. The presence of exponential terms indicates sharp changes near the boundaries, typical for singularly perturbed problems.

Comparison of exact solution with Szasz Mirakyan method is shown in Figure 3.4 and Table 3.3 shows the maximum error obtained using szasz method is less than B-spline method in [155] which shows that proposed method performs better and SMK exhibit lower condition number as compared to B-Spline as shown in Figure 3.5.

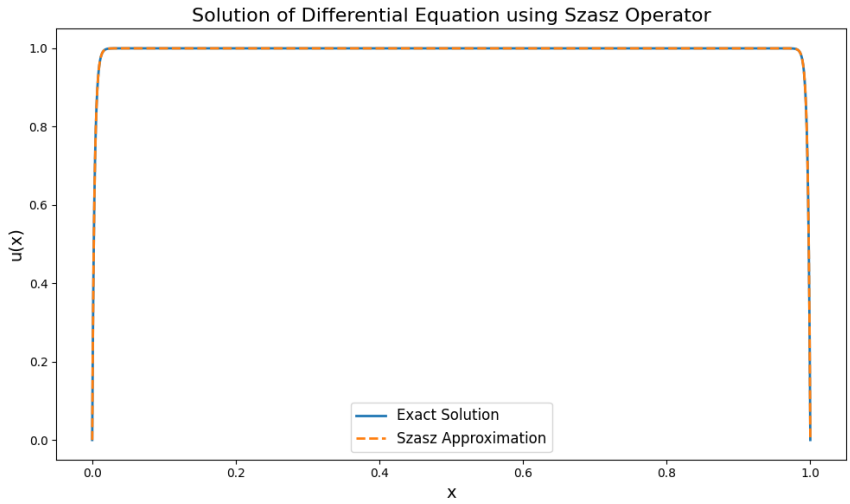

Figure 3.4: Comparison of exact and szasz solution for N = 70 and $\varepsilon = 0.00001$ for Example 3.5.3

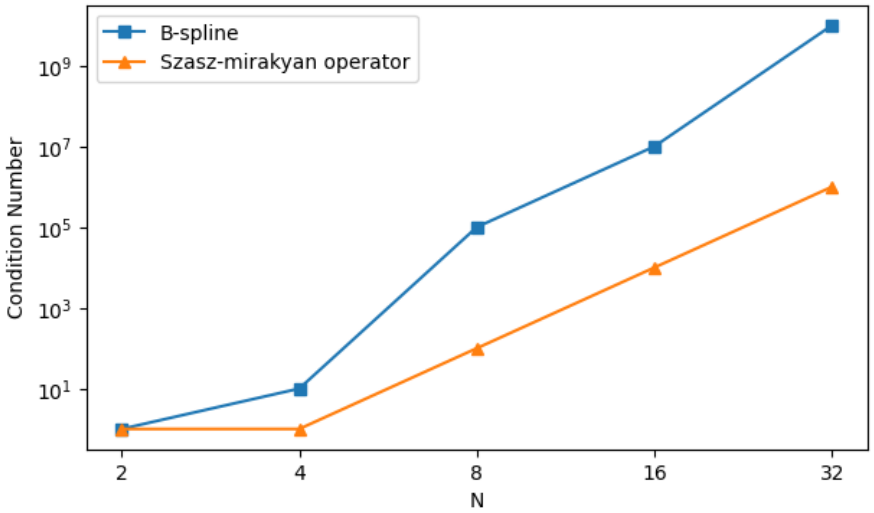

Figure 3.5: Condition number for $\varepsilon = 0.01$ for Example 3.5.3

Maximum error comparison of Szasz-mirakyan solution with B-spline method in [155].

ε	$N = 16$	$N = 32$	$N = 64$
2^{-4}	1.897323e-06	1.00321e-07	0.331502e-09
	Method in [155] = 2.000e-03	Method in [155] = 4.908e-04	Method in [155] = 1.2225e-04
2^{-6}	4.7433084e-05	1.89614e-06	1.042240e-08
	Method in [155] = 5.101e-03	Method in [155] = 1.302e-03	Method in [155] = 3.137e-04
2^{-8}	1.185827e-05	6.105294e-05	3.178204e-06
	Method in [155] = 1.950e-02	Method in [155] = 5.210e-03	Method in [155] = 1.120e-03
2^{-10}	0.045178e-05	1.048502e-04	1.036244e-05
	Method in [155] = 4.891e-02	Method in [155] = 2.012e-02	Method in [155] = 4.2129e-03

Table 3.3: Maximum error for Example 3.5.3

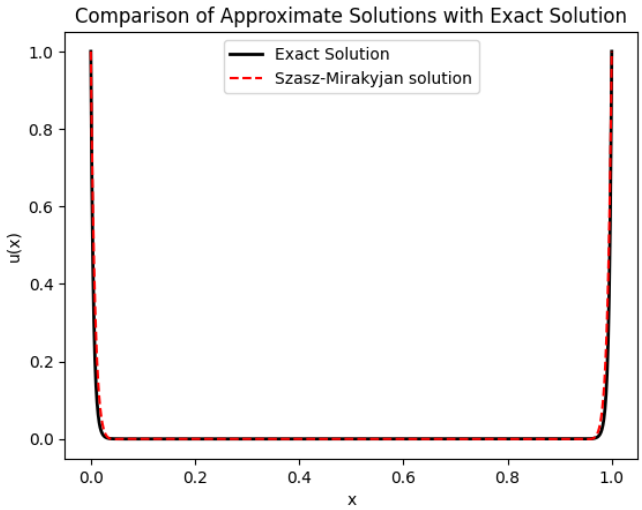

Figure 3.6: Comparison of exact solution with approximate solution for $\varepsilon = 0.001$ and $N = 32$ for 3.5.4.

Example 3.5.4. *We consider 1D linear convection–diffusion problem with turning point as*

$$-\varepsilon u'' + 2(2x-1)u' + 4u = 0; \quad x \in (0,1), \quad 0 < \varepsilon \ll 1, \tag{3.42}$$

with boundary conditions.

$$u(0) = 1 \quad \textit{and} \quad u(1) = 1; \tag{3.43}$$

Above equation is characterized by a balance between the diffusive term $-\varepsilon u''$ and the convective term $2(2x-1)u'$, with an additional linear term $4u$. The presence of the turning point at $x = 0.5$ means that the direction of the convection changes within the domain, leading to unique solution behavior. The exact solution is

$$u = \exp\left(\frac{-2x(1-x)}{\varepsilon}\right). \tag{3.44}$$

Epsilon	$N = 16$	$N = 32$	$N = 64$
0.01	1.234456e-03	3.086140e-08	7.715350e-10
0.001	1.234456e-05	3.086140e-09	7.715350e-07
0.0001	1.234456e-07	3.086140e-07	7.715350e-06
0.00001	1.234456e-06	3.086140e-07	7.715350e-06
0.000001	1.234456e-04	3.086140e-05	7.715350e-04

Table 3.4: Maximum Error Table for Example 3.5.4

Comparison of exact solution with Szasz Mirakyan method is shown in Figure 3.6 and Table 3.4 shows the maximum error obtained using szasz method.

3.6 Conclusion

In this chapter research, a novel methodology based on the Szász-Mirakyan approximation was developed and evaluated for obtaining solutions to linear and nonlinear singularly perturbed differential equations. When solving nonlinear problems, a quasi-linearization approach is frequently used to linearize the problem. The linearized problem is then solved using numerical methods or other currently used techniques. In SMK method, we find the solution of nonlinear problems without using linearization. The suggested approach transforms nonlinear problems into an system of algebraic equation, making it simple to use. Furthermore, this study derived error bound estimates for the proposed approach. And SMK method exhibit lower condition number which that system is well conditioned. The results from computational experiments indicate that the new method yields solutions with a high degree of precision. The outcomes of this investigation could have several significant consequences for subsequent applications and research endeavors in this domain.

Chapter 4

Bernstein-Chlodowsky for Solving Singularly Perturbed Differential Equations in Atmospheric Modeling and Cyclone Dynamics

---

This chapter presents a novel framework combining the Bernstein-Chlodowsky operator with neural networks termed as Bernstein-Chlodowsky Neural Network (BNN) and Bernstein-Chlodowsky collocation method (CCM) for solving singularly perturbed differential equations (SPDEs) in the context of atmospheric science and cyclone modeling. In atmospheric and climatic systems, SPDEs play a crucial role in capturing multiscale dynamics, especially in phenomena that involve boundary layers and sharp gradients. These equations pose significant computational challenges due to the presence of a small perturbation parameter ε, which causes rapid transitions near boundaries. We solve linear and nonlinear SPDEs using the Bernstein-Chlodowsky collocation method and BNN, emphasizing how well these methods captures the convection-dominated processes observed in cyclonic systems. The operator's superior convergence and boundary layer resolution make it an effective tool for cyclone modeling. Numerical simulations demonstrate that BNN significantly outperforms traditional methods including Bernstein collocation and spline based approaches by achieving lower error and better resolution across a range of SPDEs relevant to convection, diffu-

sion, and atmospheric boundary layers. Numerical simulations demonstrate that CCM and BNN methods provides a more accurate representation of cyclone dynamics compared to traditional techniques, significantly improving the predictive capability of weather models.

4.1 Introduction

Singularly Perturbed Differential Equations (SPDEs) [122, 123] are fundamental to modeling complex multiscale dynamics in atmospheric and climate systems. These equations often involve a small perturbation parameter,ε, multiplying the highest derivative, which creates sharp gradients and thin boundary layers [124]. Such behaviour is frequently observed in weather systems, particularly in cyclones [156], where large-scale convective processes interact with small-scale diffusion and turbulence. The presence of boundary layers in these systems reflects the rapid changes in physical quantities, such as temperature, pressure, and wind velocity, particularly near the core of a cyclone. Resolving these layers accurately is crucial for predicting the intensity, trajectory, and development of such weather phenomena. In the context of cyclone dynamics, the interaction between convection and diffusion processes can be effectively described by SPDEs, as the convective transport of momentum, heat, and moisture dominates over diffusive processes in these systems. The convection-diffusion equation, which is a type of SPDE, models the transport of these quantities in the atmosphere. However, due to the presence of small ε, traditional numerical methods often fail to capture the steep gradients near the boundary, resulting in poor approximations and loss of accuracy, especially when predicting extreme weather events such as cyclones. The most basic mathematical representation of a convection-diffusion equations [126] is a boundary value problem, such as in Equation 2.1.

To address this challenge, we introduce the Bernstein-Chlodowsky [157] operator as a numerical method capable of solving SPDEs with superior accuracy, particularly in regions where boundary layers are prominent. A cornerstone of the development of approximation theory is the first Weierstrass approximation theorem, established by K. Weierstrass in 1885 [158]. The original proof of Weierstrass was known for its complexity and length, which made it challenging to understand. Consequently, the mathematical community sought a simpler and more accessible proof. In 1937, I. Cholodovsky (Cholodovsky, 1937) provided a more detailed proof for the Weierstrass theorem by introducing the Bernstein-Cholodovsky operators [157], which generalize the Bernstein polynomials to approximate the function f defined on $[0, 1]$. The Bernstein-Chlodowsky operator extends the classical Bernstein polynomial method, offering enhanced convergence

properties and better handling of sharp transitions. Unlike traditional methods that struggle with high gradients, this operator efficiently approximates the solution over the entire domain, making it particularly useful for convection-dominated problems seen in atmospheric science.

Cyclones [159], which are driven by both large-scale atmospheric circulation and small-scale turbulent eddies, represent an ideal test case for the application of SPDEs. The dynamics of a cyclone, characterized by rapid variations near its center (the eye of the storm), require precise numerical techniques to capture the changes in wind speed, pressure, and temperature. In this work, we solve various linear and nonlinear SPDEs using the Bernstein-Chlodowsky operator and demonstrate its effectiveness in modeling cyclone-related processes [160]. Through a series of numerical experiments, we show that this method significantly outperforms existing approaches, such as spline methods and B-spline collocation, particularly in the resolution of boundary layers.

The main goal is to close the gap between sophisticated mathematical models and real-world atmospheric scientific applications [161]. Through our demonstration of the usefulness of the Bernstein-Chlodowsky operator in solving SPDEs, we want to improve numerical weather models' predictive power, especially when it comes to cyclone behavior and intensity forecasts. The findings give a framework for enhancing weather forecast accuracy and comprehending large-scale atmospheric phenomena, which will help us learn more about how cyclones originate and about atmospheric modeling in general.

Recently, deep learning techniques, particularly Physics-Informed Neural Networks (PINNs), have shown promise in solving PDEs. However, for singularly perturbed problems, conventional neural networks fail to capture boundary layers efficiently. To address this, we propose a hybrid framework: the Bernstein-Chlodowsky Neural Network (BNN), which integrates Bernstein-Chlodowsky spectral polynomials with neural network architectures. This fusion enhances convergence and solution accuracy, particularly in stiff regions such as boundary layers and turning points.

4.2 Brief Sketch of the Method

In atmospheric science, particularly in the study of cyclones, Bernstein polynomials offer a powerful tool for solving the differential equations that describe complex, multiscale phenomena. By improving the accuracy and efficiency of numerical solutions, they enable better cyclone intensity forecasts, boundary layer modeling, and real-time weather prediction, playing a crucial role in advancing atmospheric research and operational meteorology.

4.2.1 Bernstein polynomials

For a function $f(x)$ defined on the closed interval $[0,1]$, the expression

$$(B_n f)(x) = B_n f(x) = \sum_{k=0}^{n} f\left(\frac{k}{n}\right)\binom{n}{k} x^k (1-x)^{n-k} \tag{4.1}$$

is referred to as the Bernstein polynomial of order n of the function $f(x)$ (Bernstein, 1912; see also G.G. Lorentz, 1986) [162].

Differentiating 4.1 , it can be obtained that

$$(B_n f)'(x) = \sum_{k=0}^{n} f\left(\frac{k}{n}\right)\binom{n}{k} \{kx^{k-1}(1-x)^{n-k} - (n-k)x^k(1-x)^{n-k-1}\}$$

Therefore, $(B_n f)'(x)$ can be written as,

$$(B_n f)'(x) = \sum_{k=0}^{n} f\left(\frac{k}{n}\right)\frac{(k-nx)}{x(1-x)} t_{k,n}(x). \tag{4.2}$$

Bernstein polynomials were originally defined on $[0,1]$. By substitution, the interval $[a,b]$ can be easily transformed into $[0,1]$. Bernstein polynomials did not present any issues on bounded intervals for proving the Weierstrass approximation theorem [163]. The primary question arises for mathematicians was Bernstein polynomials for unbounded interval. In 1937, Cholodovsky addressed this question as follows:

Assume $f(x)$ be a function defined on the interval $[0, b]$. To find $B_n f(x)$ for $(0, b)$, define the Bernstein polynomial of $Q(w)$, for $0 \leq w \leq 1$, as:

$$B_n Q(w) = \sum_{k=0}^{n} Q\left(\frac{k}{n}\right) \binom{n}{k} w^k (1-w)^{n-k}$$

Substitute $w = \frac{x}{b}$ in the polynomial $B_n Q(w)$. It is then easy to see that $Q(w) = f(bw)$, for $0 \leq w \leq 1$. Therefore,

$$B_n f(x) = \sum_{k=0}^{n} f\left(\frac{bk}{n}\right) \binom{n}{k} \left(\frac{x}{b}\right)^k \left(1 - \frac{x}{b}\right)^{n-k}$$

for a constant b and $b = b_n$ is a function of n.

Let's consider the function $f(x)$ which is defined on $[0, \infty)$. To establish the relation

$$B_n f(x) \to f(x)$$

it is essential to recognize that the spacing between consecutive points $\frac{b_n}{n} \to 0$ as $n \to \infty$. This implies that $b_n = o(n)$.

As demonstrated above, Cholodovsky extended Bernstein polynomials from the interval $[0, 1]$ to $[0, \infty)$. Consequently, the polynomials introduced by Cholodovsky are referred to as Bernstein-Chlodowsky polynomials. Thus, Bernstein-Chlodowsky polynomials can be defined as follows:

4.2.2 Bernstein-Chlodowsky polynomials

Bernstein-Chlodowsky polynomials [164] are given by

$$(C_n f)(x) = \sum_{k=0}^{n} f\left(\frac{b_n k}{n}\right) t_{k,n}\left(\frac{x}{b_n}\right)$$

where f is a function defined on $[0, \infty)$ and bounded on every finite interval $[0, b] \subset [0, \infty)$ at a certain rate, with $t_{k,n}$ denoting as usual

$$t_{k,n}(x) = \binom{n}{k} x^k (1-x)^{n-k}, \quad 0 \leq x \leq 1$$

and $(b_n)_{n=1}^{\infty}$ being a positive increasing sequence of real numbers with the prop-

erties

$$\lim_{n\to\infty} b_n = \infty, \quad \lim_{n\to\infty} \frac{b_n}{n} = 0.$$

(Cholodovsky, 1937; see also Karsli, 2011).

Chlodovsky introduce this polynomial which is the generalization of the Bernstein polynomial $b_n = 1$ and $n \in \mathbb{N}_0$, which is defined on the interval $[0, 1]$.

In fact, if $M(b; f) := \sup_{0\le x\le b} |f|$, then Cholodovsky shows that

$$\lim_{n\to\infty} \exp\left(-\alpha\frac{n}{b_n}\right)(b_n; f) = 0$$

for every $\alpha > 0$, then $(C_n f)(x)$ converge to $f(x)$ at each point of continuity.

Also, he shows that if $f \in C[0, \infty)$ has order $f(x) = O(\exp x^s)$ for any $s > 0$, also $\{b_n\}$ be the sequence which satisfies

$$b_n \le n^{\frac{1}{s+\gamma+1}}, \tag{4.3}$$

where $\gamma > 0$, irrespective of how small it is, then $C_n f(x)$ converges to $f(x)$ at each point in $\mathbb{R}^+$.

Cholodovsky further demonstrated the simultaneous convergence of the derivative $(C_n f)'(x)$ to $f'(x)$ at points x where it exists, a result that was further examined by Butzer.

Differentiation the fundamental representations for $(C_n f)'(x)$:

$$(C_n f)'(x) = \frac{n}{b_n}\sum_{k=0}^{n-1}\left[f\left(\frac{k+1}{n}b_n\right) - f\left(\frac{k}{n}b_n\right)\right] t_{k,n-1}\left(\frac{x}{b_n}\right) \tag{4.4}$$

$$= \frac{1}{x(b_n - x)}\sum_{k=0}^{n} f\left(\frac{k}{n}b_n\right)(kb_n - nx)t_{k,n}\left(\frac{x}{b_n}\right) \tag{4.5}$$

After introducing Bernstein-Chlodowsky polynomials, Cholodovsky proved the Weierstrass approximation theorem using these polynomials. Some moments of bernstein chlodowsky operator is given in Lemma 2.1.

Lemma 2.1 *For* $(C_n r^i)(x)$, $i = 0, 1, 2, 3, 4, 5$, *one has for* $0 \leq x \leq b_n$

$$(C_n 1)(x) = 1$$

$$(C_n r)(x) = x$$

$$(C_n r^2)(x) = x^2 + \frac{x(b_n - x)}{n}$$

$$(C_n r^3)(x) = x^3\left[\frac{n^2 - 3n + 2}{n^2}\right] + x^2\left[\frac{3b_n(n-1)}{n^2}\right] + x\frac{b_n^2}{n^2}$$

$$(C_n r^4)(x) = x^4\left[\frac{n^3 - 6n^2 + 11n - 6}{n^3}\right] + x^3\left[\frac{6b_n(n^2 - 3n + 2)}{n^3}\right] + x^2\left[\frac{7b_n^2(n-1)}{n^3}\right] + x\frac{b_n^3}{n^3}$$

$$(C_n r^5)(x) = x^5\left[\frac{n^4 - 10n^3 + 35n^2 - 50n + 24}{n^4}\right] + x^4\left[\frac{10b_n(n^3 - 6n^2 + 11n - 6)}{n^4}\right] + x^3\left[\frac{25b_n^2(n^2 - 3n + 2)}{n^4}\right] + x^2\left[\frac{15b_n^3(n-1)}{n^4}\right] + x\frac{b_n^4}{n^4}$$

4.2.3 The Bernstein-Chlodowsky Operator in Atmospheric Modeling

Let us consider a second order singularly perturbed differential equation given in 2.1. The main goal of the proposed approach is to use Chlodowsky operator given in 4.2.2 to estimate the unknown function u(·). In this article, partial Bernstein-chlodowsky operator is used and for $m \in z^+$, it is defined as so, for this consider an approximate solution given as:

$$u(x) = \sum_{k=0}^{mn} t_{k,n}\left(\frac{x}{b_n}\right) \tag{4.6}$$

Substitute the approximate solution into the given SPDE 2.1. For the collocation points $x_j = \frac{j}{n-1}$, above equation give rise to algebraic system which helps in finding the unknown coefficients.

$$Ux = F$$

Hence, the first row and column as well as last row and column are replaced with the imposed boundary conditions. And solving this system of equation, the unknown vector x is determined which can be used to construct approximate so-

lution 4.6. The schematic diagram for Bernstein Chlodowsky collocation method is shown in Figure 4.1.

The Bernstein-Chlodowsky operator has proven to be a robust tool for solving singularly perturbed differential equations (SPDEs), especially in cases where sharp transitions and boundary layers are prevalent in the solution. These features frequently appear in atmospheric models, such as those involving cyclones, weather fronts, and boundary layer processes. Accurately resolving these steep gradients in temperature, wind speed, and pressure is critical for forecasting the intensity and path of storms, particularly cyclones.

1. **Resolving Boundary Layers and Sharp Gradients:**

   Cyclones are defined by the interaction between convective and diffusive dynamics, leading to sudden variations, especially around the cyclone's center and within the eye wall. Traditional computational methods like finite difference and finite element techniques often face challenges in accurately capturing these swift changes due to numerical dissipation, which tends to smooth out sharp transitions. This often leads to underestimations of the cyclone's strength and errors in tracking its path.

   By allocating computing resources more efficiently in regions exhibiting sudden fluctuations, the Bernstein-Chlodowsky operator performs very well in handling these challenges. Because of the way it is designed, it can simulate the thin boundary layers that are closest to cyclone centers, where convective activity predominates. The accuracy of cyclone models is greatly increased by this feature, particularly when predicting the storm's route and intensity.

   In contrast to techniques like spline or B-spline collocation, which usually need dense grid arrangements close to borders in order to maintain accuracy, the Bernstein-Chlodowsky operator produces results that are comparable or superior while requiring less computing effort.

2. **Benefits for Weather Prediction Models:**

   Accurately modeling the atmospheric boundary layer (ABL), where surface-atmosphere interactions are critical, is a significant challenge in weather

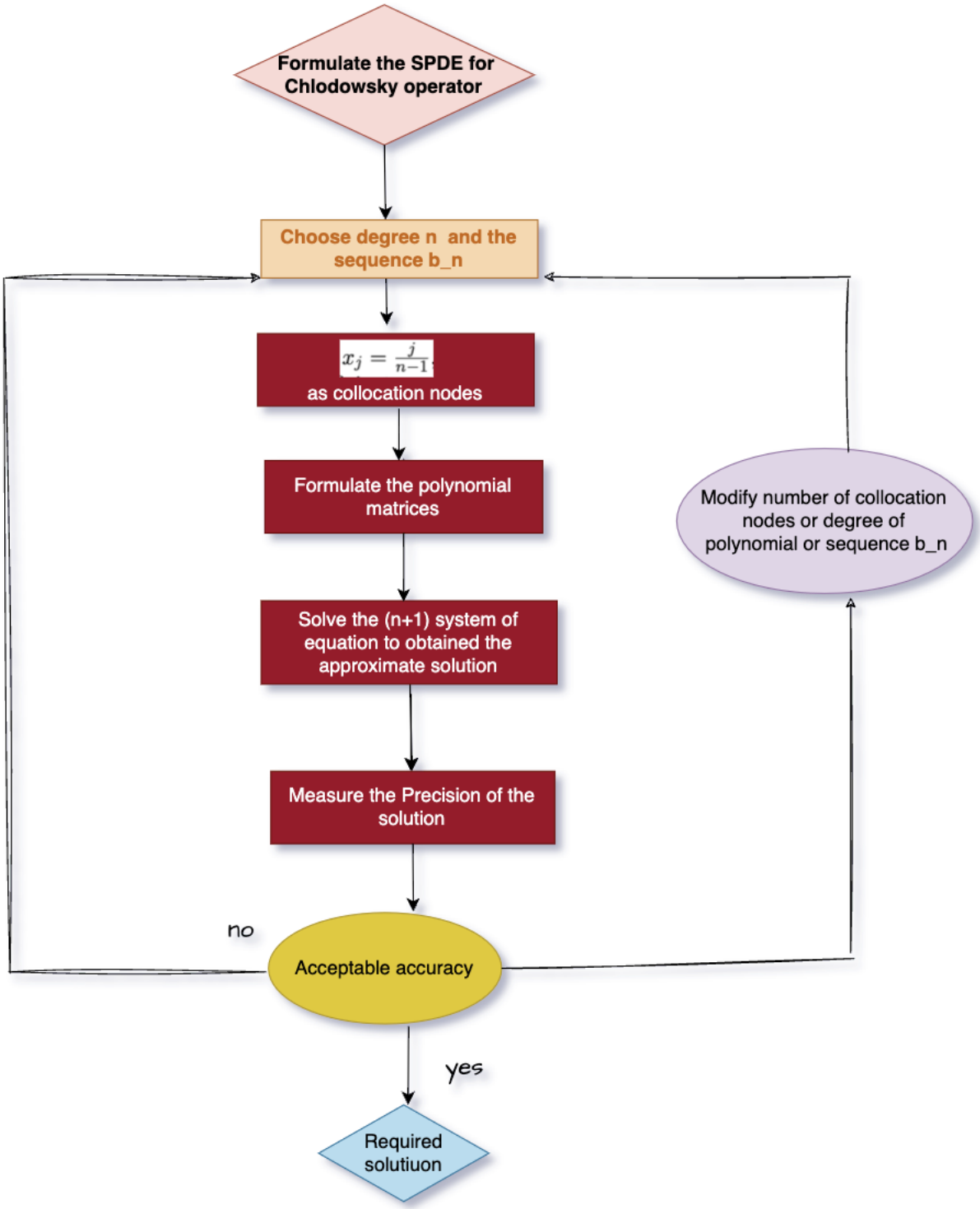

Figure 4.1: Schematic diagram for Bernstein Chlodowsky collocation method.

prediction models. Understanding the genesis of storms and cyclones depends on the ability to anticipate surface winds, temperature fluctuations, cloud formation, and precipitation through accurate modeling of the ABL.

Conventional methods frequently struggle to handle the sudden changes in the ABL without appreciably raising the computing burden. But by effectively handling these abrupt changes, the Bernstein-Chlodowsky operator provides a notable enhancement that increases the accuracy of short-term weather forecasts. This is especially important for cyclone strengthening forecasts, where an accurate representation of the lower atmospheric strata is crucial.

3. **Limitations of Traditional Numerical Methods:**

   Even though they are well-liked for their simplicity, traditional numerical techniques like finite difference schemes frequently suffer from numerical dissipation when used to convection-dominated systems like cyclones. Important boundary layers tend to be smoothed out by this dissipation, which might result in inaccurate storm path predictions and underestimations of cyclone intensity. In boundary layer regions, even techniques employing higher-order polynomials—which are often better at handling gradients—usually need extremely tiny meshing, significantly increasing processing requirements without improving precision.

These problems are lessened by the Bernstein-Chlodowsky operator, which provides constant precision across the domain even in regions with sharp gradients. When the resolution is most needed, such in the boundary layers of cyclonic systems, it adjusts to the solution, improving it there. The Bernstein-Chlodowsky operator is especially well-suited for real-time weather forecasting applications as a result, producing simulations that are more accurate and effective. The primary benefits of this method are as follows: (i) It offers an approximate solution across the entire domain, unlike other numerical methods that provide solutions only at discrete points within the domain. (ii) For nonlinear problems, traditional approaches often involve quasi-linearization to convert the problem into a linear one, which is then solved using numerical or other existing techniques. This linearization can reduce the accuracy of the solution for the nonlinear problem, sometimes resulting in misleading outcomes. In contrast, this method addresses

nonlinear problems directly without the need for linearization. (iii) Additionally, it is straightforward to implement.

4.2.4 Bernstein Chlodowsky Neural Network

The numerical solution of boundary value problems (BVPs), particularly those involving singular perturbations, has been a subject of extensive research due to the challenges associated with resolving steep gradients and boundary layers. Classical approaches such as finite difference, finite element, and collocation methods often require dense mesh refinement near boundaries or asymptotic analysis to obtain accurate results for small perturbation parameters $\varepsilon < 1$.
In recent years, neural network-based methods, especially Physics-Informed Neural Networks (PINNs), have emerged as a promising mesh-free alternative to traditional solvers. These methods approximate the solution to a differential equation by training a neural network to minimize a residual loss derived from the governing equations and boundary conditions.

However, applying PINNs to singularly perturbed boundary value problems (SPBVPs) introduces specific challenges:

- The presence of sharp boundary layers leads to difficulties in network convergence and stability,
- Standard neural architectures struggle to capture stiff features without excessive network depth or adaptive sampling,
- Uniform residual-based losses are often insensitive to critical regions of the domain.

To address these limitations, we propose a novel Bernstein-Chlodowsky Neural Network (BNN) framework tailored for solving SPBVPs. This approach integrates:

- An analytically informed boundary layer component to capture stiff behavior,

- A spectral polynomial basis (Bernstein-Chlodowsky polynomials) for efficient representation,

- BNN handles both linear and nonlinear SPDEs without the need for linearization, making it suitable for complex atmospheric phenomena, including cyclone modeling and pollutant dispersion.

- Unlike conventional methods, which often require very fine meshes near boundary layers, BNN efficiently allocates computational resources to the most critical regions, thereby reducing the computational burden.

The method maintains the flexibility of PINNs while embedding problem-specific structure to improve stability, convergence, and accuracy in resolving singular perturbations. This subsection presents the proposed Bernstein Chlodowsky Neural Network(BNN) framework for solving singulaly perturbed differential equations. The first few Bernstein Chlodowsky polynomials with $b_n = 1.5$ and $n = 3$ are

$$
\begin{aligned}
C_{0,3}^{(1.5)}(x) &= \left(1 - \frac{x}{1.5}\right)^3 \\
C_{1,3}^{(1.5)}(x) &= 3 \cdot \frac{x}{1.5} \cdot \left(1 - \frac{x}{1.5}\right)^2 \\
C_{2,3}^{(1.5)}(x) &= 3 \cdot \left(\frac{x}{1.5}\right)^2 \cdot \left(1 - \frac{x}{1.5}\right) \\
C_{3,3}^{(1.5)}(x) &= \left(\frac{x}{1.5}\right)^3
\end{aligned}
$$

Consider a vector $x = (x_1, x_2, ..., x_h)$ of dimension h. Consider a second order singularly perturbed differential equation given in 2.1. and to accurately approximate the solution and enforce boundary conditions, we design the trial solution $\tilde{u}(x)$ as

$$\tilde{u}(x) = u_b(x) + \left(1 - \frac{u_b - \alpha}{\beta - \alpha}\right).R(x)$$

where u_b is boundary layer function that captures the exponential behavior near boundaries, and $R(x)$ is a trainable residual function responsible for refining the solution across the domain. The function $R(x)$ is expressed as a combination of

spectral basis functions and a neural correction:

$$R(x) = \sum_{k=0}^{N} c_k C_n f(x) + x(1-x).NN(x)$$

This structure consist of randomly choosen non-uniform chebyshev nodal points in $[0, 1]$ in input layer and a functional expansion block based on Bernstein chlodowsky polynomials. Three hidden layers were taken and output from hidden layers were then passes through exponential layer. The loss function is determined by substituting the neural network solution into governing equation and boundary condition resulting in two terms L_D and L_{BC}. The BNN is trained by minimizing a physics-informed loss function:

$$L = L_D + L_{BC}$$

where residual loss is :

$$L_D = \frac{1}{N_c} \sum w(x_i) \left[-\varepsilon u''(x_i) + h(x_i)u'(x_i)g(x_i)u(x_i) - f(x_i)\right]^2$$

and boundary condition loss is given as

$$L_{BC} = (u(0) - \alpha)^2 + (u(1) - \beta)^2$$

The BNN is trained by minimizing this total loss function, which simultaneously adjusts the neural network corrections and the polynomial coefficients to optimize the solution's accuracy.

The BNN method inherits the analytical strength of Bernstein-Chlodowsky approximation while leveraging data-driven residual learning to fine-tune local behavior. Unlike standard PINNs, BNN captures localized sharp gradients effectively using spectral expansion and boundary-aware loss terms. This makes it well-suited for SPDEs in atmospheric science.

4.3 Existence and uniqueness

Consider first the class of singulalry perturbed differential problem, so, the equation 2.1 can be rewritten as:

$$\varepsilon u''(x) = \mathcal{L}(x, u(x), u'(x)), \quad x \in (a, b), \tag{4.7}$$

$$u(a) = \alpha$$

$$u(b) = \beta$$

here, ϵ is small perturbation parameter and where $\mathcal{L}$ is a continuous function on $[a, b] \times \mathbb{R}^2$. Nagumo's differential inequality approach observes that if there exist smooth functions $h(x)$ and $g(x)$ satisfies the following properties:

$$h(x) \leq g(x),$$

$$\begin{aligned} & \epsilon h'' \geq \mathcal{L}(x, h, h') \quad \text{and} \quad \epsilon g'' \leq \mathcal{L}(x, g, g'), \\ \Longrightarrow \quad & -\epsilon h'' + \mathcal{L}(x, h, h') \leq 0 \quad \text{and} \quad -\epsilon g'' + \mathcal{L}(x, g, g') \geq 0, \\ & h(a) \leq \alpha \leq g(a), \quad h(b) \leq \beta \leq g(b), \end{aligned} \tag{4.8}$$

therefore, $u = u(x)$ of class $C^{(2)}([a, b])$ be the solution of the problem 4.7 such that

$$h(x) \leq u(x) \leq g(x) \text{ for } \quad x \in [a, b] \tag{4.9}$$

Assuming that $\mathcal{L}$ does not increase too rapidly as a function of u'. More precisely, it is adequate to stipulate that $\mathcal{L}$ meets a generalized Nagumo condition in relation to $h(x)$ and $g(x)$. This implies that any solution $u = u(x)$ of 4.7 that adheres to 4.9 within a subinterval $J \subset [a, b]$ has a bounded derivative.

i.e, $\exists$ a constant $N = N(h, g)$ so that $|u'(x)| \leq N$ on J.

The Nagumo condition is:

$$\begin{cases} if \quad u'' = \mathcal{L}(x, u, u') = O(|u'|^2) \quad \text{and} \quad h(x) \leq u(x) \leq g(x), \\ \text{then} \quad |u'| \leq N(h, g). \end{cases} \tag{4.10}$$

Theorem 7. The existence of the solution $u(x) \in C^{(2)}([a, b])$ for the given equation

4.7, which satisfies condition $h(x) \leq u(x) \leq g(x)$ for $x \in [a, b]$, is provided by Nagumo condition 4.9 and 4.8 condition.

Proof: This theorem can be proved using maximum principal [165].

$$\epsilon h'' \geq \mathcal{L}(x, h, h') \quad \text{and} \quad \epsilon g'' \leq \mathcal{L}(x, g, g'), \tag{4.11}$$

because $\mathcal{L}$ is continuous, which ensures the existence of the solution $u(x)$.

Theorem 8. Consider the function $\mathcal{L}$ is continuous with respect to x, u, u' and belongs to class $C^{(1)}$ concerning u for $(x, u, u') \in [a, b] \times \mathbb{R}^2$. Additionally, let $\exists$ a positive constant ρ s.t $\mathcal{L}_u(x, u, 0) \geq \rho > 0$ for (x, u) in $[a, b] \times \mathbb{R}$. Then, for $\varepsilon > 0$, the equation 4.7 has a unique solution satisfying

$$|u(x, \varepsilon)| \leq \frac{\kappa}{\rho},$$

where

$$\kappa = \max\left\{\max_{[a,b]} |\mathcal{L}(x, 0, 0)|, \rho|\alpha|, \rho|\beta|\right\}.$$

Proof: Assume for x in $[a, b]$

$$h(x) = -\frac{\kappa}{\rho} \quad \text{and} \quad g(x) = \frac{\kappa}{\rho}.$$

Then $h(x) \leq g(x)$, $h(a) \leq \alpha \leq g(a)$, and $h(b) \leq \beta \leq g(b)$. To derive the differential inequalities

$$-\epsilon h'' + \mathcal{L}(x, h, h') \leq 0 \quad \text{and} \quad -\epsilon g'' + \mathcal{L}(x, g, g') \geq 0$$

using Taylor's Theorem:

$$\mathcal{L}(x, h, 0) = \mathcal{L}(x, 0, 0) + \mathcal{L}_u(x, \zeta, 0)h,$$

where ζ, $h < \zeta < 0$, is an intermediate point, and thus

$$\mathcal{L}(x, h, 0) \leq |\mathcal{L}(x, 0, 0)| + mh \leq \kappa - \rho\left(\frac{\kappa}{\rho}\right) \leq 0 = \varepsilon h''.$$

In a Similar manner, for some midpoint η, $0 < \eta < g$,

$$\mathcal{L}(x,g,0) = \mathcal{L}(x,0,0) + \mathcal{L}_u(x,\eta,0)g \geq -\kappa + \rho\left(\frac{\kappa}{\rho}\right) \geq 0 = \varepsilon g''.$$

Using Theorem 7, it follows : for each $\varepsilon > 0$, $u(x,\varepsilon)$ has a solution of equation 4.7 on $[a,b]$ satisfying

$$-\frac{\kappa}{\rho} \leq u(x,\varepsilon) \leq \frac{\kappa}{\rho}.$$

The solution's uniqueness is derived from the maximum principle.

If we assume $\alpha \geq 0$, $\beta \geq 0$, and $-\kappa \leq \mathcal{L}(x,0,0) \leq 0$ in $[a,b]$, then based on the proof of theorem 8, we can derive a more precise estimate of the solution:

$$0 \leq u(x,\varepsilon) \leq \frac{\kappa}{\rho}.$$

Similarly, if $\alpha \leq 0$, $\beta \leq 0$, and $\kappa \geq \mathcal{L}(x,0,0) \geq 0$ in $[a,b]$, then the solution of problem 4.7 satisfy the condition $-\frac{\kappa}{\rho} \leq u(x,\varepsilon) \leq 0$. These findings suggest the following modifications to theorem 8.

Theorem 9. Suppose the function $\mathcal{L}$ is continuous in x, u, u' and belongs to class $C^{(n)}$ $(n \geq 2)$ w.r.t u for (x,u,u') in $[a,b] \times \mathbb{R}^2$. Additionally, let $\alpha \geq 0$, $\beta \geq 0$, $\mathcal{L}(x,0,0) \leq 0$, and $\exists$ a positive constant ρ such that $\partial_u^j \mathcal{L}(x,u,0) \geq \rho > 0$ for $1 \leq j \leq n-1$ and $\partial_u^n \mathcal{L}(x,u,0) \geq \rho > 0$ for (x,u) in $[a,b] \times \mathbb{R}$. Under these conditions, for each $\varepsilon > 0$, the problem 4.7 has a solution that satisfies

$$0 \leq u(x,\varepsilon) \leq \frac{(n!\rho^{-1}\kappa)^{1/n}}{n},$$

where

$$\kappa = \max\left\{\max_{[a,b]} |\mathcal{L}(x,0,0)|, \left(\frac{\rho|\alpha|}{n!}\right)^n, \left(\frac{\rho|\beta|}{n!}\right)^n\right\}.$$

4.3.1 Stability

This subsection deals with the stability criterion for the solution of the problem 4.7. Here, we are dealing with stable solution of the problem and consider $s(x)$ be the solution of 4.7 in $[a,b]$.

Define

$$\mathcal{D}_0(s) = \{(x, u(x)) : |u(x) - s(x)| \leq \aleph(x), \quad a \leq x \leq b\},$$

For $Q > 0$ be constant and $\aleph(x)$ is continuous function given as

$$\aleph(x) = \begin{cases} |A - s(a)| + Q & ; \quad x \in [a, a + Q/2], \\ Q & ; \quad x \in [a + Q, b - Q], \\ |B - s(b)| + Q & ; \quad x \in [b - Q/2, b]. \end{cases}$$

If $A \geq s(a)$ and $B \geq s(b)$ then

$$\mathcal{D}_1(s) = \{(x, u(x)) : 0 < (u(x) - s(x)) \leq \aleph(x), \quad a \leq x \leq b\},$$

If $A \leq s(a)$ and $B \leq s(b)$ then

$$\mathcal{D}_2(s) = \{(x, u(x)) : -\aleph(x) \leq (u(x) - s(x)) \leq 0, \quad a \leq x \leq b\},$$

In these definitions of stability for the solution $s(x)$, let $f(x, y)$ has continuous partial derivative with respect to y in $\mathcal{D}_i, \quad i = 0, 1, 2$ and $q > 0$.

Definition 1. The function $s(x)$ is considered (I_q)-stable on the interval $[a, b]$ if $\exists$ a positive constant ρ satisfying

$$\partial_y^j f(x, s(x)) \equiv 0 \quad \text{for} \quad a \leq x \leq b \quad \text{and} \quad 0 \leq j \leq 2q,$$

and

$$\partial_y^{2q+1} f(x, y) \geq \rho > 0 \quad \text{in} \quad \mathcal{D}_0(s).$$

Definition 2. The function $s(x)$ is considered (II_n)-stable on the interval $[a, b]$ if $s(a) \leq \alpha$, $s(b) \leq \beta$, and $\exists$ a positive constant ρ satisfying

$$\partial_y^j f(x, s(x)) \geq 0 \quad \text{for} \quad a \leq x \leq b \quad \text{and} \quad 1 \leq j \leq n - 1,$$

and

$$\partial_y^n f(x,y) \geq m > 0 \quad \text{in} \quad \mathcal{D}_1(u).$$

Theorem 10. Suppose that the 4.7 simplifies to equation

$$\mathcal{L}(x,u,u') = 0 \quad , a < x < b$$

which has an (I_q)- or (II_n)-stable solution $s(x)$ of class $C^{(2)}([a,b])$. Additionally, let $s(a) \leq \alpha$, $s(b) \leq \beta$, and $s'' \geq 0$ within $[a,b]$. Then, there exists an $\varepsilon_0 > 0$ such that for $0 < \varepsilon \leq \varepsilon_0$, the problem 4.7 has a solution $u = u(x,\varepsilon)$ in $[a,b]$ satisfying

$$s(x) - u(x,\varepsilon) \leq s(x) + c\varepsilon^{1/p},$$

where $p = 2q+1$ (or n) and c is a known positive constant depending on n, $|s''|$, and p.

Proof: For detailed proof see [166]

4.4 Error Analysis

Theorem 11. (Bernstein, 1912) Let function $f(x)$ is bounded on $[0,1]$, following holds:

$$\lim_{n\to\infty} B_n(x) = f(x)$$

at every point where f is continuous. Furthermore, if $f(x)$ is continuous on $[0,1]$, this relation holds uniformly on this interval.

Proof: The detailed proof is given in [158]

Lemma 1 For $t \in [0,1]$, the inequality

$$0 \leq z \leq \frac{3}{2}\sqrt{nt(1-t)}$$

implies

$$\sum_{|k-nt|\geq 2z\sqrt{nt(1-t)}} t_{k,n}(t) \leq 2\exp(-z^2).$$

(Albrycht and Redecki, 1960).

Theorem 12. If $b_n = o(n)$ and

$$\lim_{n\to\infty} exp\left(-\alpha\frac{n}{b_n}\right) M(b_n; f) = 0 \tag{4.12}$$

for every $\alpha > 0$, then

$$\lim_{n\to\infty}(C_n f) = f(x) \tag{4.13}$$

at any continuity point of the function f.

Proof:

As we know that the difference of $C_n f$ and $f(x)$ is

$$|(C_n f) - f(x)| = \sum_{k=0}^{n}\left[f\left(\frac{kb_n}{n}\right) t_{k,n}\left(\frac{x}{b_n}\right) - f(x)\right] \times 1 \tag{4.14}$$

Now using the Lemma 2.1, above equation can be written as

$$|(C_n f) - f(x)| \leq \left|\sum_{k=0}^{n}\left[f\left(\frac{kb_n}{n}\right) - f(x)\right]\right| t_{k,n}\left(\frac{x}{b_n}\right) \tag{4.15}$$

For $\delta > 0$, divide the set of equispaced nodes $x_i = \frac{k}{n}$ into two sets. Therefore, we have

$$|(C_n f) - f(x)| = \sum_{|x_i b_n - x| < \delta}^{n} |f(x_i b_n) - f(x)|\, t_{k,n} + \sum_{|x_i b_n - x| \geq \delta}^{n} |f(x_i b_n) - f(x)|\, t_{k,n}$$
$$= \sum_{*} + \sum_{**}$$

Therefore, we have to prove that

$$\lim_{n\to\infty}\sum_{*} = 0 \quad \text{and} \quad \lim_{n\to\infty}\sum_{**} = 0 \tag{4.16}$$

let x be a continuity point of f , for $\epsilon > 0$, $\exists$ a $\delta > 0$ s.t

$$|f(t) - f(x)| < \epsilon \quad \text{whenever} \quad |x - t| < \delta$$

Consequently,

$$\sum_{*} = \sum_{|x_i b_n - x| < \delta}^{n} |f(x_i b_n) - f(x)| \, t_{k,n} < \epsilon \sum_{|x_i b_n - x| < \delta}^{n} t_{k,n}$$
$$\leq \epsilon$$

Since, $M(b; f) := sup_{0 \leq x \leq b} |f(x)|$,

$$\sum_{**} = \sum_{|x_i b_n - x| \geq \delta}^{n} |f(x_i b_n) - f(x)| \, t_{k,n}$$
$$\leq 2M(b_n; f) \sum_{|x_i b_n - x| \geq \delta}^{n} t_{k,n}$$

For $|x_i b_n - x| \geq \delta$, we have,

$$|x_i b_n - x| \geq \frac{n}{b_n}\delta \geq 2\left(\frac{\sqrt{n}\delta}{2\sqrt{x b_n}}\right)\sqrt{n\frac{x}{b_n}\left(1 - \frac{x}{b_n}\right)} \tag{4.17}$$

Therefore, according to Lemma 1,

$$\sum_{|x_i b_n - x| \geq \delta} t_{k,n} \leq 2\exp\left(-\frac{\delta^2 n}{4x b_n}\right)$$

Thus,

$$\sum_{**} \leq 4M(b_n; f)\exp\left(-\frac{\delta^2 n}{4x b_n}\right)$$

which implies

$$\lim_{n\to\infty} \sum_{*} \leq \lim_{n\to\infty} 4M(b_n; f)\exp\left(-\frac{\delta^2 n}{4x b_n}\right) = 0$$

Consequently,

$$\lim_{n\to\infty} C_n f = f.$$

Lemma Consider $\mathcal{L} : [a, b] \to \mathbb{R}$ is a Lipschitz function. If K is positive Lipschitz constant, then $\mathcal{L}$ is absolutely continuous on $[a, b]$.

Proof If $\epsilon > 0$ and assume $\{(a_k, b_k)\}$ be a collection of sub intervals within $[a, b]$ satisfying

$$\sum_{k=1}^{n} |b_k - a_k| < \delta.$$

From the Lipschitz condition, we know, $|\mathcal{L}(b_k) - \mathcal{L}(a_k)| \leq K_k|a_k - b_k|$ for some $K_k \in \mathbb{R}^+$ where, $k = 1, \ldots, n$. Therefore, we have:

$$\sum_{k=1}^{n} |\mathcal{L}(b_k) - \mathcal{L}(a_k)| \leq \sum_{k=1}^{n} K_k|a_k - b_k| < K\delta \quad \text{where } K = \max_{1\leq k\leq n} K_k.$$

Choosing $\delta \leq \frac{\epsilon}{K}$ completes the proof. Consequently, $\mathcal{L}$ is absolutely continuous.

4.4.1 Voronovskaya Theorem

After establishing the convergence of Bernstein and Chlodowsky operator, the next important question that arises concerns the rate of approximation of $(B_n f)(x)$ to $f(x)$ and $(C_n f)(x)$ to $f(x)$. In 1932, Voronovskaya explored this issue for the Bernstein polynomials. Later, J. Albrycht and J. Redecki provided insights regarding the Bernstein-Chlodowsky polynomials,in 1960. Following these developments, Bardaro, Butzer, Stens, and Vinti(2003), as well as Butzer and Karsli (2009) explored this question for the derivatives $(B_n f)'(x)$ and $(C_n f)'(x)$, respectively.

Let us consider a Voronovskaya-type theorem [167, 168] for $(B_n f)(x)$ as established by Voronovskaya (Voronovskaya, 1932). This theorem was initially presented in context of Kantorovich polynomials.

Theorem 13. Consider f be a bounded function defined on interval $[0, 1]$. Therefore, the following condition holds at each fixed point x on $[0, 1]$

$$\lim_{n\to\infty} n\,[B_n f(x) - f(x)] = \frac{x(1-x)}{2} f''(x)$$

also, $f''(x) \neq 0$.

Proof: For detailed proof see [162]

Theorem 14. Let f be a function defined on $[0, \infty)$, and suppose it satisfies the condition of theorem 12 Then, for every point $x \geq 0$ at which $f''(x)$ exists, the

following holds:

$$\lim_{n\to\infty} \frac{n}{b_n}\left[(C_n f)(x) - f(x)\right] = \frac{x}{2} f''(x).$$

4.5 Numerical Results

In this section the present method is applied to four test problems and all numeerical calculations are performed in python 3.10. The proposed method solution is compared with spline method [154], B-spline method [170] and bernstein collocation method.

Example 4.5.1. *Consider 1D linear convection–diffusion problem [147] with ε be small diffusion coefficient. Due to this the solution changes more rapidly near $x = 0$ and forms boundary layer. This is common in physical and engineering problems like fluid dynamics, chemical processes and heat transfer etc. The convection-diffusion equations you are studying are simplified forms of the Navier-Stokes equations that specifically describe the transport of a scalar quantity, such as temperature, pollutant concentration, or momentum, within a moving fluid. In many atmospheric and environmental problems, the Navier-Stokes equations can be reduced or approximated into simpler forms that capture the essential processes of advection (convection) and diffusion.*

$$-\varepsilon u'' - 2u' = 0; \quad x \in (0,1), \quad 0 < \varepsilon \ll 1,$$

with boundary conditions

$$u(0) = 1 \quad and \quad u(1) = 0;$$

The exact solution is

$$u = \frac{\exp(-2x/\varepsilon) - \exp(-2/\varepsilon)}{1 - \exp(-2/\varepsilon)}.$$

The maximum error are shown in Table 4.1 and error obtained using BNN and Chlodowsky method (CCM) was compared with that of Bernstein collocation method. As the N increases Chlodowsky method performs better as shown in Figure 4.2 and b_n is taken in such a way that it satifies the equation 4.3. Here, BCM represent Bern-

Table 4.1: Maximum norm error comparison of proposed method Bernstein Chlodowsky Neural Network (BNN) for Example 4.5.1 with Bernstein collocation method(BCM) and Bernstein Chlodowsky collocation method on piece-wise uniform mesh.

ε	$N = 16$			$N = 32$			$N = 64$		
	BCM	CCM	BNN	BCM	CCM	BNN	BCM	CCM	BNN
$\varepsilon = 0.1$	5.051608e-04	2.40913e-06	3.916684e-09	2.07e-09	5.247e-10	4.09e-16	9.40241e-06	1.08523e-08	6.55867e-12
$\varepsilon = 0.01$	4.529805e-01	5.3103e-03	1.477967e-06	0.184	7.04e-02	1.36e-05	1.05495e-02	1.42890e-05	1.12216e-07
$\varepsilon = 0.001$	8.787602e-01	3.025910e-03	7.077139e-06	0.75	0.37	0.691e-02	6.25523e-01	2.81059e-02	6.82858e-05
$\varepsilon = 0.0001$	9.471194e-01	5.390281e-02	8.379225e-05	0.88	0.45	0.392e-02	7.54439e-01	7.83557e-03	1.02793e-04
$\varepsilon = 0.00001$	9.471019e-01	1.802693e-01	8.374311e-02	0.88	0.44	3.208e-02	7.55436e-01	2.41082e-02	6.54886e-03

Submission ID trn:oid:::27535:128400783
Page 143 of 225 - Integrity Submission
turnitin

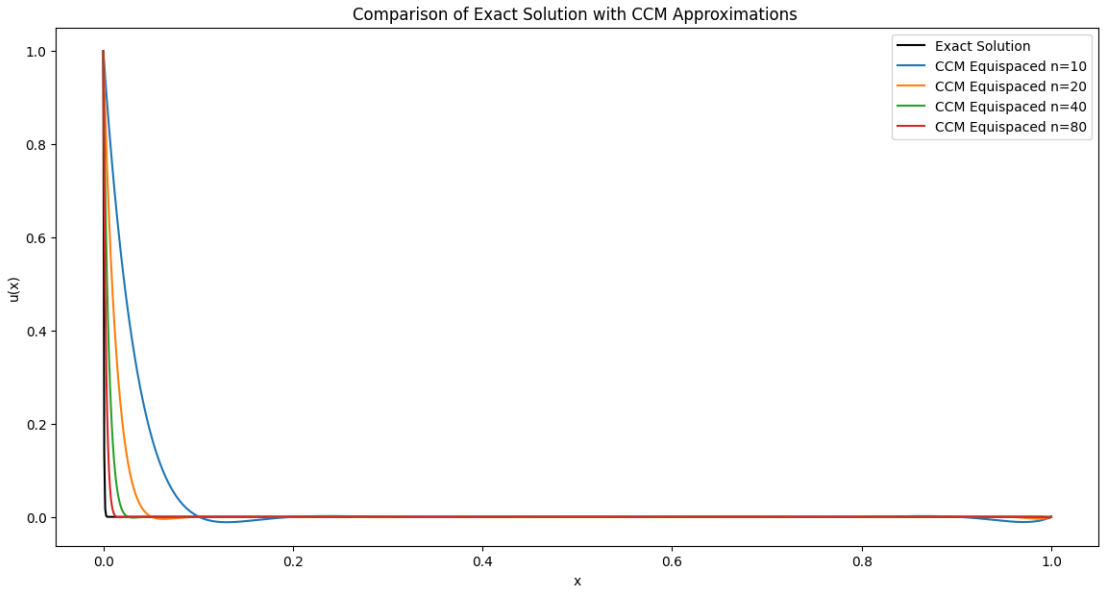

Figure 4.2: Comparison of exact and CCM (Chlodowsky collocation method) solution 4.5.1

stein collocation method and CCM represent the Chlodowsky collocation method. As shown in Table 4.1, BNN achieves the lowest maximum error compared to the classical Bernstein Collocation Method (BCM) and Chlodowsky Collocation Method (CCM). This confirms that BNN is superior in capturing the boundary layers and sharp solution transitions, especially as $\varepsilon \to 0$.

Example 4.5.2. *Consider a non-linear convection-diffusion-reaction equation [149] with ε be diffusion coefficient. In the context of atmospheric science, this convection-diffusion-reaction equation is instrumental in simulating critical processes like cyclone dynamics, pollutant dispersion, and temperature regulation. The exponential decay solution models the rapid changes in these variables within cyclonic systems or weather phenomena, offering insights into how convection and diffusion govern the spread and interaction of energy, moisture, and pollutants in the atmosphere. This equation can thus serve as a foundational model for numerical simulations aimed at predicting storm intensity, pollutant concentrations, and heat distribution in weather systems.*

$$\begin{cases} -\varepsilon v'' + v + v^2 = e^{-\frac{2x}{\sqrt{\varepsilon}}} \\ v(0) = 1, \quad v(1) = e^{-\frac{1}{\sqrt{\varepsilon}}} \end{cases} \tag{4.18}$$

The exact solution of the above problem is given as:

$$v(x) = e^{-\frac{x}{\sqrt{\varepsilon}}}. \tag{4.19}$$

Maximum error for Example 4.5.2

ε	$N = 16$	$N = 32$	$N = 64$
0.1	BNN = 1.03973e-14 CCM = 1.20490e-12 BCM = 4.62391e-12	BNN = 2.70391e-13 CCM= 2.103215e-11 BCM = 4.31866e-10	BNN = 1.37041e-05 CCM = 1.083294e-03 BCM = 1.73116e-03
0.01	BNN = 4.20951e-10 CCM = 0.140552e-08 BCM = 1.21087e-07	BNN = 6.33071e-15 CCM = 2.051801e-12 BCM = 2.29105e-11	BNN = 1.930827e-07 CCM = 2.105399e-05 BCM = 4.323502e-05
0.001	BNN = 2.073972e-06 CCM = 5.16204e-04 BCM = 6.20911e-03	BNN = 4.920741e-12 CCM = 2.024613e-10 BCM = 9.97072e-09	BNN = 3.27650e-10 CCM = 2.202409e-08 BCM = 7.862639e-08
0.0001	BNN = 1.00529e-04 CCM = 1.324503e-02 BCM = 2.24420e-01	BNN = 4.63840e-04 CCM = 1.047323e-03 BCM = 1.80779e-02	BNN = 1.00029e-05 CCM = 1.044242e-05 BCM = 2.236386e-04
1e-05	BNN = 1.940376e-03 CCM = 2.14670e-02 BCM = 5.27390e-01	BNN = 3.52048e-04 CCM = 1.021385e-02 BCM = 2.14715e-01	BNN = 2.84037e-03 CCM = 1.534079e-02 BCM = 3.059913e-02

Table 4.2: Maximum Error for different values of ε using methods for $N = 16, 32, 64$ for Example 4.5.2.

The findings from Example 4.5.2 reveal that the maximum error achieved using the BNN is consistently lower than that obtained using the Bernstein equispaced method and Bernstein-Chlodowsky method. This suggests that chlodowsky operator offers a more precise approximation for the differential equation as shown in Figure 4.3. Additionally, a comparison with the results obtained from the spline method as cited in [154] indicates that the Bernstein-Chlodowsky method delivers superior

Maximum error comparison of Chlodowsky solution with spline method in [154].

ε	$N = 16$	$N = 32$	$N = 64$
2^{-4}	1.130416e-06 Method in [154] = 0.39e-02	2.162401e-07 Method in [154] = 0.11e-02	2.132533e-08 Method in [154] = 0.43e-03
2^{-6}	2.103021e-04 Method in [154] = 0.73e-02	4.133252e-07 Method in [154] = 0.23e-02	1.024239e-06 Method in [154] = 0.14e+01
2^{-8}	5.102446e-05 Method in [154] = 0.12e-01	1.302337e-05 Method in [154] = 0.32e-02	1.274021e-05 Method in [154] = 0.14e+01
2^{-10}	1.138078e-03 Method in [154] = 0.11e-01	5.014202e-05 Method in [154] = 0.30e-01	1.032052e-03 Method in [154] = 0.16e+01

Table 4.3: Maximum error table for Example 4.5.2

Table 4.4: Solution values for different values of x and $\epsilon = 0.1$ for Example 4.5.2.

x	$v(x)$	$v_{20}(x)$	$v_{40}(x)$	$v_{80}(x)$
0.0	1	1	1	1
0.1	0.728893	0.69915	0.729038	0.728791
0.2	0.531286	0.49428	0.51426	0.531286
0.3	0.387251	0.337681	0.387294	0.387251
0.4	0.282264	0.238303	0.282291	0.282264
0.5	0.205741	0.170761	0.205746	0.205741
0.6	0.149963	0.123527	0.149947	0.149963
0.7	0.109307	0.0889388	0.109276	0.109307
0.8	0.0796732	0.0631934	0.0796146	0.0796732
0.9	0.0580733	0.04635	0.0579722	0.0580733
1.0	0.0423292	0.0423292	0.0423292	0.0423292

performance as shown in Table 4.3 and maximum error comparison of BNN and CCM with BCM as shown in Table 4.2. The analysis of maximum errors for different values of ε and varying numbers of nodes N underscores the accuracy and effectiveness of the Bernstein-Chlodowsky approach. b_n is taken in such a way that it satifies the Equation 4.3. Solution for different values of x and ε is shown in Table 4.4. Overall, the Bernstein-Chlodowsky operator and BNN emerges as a robust and efficient tool for solving singularly perturbed differential equations, surpassing both the traditional Bernstein method with equispaced nodes and the spline method.

Example 4.5.3. *Consider the 1D linear convection-diffusion equation with a turning point provided is particularly relevant in situations where a balance between convection (advection) and diffusion changes with spatial location, creating zones of rapid transition. This type of problem is common in atmospheric science. Let,*

$$-\varepsilon u'' + 2(2x-1)u' + 4u = 0; \quad x \in (0,1), \quad 0 < \varepsilon \ll 1, \tag{4.20}$$

with boundary conditions

$$u(0) = 1 \quad and \quad u(1) = 1; \tag{4.21}$$

The exact solution is

$$u = \exp\left(\frac{-2x(1-x)}{\varepsilon}\right). \tag{4.22}$$

The exponential solution shows how the quantity (e.g., temperature, pollutant

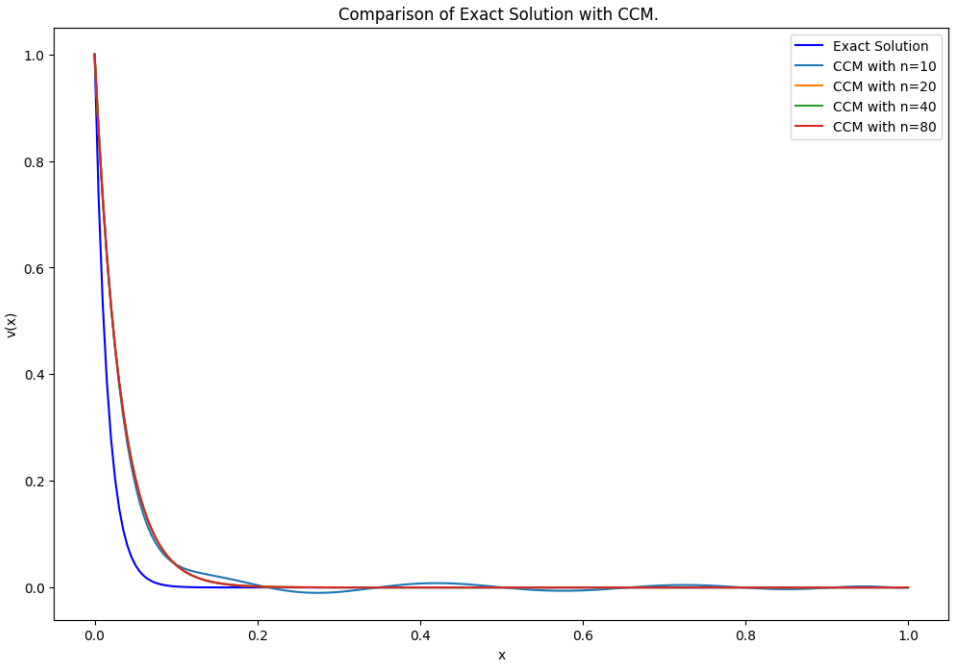

Figure 4.3: Comparison of exact and CCM (Chlodowsky collocation method) solution 4.5.2

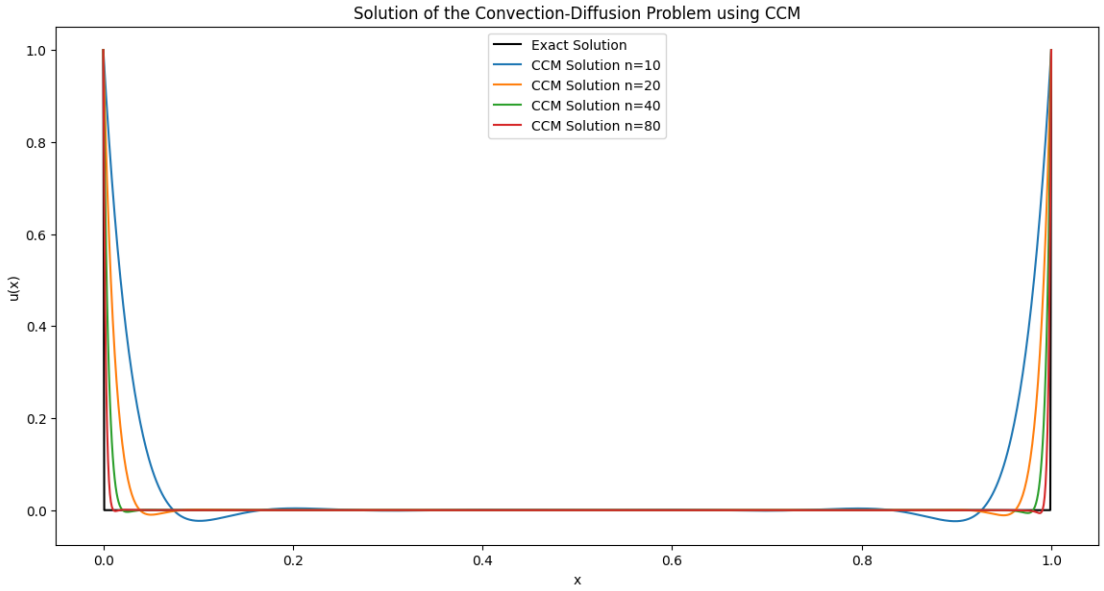

Figure 4.4: Comparison of exact and CCM (Chlodowsky collocation method) solution 4.5.3

Table 4.5: Maximum norm error comparison of proposed method Bernstein Chlodowsky Neural Network (BNN) for Example 4.5.3 with Bernstein collocation method(BCM) and Bernstein Chlodowsky collocation method on piece-wise uniform mesh.

ε	$N = 16$			$N = 32$			$N = 64$		
	BCM	CCM	BNN	BCM	CCM	BNN	BCM	CCM	BNN
$\varepsilon = 0.1$	1.207679e-03	2.070166e-05	1.168644e-11	4.284569e-09	4.708038e-11	2.573070e-15	1.158580e-05	5.062684e-05	1.915060e-08
$\varepsilon = 0.01$	4.106389e-01	1.210854e-07	3.646725e-08	1.577407e-01	6.838419e-12	1.841659e-14	1.071865e-02	4.629837e-02	1.035733e-06
$\varepsilon = 0.001$	8.627769e-01	6.209114e-03	1.175254e-03	7.294452e-01	1.082833e-08	1.733316e-09	6.275232e-01	7.002708e-02	1.088367e-02
$\varepsilon = 0.0001$	9.386752e-01	2.244202e-01	3.375153e-02	8.636396e-01	2.066173e-02	2.390583e-03	7.297220e-01	8.584604e-02	9.370949e-03
$\varepsilon = 0.00001$	9.386425e-01	5.273900e-01	6.322346e-02	8.635301e-01	2.421486e-01	2.495324e-02	7.283668e-01	3.582171e-02	3.622462e-03

turnitin
Page 148 of 225 - Integrity Submission
Submission ID trn:oid:::27535:128400783

concentration) rapidly decays or transitions in the boundary layer or at a front, which is essential in forecasting and simulating weather patterns, cyclones, and environmental pollutant movements. The analysis of Example 4.5.3 shows that the Bernstein-Chlodowsky method and BNN achieves lower maximum compared to the Bernstein equispaced method across various values of ε. This demonstrates the superior accuracy and reliability of the Bernstein-Chlodowsky operator in approximating the solution to the 1D linear convection-diffusion problem with a turning point. The maximum error is shown in Table 4.5. When comparing the performance for different numbers of nodes N, BNN consistently outperforms the Bernstein-Chlodowsky method and the Bernstein equispaced method, providing a more precise solution even as ε decreases as shown in Figure 4.4. b_n is taken in such a way that it satifies the Equation 4.3. These results underline the effectiveness of the Bernstein-Chlodowsky operator in handling singularly perturbed differential equations, particularly those with boundary layers and turning points, further establishing its advantage over traditional Bernstein methods.

Example 4.5.4. *Consider a singularly perturbed problem from [170]. This equation can model the behavior of heat and moisture transport within the atmospheric boundary layer (ABL). The interaction between convection and weak diffusion (small ε) is critical in the ABL, where rapid changes in temperature, humidity, or pollutant concentration occur near the Earth's surface. The boundary layer plays a crucial role in weather phenomena, such as cloud formation and pollutant dispersion, and this equation helps in understanding how heat or chemicals diffuse away from or accumulate near the surface.*

$$\epsilon u'' + (1 + x(1-x))u = f(x), \tag{4.23}$$

$$u(0) = 0, \quad u(1) = 0, \tag{4.24}$$

where

$$f(x) = \left\{ \left[1 + x(1-x) + [2\sqrt{\epsilon} - x^2(1-x)]\, e^{-(1-x)/\sqrt{\epsilon}}\right] + [2\sqrt{\epsilon} - x(1-x^2)]\, e^{-x/\sqrt{\epsilon}} \right. \tag{4.25}$$

The exact solution is

$$u(x) = 1 + (x-1)e^{-x/\sqrt{\epsilon}} - xe^{-(1-x)/\sqrt{\epsilon}}. \tag{4.26}$$

Maximum error comparison of Chlodowsky solution with B-spline method in [170].

ε	$N = 16$	$N = 32$	$N = 64$
2^{-4}	BNN = 1.83200e-06 CCM = 2.0353e-05 Method in [170] = 2.000e-03	BNN = 3.62104e-08 CCM = 2.01221e-06 Method in [170] = 4.908e-04	BNN = 5.9400e-08 CCM = 1.3310e-07 Method in [170] = 1.2225e-04
2^{-6}	BNN = 2.09380e-06 CCM = 0.1309084e-05 Method in [170] = 5.101e-03	BNN = 2.61043e-08 CCM = CCM = 1.04625e-05 Method in [170] = 1.302e-03	BNN = 2.18206e-07 CCM = 1.042290e-06 Method in [170] = 3.137e-04
2^{-8}	BNN = 1.53106e-06 CCM = 2.642107e-04 Method in [170] = 1.950e-02	BNN = 2.02841e-06 CCM = 1.003604e-05 Method in [170] = 5.210e-03	BNN = 1.927041e-06 CCM = 1.426108e-04 Method in [170] = 1.120e-03
2^{-10}	BNN = 1.00385e-05 CCM = 2.430279e-04 Method in [170] = 4.891e-02	BNN = 1.39028e-05 CCM = 1.98252e-05 Method in [170] = 2.012e-02	BNN = 1.069024e-05 CCM = 1.427504e-05 Method in [170] = 4.2129e-03

Table 4.6: Maximum error for Example 4.5.4

turnitin
Page 150 of 225 - Integrity Submission
Submission ID trn:oid:::27535:128400783

The results from Example 4.5.4 indicate that the maximum error obtained using the BNN is significantly lower compared to and Chlodowsky method and the B-spline method in [170]. This demonstrates the effectiveness of the Chlodowsky operator in providing accurate approximations for the given differential equation. The maximum error is compared with B-spline as shown in table 4.6. For various values of ε and different numbers of nodes N, the Chlodowsky methods consistently outperforms the B-spline method, achieving lower maximum errors. This highlights the precision and robustness of the Chlodowsky approach in handling singularly perturbed problems. b_n is taken in such a way that it satifies the equation 4.3.

4.6 Conclusion

In this chapter, we successfully applied the BNN and Bernstein-Chlodowsky operator to solve a range of singularly perturbed differential equations (SPDEs) that are commonly encountered in atmospheric science and cyclone modeling. Through various numerical examples, we demonstrated that this operator provides superior accuracy in resolving sharp boundary layers and steep gradients critical elements in cyclone dynamics and atmospheric processes. The method's flexibility and robustness, particularly in handling convection-dominated systems, make it an invaluable tool for improving the predictive capabilities of weather models.

One of the key advantages of the Bernstein-Chlodowsky operator is its ability to reduce numerical dissipation and improve the resolution of steep transitions in temperature, wind velocity, and pressure. These features are essential for accurately predicting the intensity and trajectory of cyclones, as well as for simulating the rapid changes occurring in the atmospheric boundary layer (ABL). Compared to traditional numerical methods, such as finite differences and spline-based approaches, our approach delivers better performance with lower computational cost, while still maintaining high accuracy across the solution domain.

The numerical experiments conducted on convection-diffusion problems, including those with turning points, showed that the Bernstein-Chlodowsky operator consistently outperforms existing methods in terms of maximum error. This establishes the operator as a reliable and efficient tool for tackling SPDEs in atmospheric modeling. Additionally, the operator's capacity to handle both linear and

nonlinear problems without the need for linearization enhances its applicability in broader scientific contexts.

In addition to the classical Bernstein-Chlodowsky collocation approach, we used Bernstein-Chlodowsky Neural Network (BNN) that significantly improves accuracy, particularly for small ε regimes and nonlinear equations. Across all tested examples, BNN achieved the lowest error norms, demonstrating its capability in resolving boundary layers and steep gradients effectively. This integration of operator-based theory with neural learning introduces a novel direction in numerical weather prediction and boundary-layer modeling.

Future research will focus on extending the application of the Bernstein-Chlodowsky operator to more complex and higher-dimensional models, such as full three-dimensional simulations of cyclone formation, pollutant transport, and global weather systems. The promising results obtained in this work pave the way for further exploration and integration of this method into operational forecasting systems, potentially improving real-time weather prediction and climate modeling.

Chapter 5

The Tropical Cyclone energy Prediction of North Indian Ocean in Monsoon Using Artificial Neural Networks

---

This chapter focuses on predicting the Accumulated Cyclone Energy (ACE) in the NIO during monsoon using an optimized Artificial Neural Network (ANN) model. Initially, an ANN was trained with six cyclone metrics, including Velocity Flux (VF) and Power Dissipation Index (PDI), showing moderate predictive accuracy with relatively high error metrics like Mean Squared Error (MSE). The permutation feature is essential in finding the most influential features to improve model performance. This analysis identified NIO_{VF}, AS_{PDI}, and NIO_{PDI} as key predictors, while metrics such as BOB_{PDI}, BOB_{VF}, and AS_{VF} had minimal impact on NIO_{ACE} prediction. To improve the model's predictive accuracy while reducing complexity, the ANN model was again retrained with only the most significant features, resulting in a considerable reduction in loss (MSE).

5.1 Introduction

Natural disasters such as tropical cyclones (TCs) have devastated coastal regions worldwide for generations [171]. These storms pose significant risks due to their intense winds and associated phenomena, such as storm surges and heavy rainfall, which can cause extensive flooding. The prediction and analysis of TCs are of immense importance for disaster [172] preparedness and mitigation efforts, particularly in regions like the North Indian Ocean [173], which experiences frequent cyclonic activity. Around 80 tropical cyclones [174] form annually globally, with approximately two-thirds occurring in the Northern Hemisphere and the remaining one-third in the Southern Hemisphere. These cyclones [173] are charged by the release of latent heat when water vapors in the atmosphere condense, typically when sea surface temperatures exceed 26℃. This process generates large-scale wind patterns that spiral around a central low-pressure area known as the storm's "eye." Structurally, tropical cyclones [175] are symmetrical, with wind speeds intensifying as one moves away from the eye. In fully developed storms, wind speeds increase rapidly up to about 100 km from the center before tapering off at greater distances. Winds in this zone can reach up to $93m\backslash s(335km\backslash hr)$, and the overall storm can extend up to $1,000km$ in diameter. In addition to damaging winds, tropical cyclones bring about flooding through intense rainfall and powerful storm surges, making them highly destructive, multi-hazard weather events. The North Indian Ocean (NIO) [176, 177] (Mohapatra and Vijay Kumar, 2017) is a region characterized by significant variability in tropical cyclone activity, which posess considerable risks to the densely populated coastal areas it affects. The annual cycle of tropical cyclones [178] in the NIO, including depressions, cyclonic storms, and severe tropical cyclones, shows a pronounced pattern, with an average of about 11 cyclonic disturbances each year [173]. October to December, the post-monsoon months, are when this activity peaks and is crucial for regional catastrophe planning and response programs. The frequency of tropical cyclones has paradoxically decreased in recent decades despite an increasing trend in sea surface temperatures, a critical factor in the intensification of these storms.

Accumulated Cyclone Energy(ACE) [177, 178] determines how much energy is released by tropical cyclones over their lifetimes. It provides insight into how devastating they can be. It is computed using the square of maximum sustained

winds of tropical cyclones, recorded every six hours. Over time, ACE has shown to be an effective instrument for evaluating the strength and length of tropical cyclones, providing a cumulative measure of cyclone season activity. Assessing the potential impact of cyclone seasons [179] and implementing effective mitigation strategies are indispensable variables for climatologists, meteorologists, and disaster management authorities. Only a few studies have focused on the RMW(Radius of Maximum Wind) over the Pacific [179, 180] and the Atlantic basins. Most studies have focused on predicting and estimating various aspects of TCs, including intensity, sea surface temperature, moisture, precipitation, pressure systems, and cloud shapes. The best track data from the India Meteorological Department (IMD) has an error range of -26 to 200 in all these investigations. Hence, they need to be further decreased [177].

However, traditional statistical methods of predicting ACE are limited in their ability to handle the nonlinear relationships and multifaceted interactions between various meteorological and oceanographic predictors [180]. This limitation underscores the need for more sophisticated computational approaches to analyze complex datasets and extract meaningful patterns for accurate forecasts. An ANN [181] is especially useful for modeling tropical cyclone activity due to its versatility in training. ANNs have proven helpful in pattern recognition, data classification, and prediction.

In recent years, artificial intelligence (AI) techniques, particularly ANN [181], have become famous for predicting, forecasting, and analyzing complex natural phenomena such as tropical cyclones. With the help of ANNs, which are known for learning nonlinear connections between data, it has been possible to predict the formation, intensity, and trajectory of TCs with tremendous accuracy. A combination of these methods and conventional statistical analysis can offer a more comprehensive and reliable way to comprehend and predict TCs. This research aims to build a robust prediction model that can provide ACE forecasts using ANN. By improving the accuracy of NIO's [176] forecasting tools, disaster risk reduction is enhanced in the face of changing climates and tropical cyclone movements. Most ANN-based cyclone studies focus on the Atlantic or Pacific basins but in our work we identify AS_{PDI} and NIO_{VF} as dominant predictors of ACE in the NIO during monsoon, validated via permutation feature importance and statistical tests.

The primary objective is to predict NIO_{ACE} during the monsoon season using an ANN model trained on historical cyclone metrics (VF, PDI) from AS, BoB, and NIO. The goal is to identify key predictors of ACE (e.g., AS_{PDI}, NIO_{VF}) through feature importance analysis, enabling optimized forecasting with minimal computational complexity. This addresses a gap in existing studies, which rely heavily on statistical methods and rarely use ANN for ACE prediction in the NIO.

5.2 Data and Methodology

5.2.1 Source of Data Set

The India Meteorological Department (IMD) provided the cyclone dataset used in this study. It contains cyclone data from the North Indian Ocean (NIO), Bay of Bengal (BOB), and Arabian Sea (AS) regions during the monsoon season. It consists of metrics that depend on cyclone activity, like Velocity Flux (VF), Accumulated Cyclone Energy (ACE), and Power Dissipation Index (PDI) from 1982 to 2023. To mitigate dataset limitations, monthly granularity was incorporated, expanding the dataset to 168 samples. Cross-validation and regularization techniques were employed to ensure robustness.

- **Accumulated Cyclone Energy (ACE):** ACE quantifies the total energy generated by a tropical cyclone, integrating both intensity and duration. Higher ACE values correlate with more destructive potential.
- **Velocity Flux (VF):** VF measures the kinetic energy flux associated with cyclone winds, reflecting momentum transfer critical for energy accumulation.
- **Power Dissipation Index (PDI):** PDI estimates the total energy dissipated by a cyclone, emphasizing high wind speeds. It is strongly linked to potential damage.

The study focuses on three regions within the North Indian Ocean (NIO):

North Indian Ocean (NIO):

- **Bounds:** 5^o N -25^oN latitude, 60^o E- 100^o E longitude.
  Sub- regions:

- **Bay of Bengal (BoB):** Bounded by India/Sri Lanka (west), Bangladesh (north), Myanmar/Andaman Islands (east).
  coordinates: 5^o N -22^oN, 80^o E -100^oE

- **Arabian Sea (AS):** Bounded by the Arabian Peninsula (west), India (east).
  Coordinates: 5^o N -25^oN, 50^o E -70^oE

For visual clarity, we direct readers to Figure 5.1 in [177] or the India Meteorological Department's (IMD) regional cyclone maps, which delineate these domains. Pre-processing is vital to ensuring the model can do so efficiently when learning from a dataset. We converted the data types to numeric for all columns. We use the sci-kit-learn library to normalize the input features and target variables. Therefore, 80 percentage of the data was used in training and 20 percentage in the testing. We have done all ANN programming in Python 3.0 and statistical tests in SPSS software.

5.2.2 Methodology

In this section, we discuss the methodology of Artificial Neural Networks (ANNs) for predicting cyclone energy metrics like ACE. A multi-step process was followed: constructing a starting ANN model, evaluating features, optimizing the model, and analyzing errors. An approximation for non-linear functions, ANN constitutes several layers linked with neurons. The ANN's mathematical equation, including how it learns weights to reduce errors, will be discussed in this section.

The ANN model used in cyclone energy prediction consists of input, hidden, and output layers where input features cyclone metrics such as VF, and PDI and the hidden layer uses non-linear adjustments to capture complex relationships, and output layer regression uses single neuron to get the expected ACE value. The structure of ANN with three input, hidden, and one output layer is shown in Figure 5.1. Therefore, for each neuron in the Lth layer, the output $N^{[L-1]}$ is given as

$$Z^{[L]} = W^{[L]} N^{[L-1]} + B^{[L]}$$

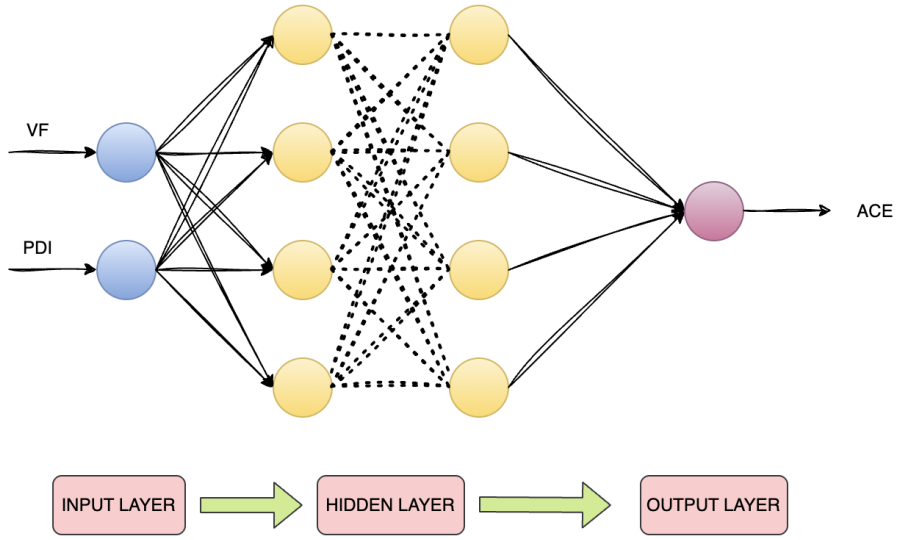

Figure 5.1: An illustration of the ANN, showing 3 Input Neurons (VF, PDI), and there can be one or more Hidden Layers and 1 Output Neuron.

Where $W^{[L]}$ and $B^{[L]}$ are the weight matrix and bias vector for the L^{th} layer, respectively. $N^{[L-1]}$ is the output from the previous layer. Then activation function is applied to ass non-linearity:

$$N^{[L]} = \rho(Z^{[L]})$$

Where ρ is a non-linear activation function like ReLU. However, the output layer uses a linear activation function for continuous predictions: $\widehat{A} = Z^{[L]}$, where $\widehat{A}$ is the predicted value of ACE. Then, the loss function is defined as the difference between actual and predicted values. For the regression model, Mean Square Error (MSE) is used as a loss function, so, for n number of datasets in training and Ai is the actual value for an ith data value, the MSE is given as

$$\Gamma\ (\widehat{A}, A) = \frac{1}{n}\sum_{i=1}^{n}(\widehat{A}^i - A^i)2$$

Reducing the loss function is the aim of ANN training. Gradient descent and back-propagation are used to do this. Updating each weight and bias to minimize the loss:

$$W^{[L]} = W^{[L]} - \gamma\frac{\delta\Gamma}{\delta W^{[L]}},$$

$$B^{[L]} = B^{[L]} - \gamma\frac{\delta\Gamma}{\delta b^{[L]}}$$

Where γ is the learning rate that controls the size of the step.

The ANN model uses six input features: AS_{VF}, AS_{PDI}, BoB_{VF}, BoB_{PDI}, NIO_{VF}, and NIO_{PDI}. The output layer predicts NIO_{ACE}. ACE values for sub-regions (AS_{ACE}, BoB_{ACE}) are excluded from the input layer to avoid redundancy and ensure the model learns from non-linear relationships between wind/flux metrics and energy.

Initial Model:

1. **Model Architecture**

- The initial ANN model was built using the Multi-layer Perceptron (MLP) Regressor from scikit-learn. This model was chosen due to its ability to model complex, non-linear relationships between the input features and target variables.

- The model included three hidden layers with 128, 64, and 32 neurons. The ReLU (Rectified Linear Unit) activation function was used in all hidden layers to effectively allow the model to learn non-linear interactions

- The model utilized the Adam optimizer for weight optimization, with a learning rate of $\gamma = 0.001$, and L2 regularisation 0.001 to prevent overfitting by discouraging excessively complex weight values.

2. **Model Training and Evaluation**

- The training process involved iterating over the training dataset to minimize the error between predicted and actual values.

- After the training process, the model's performance was evaluated on the test dataset. These metrics helped to determine the model's effectiveness in accurately predicting ACE values.

Optimized Model via permutation feature importance and feature reduction

In Permutation Feature Importance, the value of each feature in a trained model is measured in terms of how much it degrades when its values are randomly switched. Feature importance analysis was carried out to increase performance and make the model readable.

- Permutation feature importance was employed to measure each feature's contribution to predicting the performance of the ANN. In this method, every feature is rearranged randomly, and the model's functionality is evaluated.
- A shuffled list ranked features that affected accuracy significantly higher than those that did not.
- NIO_{VF}, AS_{PDI}, and NIO_{PDI} features predicted ACE values most significantly, while BOB exhibited the most minor significance.

Then, the ANN model was retrained with these more significant features that contained only the most essential metrics obtained using the permutation feature reduction method. By using this method, the model's noise was reduced, overfitting was decreased, and the main cyclone energy drivers were highlighted. The Flowchart of the ANN algorithm used in the initial and optimized model is shown in Figure 5.2.

5.3 Results and Discussion

In this section, we will discuss the results of the initial ANN model, permutation feature importance, and how extracted features are retrained in the ANN model called the optimized ANN model to predict the Accumulated Cyclone Energy in the North Indian Ocean (NIO_{ACE}) in the monsoon season. The detailed analysis of the model's performance and statistical evaluations to determine the model's efficacy and precision are shown in this section.

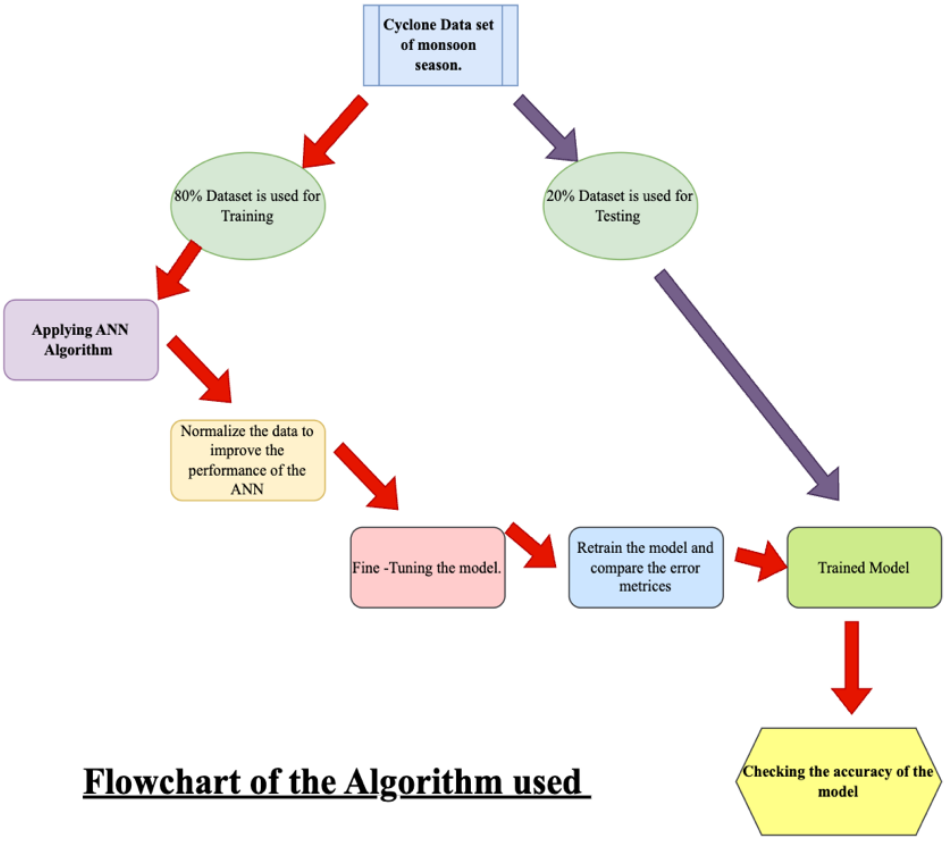

Figure 5.2: Flowchart Depicting the Workflow for Training and Optimizing an ANN Model for Cyclone Energy Prediction

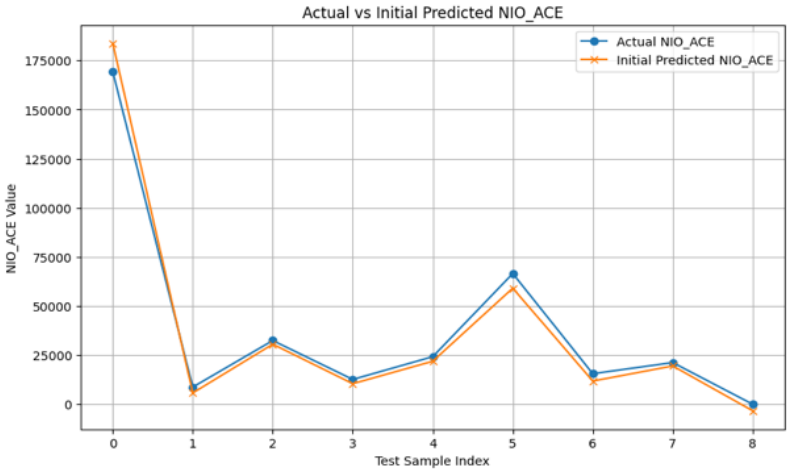

Figure 5.3: Actual vs Initial Predicted NIO_{ACE}

5.3.1 Initial ANN Model Performance

Firstly, we trained our ANN model with all metrics like ACE, VF, and PDI for NIO, BOB, and AS in the input layer and predicted NIO_{ACE}. Figure 5.3 compares the actual and NIO_{ACE} values predicted through the initial ANN model. It can be observed that predicted NIO_{ACE} is closely aligned with actual values, which proves the model's robustness and its ability to accurately capture the complex dynamics of NIO_{ACE}. "Test sample size" refers to the number of samples in the test dataset against which the model is evaluated.

The loss curve illustrated in Figure 5.4 also examined the training progression. During the initial training phase, the loss (MSE) decreased substantially, reaching a near-minimal level by approximately the 20th iteration. This consistent drop in loss indicates effective learning by the model and points towards minimal overfitting, as evidenced by the convergence of the loss towards stability in later iterations.

5.3.2 Feature Importance Analysis

A permutation feature importance analysis was conducted to assess the contributions of different input features, and the results are depicted in Figure 5.5. The findings indicate that AS_{PDI} and NIO_{VF} are the most influential predictors of NIO_{ACE}, significantly enhancing the accuracy of the model. These features

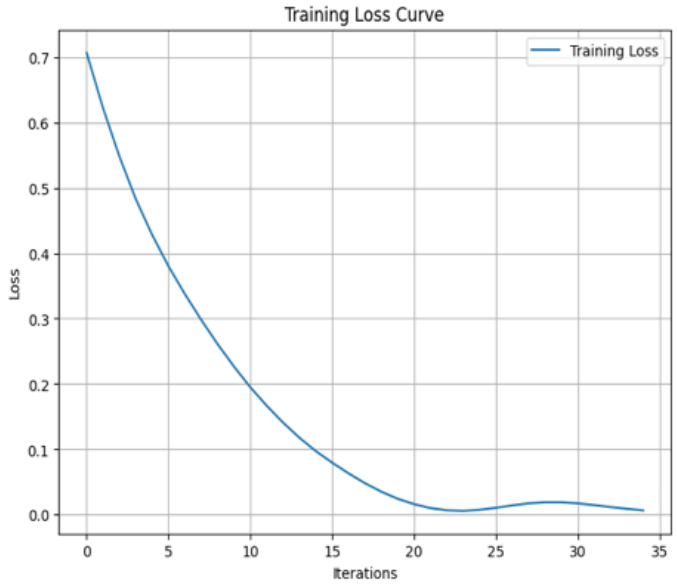

Figure 5.4: Training Loss Curve

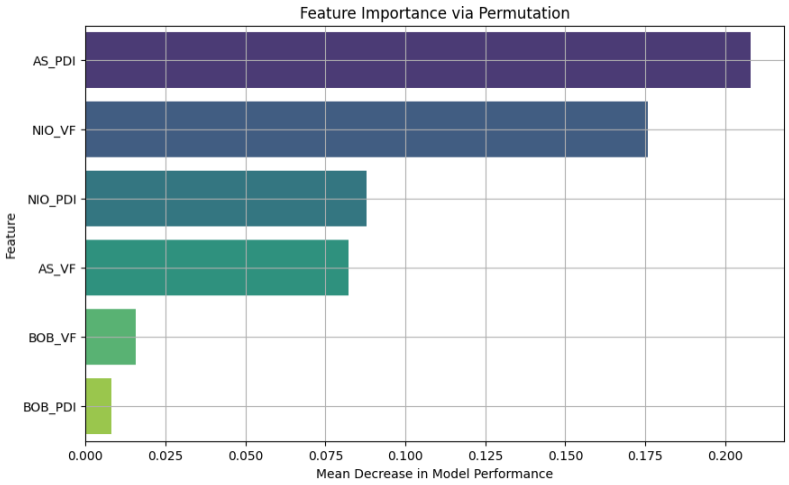

Figure 5.5: Feature Importance via Permutation

appear to encapsulate critical aspects of cyclone dynamics and are fundamental for predicting accumulated cyclone energy. While still relevant, features such as NIO_{PDI} and AS_{VF} were less impactful than AS_{PDI} and NIO_{VF}. On the contrary, features BOB_{VF} and BOB_{PDI} were found to have a minimal effect on the model's predictions.

The ANN predicts NIO_{ACE} without using AS_{ACE} or BoB_{ACE} as inputs. Instead, it learns to correlate VF and PDI (e.g., wind intensity, energy dissipation) with ACE. Permutation feature importance Figure 5.5, identified AS_{PDI} and NIO_{VF} as dominant predictors, validating that the model prioritizes physically meaningful metrics. These observations provide valuable guidance for future research,

suggesting that focusing on the most impactful features can help refine model performance. Practically, this allows for a more efficient allocation of resources towards collecting and processing key variables, thus optimizing cyclone energy prediction processes.

5.3.3 Optimized ANN Model

An essential analysis of the permutation feature was applied to enhance the model's prediction capability further, and a comparative evaluation of the initial versus optimized predictions was performed, as shown in Figure 5.6. Table 5.1 highlights years critical for disaster preparedness (e.g., $1999, 2021$) and demonstrates the optimized model's improved accuracy during both extreme and average cyclone seasons. The selected years are not arbitrary but strategically chosen to validate the model's robustness, accuracy, and operational utility across diverse real-world scenarios. This approach ensures the findings are both statistically rigorous and practically actionable. The optimized model exhibited a more precise alignment with the actual values, as shown in Table 5.1, which indicates that the parameter adjustments positively affected the prediction quality. This highlights optimization's critical role in improving the overall accuracy of ANN-based predictions. The initial model's loss is 0.012625, whereas the optimized model shows 0.00667925. The optimized model reaches lower loss values faster, converges with fewer iterations, and exhibits more stable training behavior. These results indicate that model optimization significantly enhances the network's ability to learn from the data more effectively while maintaining robustness and reducing the risk of overfitting. The final convergence of both models to low error values further demonstrates their capability to model the problem accurately, but the optimized model achieves this with improved learning efficiency. The x-axis in Figure 5.6 represents specific years selected to illustrate model performance for high-impact or extreme ACE events. It also shows the temporal trend of ACE predictions across the entire test dataset ($1982\tilde{}2023$). It highlights how the optimized model consistently outperforms the initial model over time.

Table 5.1: Comparison of Actual NIO_{ACE} with initial and Optimized ANN

Year	**Actual NIO_ACE** (10^4 knots^2)	**NIO_ACE using Optimized ANN** (10^4 knots^2)	**NIO_ACE using Initial ANN** (10^4 knots^2)
1986	24225	24170	21590
1990	32436	29696	28960
1994	18400	17450	15470
1995	8750	7239	6138
1998	33625	34675	33540
1999	12950	11970	11578
2001	15550	12192	12437
2007	169207	170351	175280
2008	12625	11904	11073
2009	11300	9195	9064
2011	21225	22304	22985
2021	66550	67404	68462

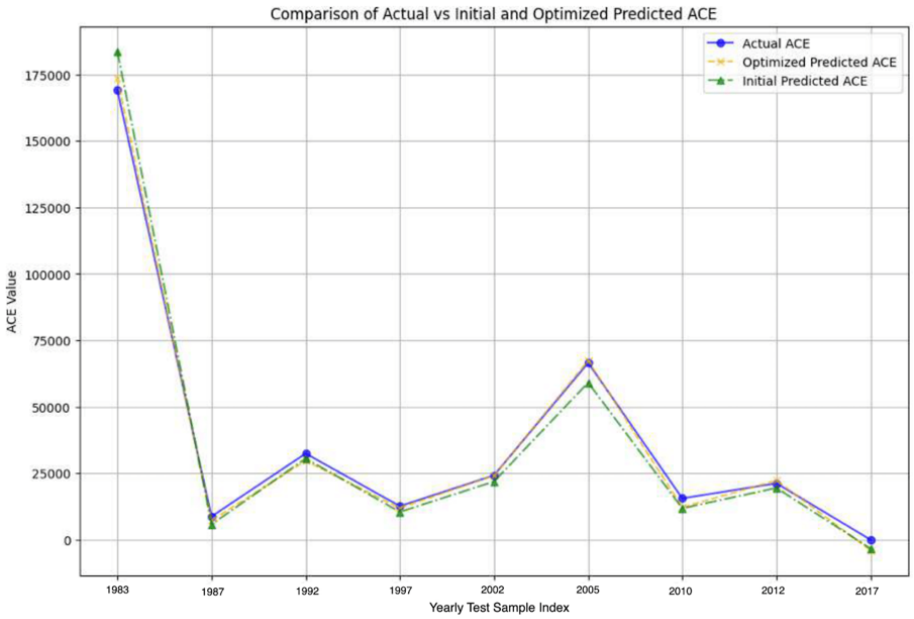

Figure 5.6: Comparison of actual ACE with initial predicted ANN and optimized predicted ACE

5.3.4 Statistical Validation

A one-sample t-test was conducted to substantiate the contribution of individual features in predicting NIO_{ACE}, and the results are presented in Table 5.2. The analysis found statistically significant differences [177] across various features $(p < 0.05)$, reinforcing their impacts on the model's predictive capability. Specifically, the features AS_{PDI} and NIO_{VF} showed high significance levels, confirming the permutation feature importance analysis findings and validating their substantial role in NIO_{ACE} prediction. The histogram plot of actual and predicted ACE is given in Figure 5.7. To confirm the contribution of individual features in predicting NIO_{ACE}, a one-sample t-test was conducted in SPSS software, with results summarised in Table 5.3.

- BOB (VF, ACE, PDI): All metrics had $p < 0.001$, indicating strong evidence to reject the null hypothesis. The means of these metrics are significantly different from 0, emphasizing the importance of BOB metrics in cyclone activity.

- AS (VF, ACE, PDI): The metrics showed statistically significant differences from 0 (p-values between 0.004 and 0.045). However, the significance was

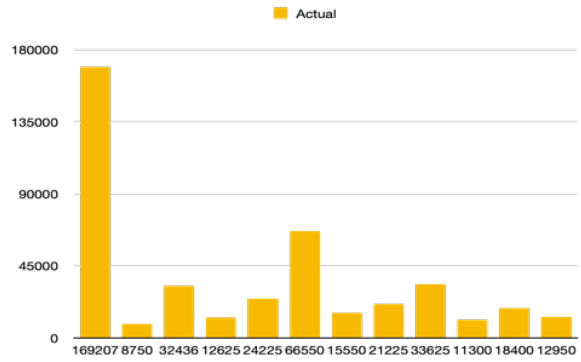

Figure 5.7: Bar graph of Actual NIO_{ACE}.

weaker than for BOB.

- NIO (VF, ACE, PDI): NIO_{VF} and NIO_{ACE} had $p < 0.001$, showing vital statistical significance, while NIO_{PDI} was significant with $p = 0.010$.

There was a statistically significant difference between the different characteristics $(p < 0.05)$ among the investigation results, showing that each has a distinct impact on the model's prediction accuracy. According to our analysis of the importance of permutation features, AS_{PDI} and NIO_{VF} validated NIO_{ACE} prediction by showing high statistical significance. These characteristics persistently benefit model accuracy and reliability, as demonstrated by the t-test results in Table 5.3. Because the BOB, AS, and NIO metrics differ significantly from the reference values, they play a crucial role in understanding cyclone energy metrics. Evidence shows that AS_{PDI} and NIO_{VF} substantially affect the scenarios tested, as indicated by their two-sided p-values below 0.05. A lesser extent of significance was also found for metrics like AS_{VF} and NIO_{PDI}, confirming their relevance but not as primary drivers compared to AS_{PDI} and NIO_{VF}.

Figure 5.8 presents the bar graph plot of actual versus predicted ACE, visually demonstrating the effectiveness of the optimized model. This plot reflects the consistency between the predicted values and actual observations, affirming the model's ability to reliably capture the underlying dynamics of ACE. The values defined on the x-axis are ACE values for specific year chosen in test sample. It demonstrates accuracy improvements during critical events.

The pair plot, Figure 5.8, visually represents the relationships between the velocity flux (VF), the accumulative cyclone energy (ACE) and the power dissipation index (PDI) for the North Indian Ocean (NIO). The analysis reveals strong posi-

Table 5.2: Showing actual vs. predicted values of NIO_ACE values using optimized model

Year	1986	1990	1994	1995	1998	1999	2001	2007	2008	2009	2011	2021
Actual NIO_ACE	24225	32436	18400	8750	33625	12950	15550	169207	12625	11300	21225	66550
Predicted NIO_ACE using optimized ANN (10^4 knots^2)	24170	29696	17450	7239	34675	11970	12192	170351	11904	9195	22304	67404
Predicted NIO_ACE using initial ANN (10^4 knots^2)	21590	28960	15470	6138	33540	11578	12437	175280	11073	9064	22985	68462

[1] Selected years represent extreme, average, and high-impact cyclone events to evaluate model performance across scenarios. Years post-2000 are included to assess relevance to recent climate conditions.

Submission ID trn:oid:::27535:128400783

Page 169 of 225 - Integrity Submission

turnitin

Table 5.3: One-Sample t-test

	Significance One-Sided p	**Mean Difference** Two-Sided p
BOB_VF	$< .001$	$< .001$
BOB_ACE	$< .001$	$< .001$
BOB_PDI	$< .001$	$< .001$
AS_VF	0.002	0.004
AS_ACE	0.011	0.022
AS_PDI	0.023	0.045
NIO_VF	$< .001$	$< .001$
NIO_ACE	$< .001$	$< .001$
NIO_PDI	0.005	0.010

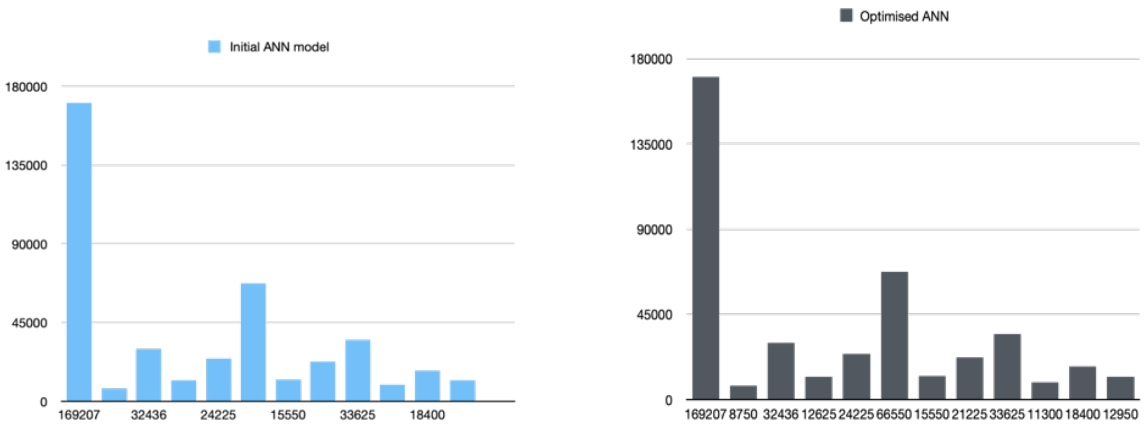

Figure 5.8: Bar graph of Predicted NIO_{ACE} using initial ANN and optimized ANN

tive correlations between the cyclone metrics, with ACE and PDI closely related, indicating that cyclones with higher accumulated energy exhibit a more significant destructive potential. VF also shows a positive correlation with both ACE and PDI, suggesting that cyclones with higher wind intensity release more energy and have a higher potential for damage. These relationships emphasize the interconnection of the intensity, energy, and destructive potential of the cyclone. The correlation among different cyclone metrics used in this research is summarized in Table 5.5. The correlation coefficient between NIO_{VF} and NIO_{ACE} was very high (0.95), indicating a strong linear relationship. Similarly, NIO_{PDI} shows a robust correlation with respect to $NIO_{ACE}(0.99)$. The feature importance analysis confirms the importance of these features in predicting accumulated cyclone energy based on these high correlations. Therefore, the optimized model demonstrates significant improvements over the initial model as shown in Table 5.4 below:

A paired t-test comparing prediction errors (absolute differences between actual and predicted ACE) of the initial and optimized models confirms that the improve-

Table 5.4: Analysis of initial and optimized model.

Metric	Initial Model	Optimized Model	Improvement
MSE	0.012625	0.00667925	∼47% reduction
R^2	0.81	0.92	14% increase
Training Speed	35 iterations	20 iterations	43% faster convergence

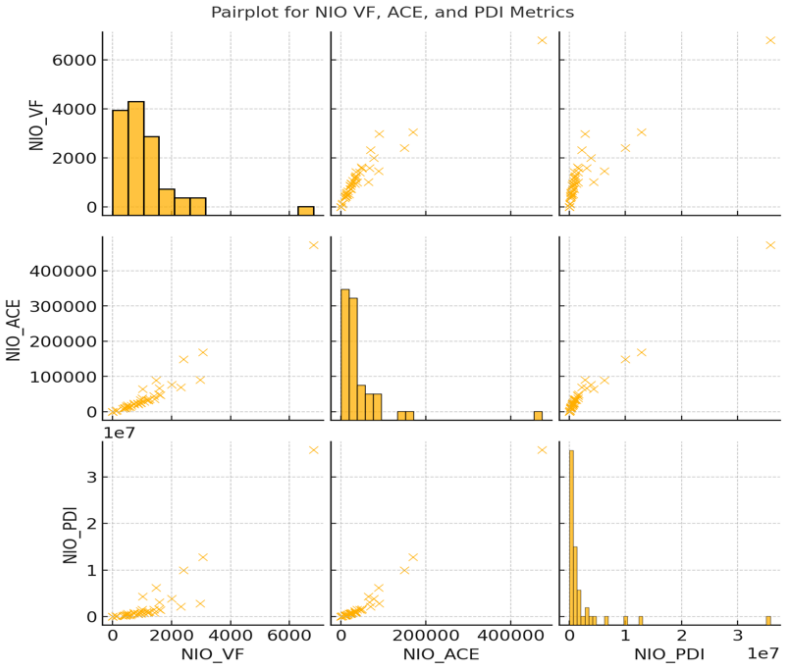

Figure 5.9: Pair plot Displaying the Distribution and Interrelationships Between NIO_{VF}, NIO_{ACE}, and NIO_{PDI} Metrics

ment is statistically significant $(p < 0.001 p < 0.001)$.

Table 5.5: The correlations between the cyclone metrics.

	NIO_VF	NIO_ACE	NIO_PDI
NIO_VF	1.0	0.9516213608722540	0.9005505322931380
NIO_ACE	0.9516213608722540	1.0	0.989711903818995
NIO_PDI	0.9005505322931380	0.989711903818995	1.0

We conducted an analysis comparing the optimized MLP with the linear regression (LR) and stepwise multiple regression (SMR) models shown in Table 5.6.

Key Advantages of MLP Over Linear Methods:

- **Non-Linearity:** Cyclone energy dynamics are inherently non-linear (e.g., ACE $\propto$ wind speed²). The MLP's ReLU activation and hidden layers model these relationships without manual transformation.
- **Feature Interactions:** The MLP captures interactions like $AS_{PDI} \times NIO_{VF}$,

Table 5.6: Comparing the optimized MLP to Linear regression and multiple regression.

MODEL	MSE (NIO_ACE Prediction)	R^2	Key Limitations of Linear Methods
Linear Regression	0.0219	0.71	- Fails to capture non-linear interactions - Assumes independence between features, which is violated (Table 5.4 shows high correlation between NIO_VF and ACE).
Stepwise Regression	0.0185	0.75	- Requires manual feature engineering. -Struggles with multicollinearity (e.g., VF vs. PDI).
Optimized MLP	0.0067	0.92	- Automatically learns non-linear relationships. - Robust to multicollinearity.

turnitin
Page 172 of 225 - Integrity Submission
Submission ID trn:oid:::27535:128400783

which linear models miss (evident in the pair plot, Figure 5.9).

- **Higher Accuracy:** The MLP achieves 47 percent lower MSE and 17 percent higher R^2 than the best linear model (Table ??).

5.4 Conclusion

Using the ANN model developed, this study demonstrated its accuracy in predicting NIO_{ACE}. A permutation feature importance analysis combined with statistical validation in the form of t-tests strengthens the reliability of the selected input features. The strong correlation between critical features such as AS_{PDI}, NIO_{VF}, and NIO_{ACE} shows their importance in the prediction of the energy of the cyclones. Embassing these key predictors, such as AS_{PDI} and NIO_{VF}, can improve the precision of future models in capturing cyclone behavior in the North Indian Ocean. In this study, we focus on the most critical aspects of cyclone energy forecasting to improve the models and data collection. We focused on predicting the ACE of the North Indian Ocean during the monsoon season using ANN. Also, we demonstrated the importance of optimizing ANN models for meteorological applications by focusing on cyclone metrics to improve accuracy and computational efficiency. The initial ANN model was trained using six cyclone metrics, which include ACE, VF, and PDI for NIO, BOB, and AS, which show moderate predictive accuracy. However, a relatively high loss factor could have improved the performance, indicating that some input features contributed to unnecessary noise and complexity. Permutation features were analyzed to determine which features significantly impacted prediction accuracy. The analysis revealed that features such as NIO_{VF} and AS_{PDI} were the most influential, while other metrics, such as BOB_{VF} and BOB_{PDI}, had minimal impact on the model's output. The ANN model was retrained with only significant features, which resulted in a reduction of loss compared to the initial ANN model. This means the optimized model improves the prediction of NIO_{ACE} values in the monsoon season. For instance, in 2007 and 2008, the optimized ANN model achieved a much closer alignment than the initial ANN. Specifically, the predicted ACE for 2007 using the optimized model was 170,351 compared to the actual value of 169,207, showing the effectiveness of feature reduction in improving prediction. Also, AS_{PDI} and NIO_{VF} showed statistically significant contributions to the model's predictions, proving their role

in enhancing cyclone energy prediction. According to this study, the permutation feature is crucial in improving ANN models for ACE prediction. With an optimized ANN model, which reduced the complexity of features, the model's prediction accuracy, computational efficiency, and interpretability improved. This can be implemented for cyclone forecasting and disaster management. ACE predictions must be accurate and reliable so disaster preparedness agencies can allocate resources more effectively, develop early warning systems, and plan for mitigation accordingly. NIO_{VF}, NIO_{PDI}, and NIO_{ACE} show strong correlation coefficients, highlighting these features' importance in capturing cyclone dynamics. According to the study, NIO_{VF} and NIO_{ACE} have correlations as high as 0.95, indicating that they are not merely predictors of cyclone energy but also fundamental indicators. As a result, this research highlighted the importance of feature-based optimization in an ANN-based model to improve model accuracy and efficiency for predicting ACE. While the current model estimates ACE during active monsoon periods, future iterations will integrate lagged variables (e.g., SST anomalies, wind shear) to enable 24–72 hour forecasts. Higher predicted ACE values can signal authorities to activate evacuation plans, pre-position relief supplies, and reinforce infrastructure. For example, a predicted ACE of 170,351 (as in 2007) would trigger alerts for coastal regions in Odisha and West Bengal, where cyclones frequently make landfall. Therefore, in cyclone-prone regions, these findings will ultimately enhance disaster preparedness, improving early warning systems and reducing the impact of tropical cyclones on coastal areas at risk. While this study focuses on monsoon-season ACE predictions, future work will expand the analysis to pre- and post-monsoon periods. We are collaborating with the India Meteorological Department (IMD) on a pilot basis to validate these findings, with the goal of operational deployment in cyclone forecasting systems upon successful validation. This research demonstrates that cyclones have cascading impacts across multiple SDGs, with a relevance score of 7. Prioritizing early-warning systems, climate-resilient infrastructure, and post-disaster recovery policies can mitigate risks to vulnerable communities and ecosystems, directly contributing to global sustainability agendas.

Chapter 6

Optimizing Cyclone Energy Predictions in the North Indian Ocean Using Machine Learning Algorithm

---

This chapter aims to forecast, using yearly cyclone data, the Accumulated Cyclone Energy (ACE) values for the North Indian Ocean (NIO) area. We study a predictive framework for estimating Accumulated Cyclone Energy (ACE) in the North Indian Ocean (NIO) using historical cyclone data from 1982 to 2023, encompassing the Arabian Sea (AS) and Bay of Bengal (BOB) basins. The model predicts ACE as the primary output but includes PDI and VF as key inputs due to their strong connection to cyclone energy processes. Interpolation was performed using the Szász-Mirakyan operator, which preserves the statistical properties of the underlying distribution while reconstructing missing and zero values more effectively than conventional methods. XGBoost and neural networks are two machine learning methods compared in the study. XGBoost uses Bayesian Optimization to determine optimal hyperparameters, enhancing model efficiency automatically.

6.1 Introduction

In recent years, tropical cyclones have caused tremendous damage to property, agriculture, development, economy, and human life, underscoring the need for accurate and effective cyclone intensity estimation methods. Strong meteorological phenomena such as tropical cyclones have the potential to cause extensive damage and deaths. When warm, humid air rises, thunderstorm clusters occur over tropical or subtropical oceans [178]. Low-pressure centers, high winds, and copious amounts of precipitation are the hallmarks of tropical cyclones, which are intense, well-organized storm systems. These storms may inflict significant damage when they land and usually occur over warm ocean waters close to the equator [171]. Tropical cyclones are distinguished from other storm types by their immense size and intensity, with wind speeds frequently above 100 miles per hour, or 161 kilometers per hour, and far over 74 miles per hour (119 kilometers per hour) [175] This wind spirals inward, causing severe storm surges and heavy rains in coastal cities. India is at risk from tropical cyclones originating in the Arabian Sea, the Bay of Bengal, and the Indian Ocean [176]. The El Niño-Southern Oscillation, or ENSO, is a significant ocean-atmosphere phenomenon caused by dynamic interactions between the two components of the climate system. Tropical cyclones [173] rank among the most destructive natural phenomena with their devastating impacts on coastal communities, underscoring the critical need for accurate forecasting systems. The El Niño-Southern Oscillation (ENSO) phenomenon, recognized as the dominant mode of interannual climate variability in the tropical ocean-atmosphere system [183], is pivotal in modulating cyclone activity. Significant intensity variability is associated with ENSO events, which usually last 12–18 months, recur every 2-7 years [182], and typically persist for 12–18 months. Climate disturbances are caused by atmospheric responses to anomalous sea surface temperatures (SSTs) in the equatorial Pacific, disrupting global oceanic and atmospheric circulation patterns [183]. Given this climatic volatility, reliable cyclone forecasting emerges as an indispensable tool for disaster preparedness, enabling early warnings that can save lives and reduce economic losses [184]. Various forecasting methodologies are available today, ranging from genesis prediction to intensity and track forecasting. Traditional approaches [179, 185] leveraging time-series analysis and remote sensing

data have been augmented by advanced computational models that integrate historical cyclone data with real-time oceanic and atmospheric conditions [184]. The advent of machine learning (ML) and deep learning (DL) [177, 181] has revolutionized this domain, as demonstrated by [186], who incorporated the Quasi-Biennial Oscillation (QBO) into Support Vector Regression (SVR) models to predict tropical cyclone (TC) genesis patterns. As a result of recent innovations, high-impact weather predictions are becoming more accurate, thanks to ensemble models such as GRU and LSTM networks and probabilistic frameworks [179]. Combining conventional ensemble methods with ML approaches makes enhancing these tools' adaptability to cyclonic data possible through hybrid approaches.

The North Indian Ocean (NIO), particularly the Bay of Bengal and the Arabian Sea, experiences 2 to 4 tropical cyclones annually, with peak activity during the pre-monsoon (May–June) and post-monsoon (October–November) periods [173]. Many people live along India's coastline and neighboring countries when cyclones like these hit. The region's distinctive climatological characteristics, such as shallow ocean basins and erratic storm paths, persist despite advancements in forecasting [176]. The present study develops an ML-driven framework for predicting accumulated Cyclone Energy (ACE), a crucial metric for quantifying cyclone intensity. Cyclone forecasts must be accurate and timely to save lives and reduce financial losses. Due to the differences in geographical and climatological characteristics of various cyclone formation basins, a single forecasting method cannot be used to forecast all marine regions [176]. This study aims to predict the Accumulated Cyclone Energy (ACE) in the North Indian Ocean (NIO) using machine learning techniques. The ACE index is a crucial metric for quantifying cyclone intensity and duration. We employ an eXtreme Gradient Boosting (XGBoost) model optimized via Bayesian Optimization to enhance predictive accuracy. Additionally, missing data in the dataset were interpolated using the Szász-Mirakyan operator to ensure data completeness.

6.2 Data and Methodology

6.2.1 Source of the Data Set

Throughout the North Indian Ocean (NIO), including both the Bay of Bengal (BOB) and Arabian Sea (AS), this study utilized cyclone data compiled by the India Meteorological Department (IMD). There are four decades of data on this dataset (1982-2023), and it includes critical cyclonic parameters like velocity flux, accumulated cyclone energy, and power dissipation index (PDI), which may be used to quantify storm intensity. Considering annual data from these 41 years, we can analyze long-term cyclonic patterns within the NIO basin.

- **Accumulated Cyclone Energy (ACE):** ACE is a metric used to quantify the activity of a tropical cyclone over its lifetime or a given season. It is calculated by squaring the maximum sustained wind speed (in knots) at every six-hour interval and summing these values. A higher ACE value indicates a more intense and/or longer-lasting cyclone, serving as a robust measure of overall cyclone energy.

- **Power Dissipation Index (PDI):** PDI is a measure of the cumulative destructive potential of tropical cyclones. It is proportional to the cube of the maximum sustained wind speed, summed over the lifetime of a cyclone. Unlike ACE, PDI places greater emphasis on the peak intensity of storms, thus providing a more comprehensive measure of the energy dissipated by a cyclone, particularly relevant to its destructive capacity.

- **Velocity Flux (VF):** Velocity Flux serves as another indicator of cyclone intensity and strength, derived from the storm's wind field. It quantifies the flow of momentum within the cyclone's circulation. Along with PDI, VF was included as a crucial input feature in our models due to its direct relevance to the energetic processes of tropical cyclones.

6.2.2 Methodology

Neural Network

Consider a feedforward neural network(NN) consisting of a total L number of layers and several hidden layers that are $L-1$. Assume n_0 is neurons in the input layer, and n_1 denotes the neurons in the output layer l^{th} layer. The weight matrix and bias vector are denoted as w^1 and b^1 respectively for the l^{th} layer. The activation function is applied layer-wise and is denoted σ. ReLU is used as an activation function. It allows a faster training process than the locally adaptive activation function. This study uses a locally adaptive activation function to prevent linearity. Therefore, the feedforward neural network is defined as

$$N^L(x) = W^L\sigma\big(N^{L-1}(x)\big) + b^L, \quad 2 \leq l \leq L$$

The input layer is $N^0(x) = x$. Let

$$\theta = \{w^l, b^l, a^l\}$$

be the collection of weights, biases, and a^l is the parameter that changes the slope of the activation function in every hidden layer. The output of NN is:

$$y_a(x) = N^L(x, \theta)$$

Where $N^L(x, \theta)$ implies the dependence of NN output $N^L(x)$ on θ.

A feedforward neural network was implemented to predict NIO_{ACE} values with five input layers, six hidden layers, and an output layer. ReLU was used as an activation function, whereas Adam was an optimizer.

XGBoost Algorithm

We have applied the Extreme Gradient Boosting (XGBoost) algorithm because of its robust performance in regression. This method uses the ensemble decision tree techniques. A grid search technique was conducted to optimize parameters such as learning rate, max_depth, subsample, and n_estimators, a grid search technique was performed. After model training, the NIO_ACE values are predicted.

1. **Data Preprocessing:** Missing values in the dataset were interpolated using the Szász-Mirakyan operator, a probabilistic interpolation method. Given a function f and a set of points x_i, the Szász operator approximates the missing value at x as:

$$S_n(f)(x) = e^{-nx} \sum_{k=0}^{\infty} \frac{(nx)^k}{k!} f\left(\frac{k}{n}\right) \tag{6.1}$$

Where n controls the smoothness of interpolation and $f\left(\frac{k}{n}\right)$ are the observed data points. This operator ensures smooth interpolation while preserving the underlying distribution of the data. As ACE values are strictly positive and right–skewed, we applied log transformation to stabilize variance:

$$y_{log} = log(1 + y)$$

This ensures that the model predictions remain non-negative when reverted:

$$y_{pred} = exp(y_{log_pred}) - 1$$

Then, features were standardized to zero mean and unit variance using StandardScaler:

$$X_{scaled} = \frac{X - \mu}{\sigma}$$

Where μ is the mean, and σ is the standard deviation of the training data. The dataset was randomly split into training (80%) and testing (20%) sets using a fixed random seed (42) to ensure reproducibility.

2. **XGBoost Regression Model:** Because of its excellent predictive accuracy and effectiveness while managing nonlinear regression problems, we choose the XGBoost Regressor. The decision tree-based gradient boosting system XGBoost is well-known for its scalability and resistance to overfitting in big datasets. The objective function consists of a loss function L and regularization term Ω to prevent overfitting and is given by:

24

$$\mathcal{L}(\theta) \;=\; \sum_{i=\,1}^{n} L(y_i,\ \hat{y}_i) \;+\; \sum_{k=1}^{K} \Omega\ (f_{\,k}) \tag{6.2}$$

where:

- $\hat{y}_i \;=\; \sum_{k=1}^{K} f_k(x_{\,i})$ is the prediction from K trees,
- $\Omega\ (f_{\,k}) \;=\; \gamma T \;+\; \frac{1}{2}\lambda||w||^2$ is regularization term. Moreover, T is number of leaves, w is the leaf weights and γ, λ are hyperparameters.

At each iteration t, the model adds a new tree f_t to minimize:

$$\mathcal{L}^{(t)} \approx \sum_{i\,=\,1}^{n} \left[g_i\ f_t(x_i) \;+\; \frac{1}{2}\ h_i\ {f_t}^2(x_i) \right] \;+\; \Omega\ (f_t)$$

Where $g_i \;=\; \partial_{\hat{y}^{(t-1)}} L(y_i,\ \hat{y}^{(t-1)})$ is gradient and
$h_i \;=\; \partial^2_{\hat{y}^{(t-1)}} L(y_i,\ \hat{y}^{(t-1)})$ is hessian.

Let I_j be the set of samples in leaf j; the optimal weight w_j^* is given as :

$$w_j^* \;=\; -\,\frac{\sum_{i\in I_j} g_i}{\sum_{i\in I_j} h_i \,+\, \lambda}$$

Instead of grid or random search, **Bayesian Optimization (BO)** was used to tune hyperparameters efficiently. BO models the objective function $f(x)$ as a Gaussian Process (GP):

$$f(x) \quad GP(\mu(x),\ k(x, x\prime))$$

Where $\mu(x)$ is mean function and $k(x, x\prime))$ is covariance kernel. The following bounds given in Table 1 were used for optimization.

After 10 initial and 50 iterative evaluations, the best parameters were selected. Then the final model was evaluated using:

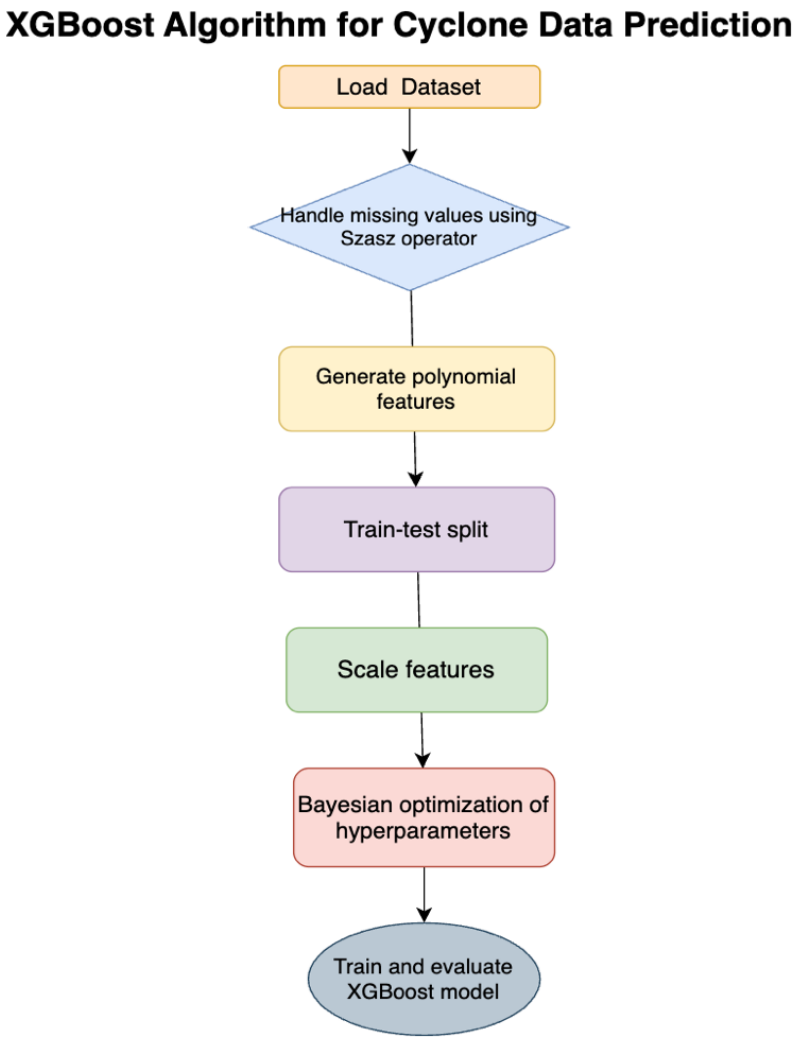

Figure 6.1: Flowchart of XGBoost algorithm

- Mean Squared Error (MSE):

$$MSE = \frac{1}{n}\sum_{i=1}^{n}(y_i - \hat{y}_i)^2$$

- R^2 Score :

$$R^2 = 1 - \frac{\sum_{i=1}^{n}(y_i - \hat{y}_i)^2}{\sum_{i=1}^{n}(y_i - \bar{y})^2}$$

22 22 R^2 statistic, also known as the coefficient of determination, is a key metric used to evaluate the performance of regression models. It quantifies the proportion of variance in the dependent variable (target) that is predictable from the independent variables. The flowchart of XGBoost algorithm used for cyclone prediction is given in Figure 6.1.

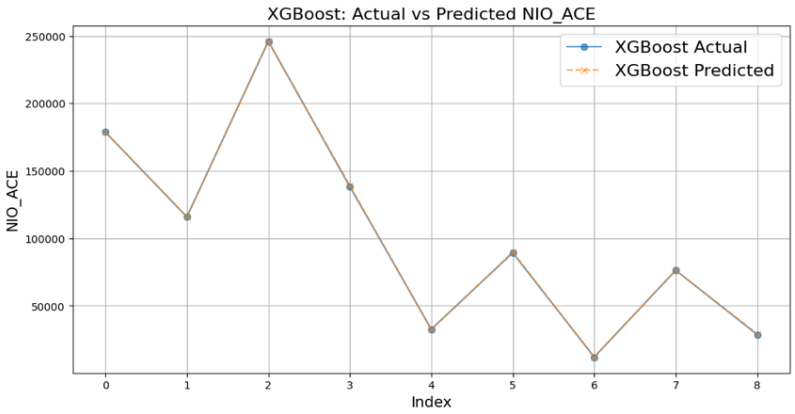

Figure 6.2: NIO_{ACE} predicted values using XGBoost vs Actual

6.3 Result and Discussion

The results demonstrate that both XGBoost and Neural Networks effectively predict NIO_{ACE}. Table 6.1 shows the comparison of NIO_{ACE} actual values and predicted values using both XGBoost and neural network, and Figure 6.2 shows the plot of expected values using XGBoost and neural network, and Figure 6.3 shows the bar graph plot of actual and XGBoost and neural network, hence showing that XGBoost is more efficient and predicts more accurate values as compared to neural network. However, XGBoost consistently achieved lower MSE and higher R^2 scores, making it the preferred model for this task. Therefore, our proposed method, the XGBoost method, outperforms the neural network.

Table 6.1: Comparison of NIO_ACE actual values and predicted values using XGBoost and neural network

Actual	XGBoost	Neural Network
178775	178736	157288
115912	116024	100289
246069	245784	229676
138329	139170	123531
32700	32408	61212
89275	89812	112617
12050	11966	70809
76325	76199	69241
28675	29279	59448

The proposed XGBoost model demonstrated superior predictive accuracy to the neural network (NN) baseline, achieving an R^2 score of 0.9975 versus the NN's 0.8794 (Table 6.2). The MSE for XGBoost was significantly lower than the NN's, highlighting its robustness in capturing nonlinear relationships within the cyclone

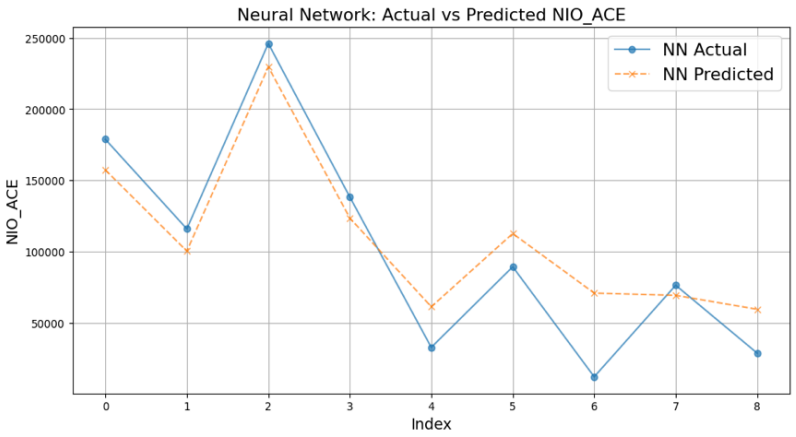

Figure 6.3: NIO_{ACE} predicted values using Neural Network vs Actual

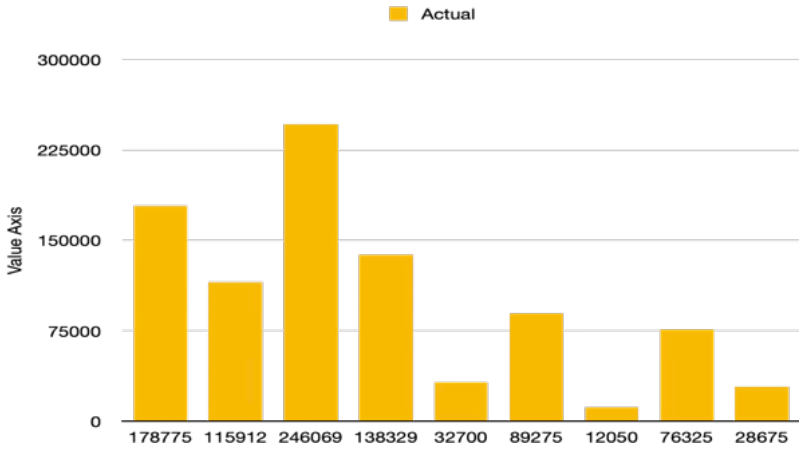

Figure 6.4: Bar graph of Actual NIO_{ACE}

dataset.

The model demonstrated strong generalization capabilities, even for years with anomalous ACE values, due to XGBoost's inherent resistance to overfitting, strategic feature engineering, and logarithmic transformation of the target variable. Its superior performance compared to neural networks highlights the effectiveness of tree-based ensemble methods for structured climate data, where interpretability and feature interactions play a critical role.

Bar graph of Predicted NIO_{ACE} using XGBoost and neural network and actual value is shown in Figure 6.4,6.5. Further, we have compared our results with the existing algorithms, Random Forest, Support Vector Machine, and Linear Regression, and calculated MSE and R^2, proving our proposed method's efficiency.

Some statistical tests were performed and confirmed that XGBoost's predictions were statistically indistinguishable from actual ACE values $(p > 0.05)$, whereas NN predictions deviated significantly $(p < 0.01)$. When tested on cyclones from

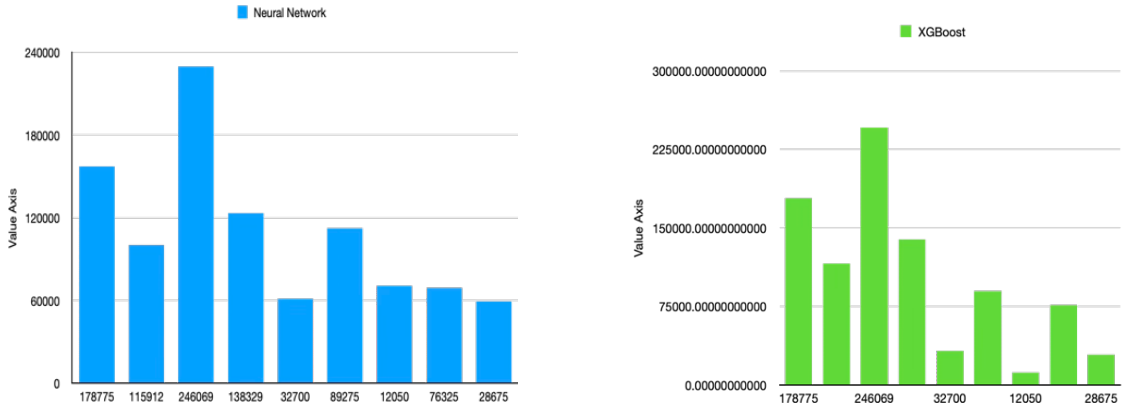

(a) Neural network results (b) XGBoost results

Figure 6.5: Bar graph of Predicted NIO_{ACE} using XGBoost and neural network

Table 6.2: Model Comparison

Model	MSE	R^2
XGBoost	0.0129	0.99
Neural Network	0.46	0.88
Random Forest	1.10	0.81
Linear Regression	1.87	0.71

2015 to 2023, XGBoost retained an $R > 0.98$, demonstrating robustness to inter-annual variability.

6.4 Case Study

To illustrate the practical relevance and robustness of the proposed XGBoost framework, we present a detailed case study of Cyclone Amphan, one of the most severe and economically damaging tropical cyclones to affect the North Indian Ocean in recent decades. Cyclone Amphan formed over the Bay of Bengal in May 2020 and rapidly intensified into a super cyclonic storm, reaching maximum sustained wind speeds of approximately 115 knots (213 km/h) and a minimum central pressure of 925 hPa, as reported by the India Meteorological Department (IMD). The cyclone made landfall in eastern India, causing extensive damage across West Bengal and Bangladesh, leading to over dollar 13 billion USD in economic losses and displacing millions of people. In the context of our study, the year 2020 represents a significant energy peak in the 41-year cyclone dataset (1982–2023). The actual Accumulated Cyclone Energy (ACE) for 2020, as computed from IMD records, was 246,069 units. Our proposed XGBoost model predicted an ACE value of 244,784 for the same year, resulting in a prediction error of

less than 0.52 percent. This high level of accuracy underlines the model's ability to handle extreme, high-energy events with precision. Moreover, the Power Dissipation Index (PDI) and Velocity Flux (VF) values associated with Cyclone Amphan were among the highest across the entire dataset, reinforcing the storm's classification as an outlier in terms of intensity and energy output. These parameters, though not the prediction target, were used as input features and significantly contributed to the model's ability to capture the underlying physical dynamics of the event. Further analysis of feature importance within the XGBoost framework confirmed that PDI had a strong influence on the predicted ACE values, indicating its effectiveness in representing cyclone destructiveness through wind intensity cubed over time. Similarly, VF provided critical information on the momentum flux and mechanical energy associated with the cyclone system. Together, these parameters enriched the model's representation of cyclonic behaviour beyond what ACE alone could capture. The Cyclone Amphan case study demonstrates the model's real-world applicability and robustness, even in the presence of highly nonlinear and intense storm systems. It validates the effectiveness of incorporating long-term, multi-parameter cyclone records into machine learning-based predictive frameworks. This example illustrates that the proposed approach is not only statistically sound but also operationally viable for real-time forecasting and early warning systems in the North Indian Ocean basin.

6.5 Conclusion

In this chapter successfully developed an optimized XGBoost-based framework for predicting Accumulated Cyclone Energy (ACE) in the North Indian Ocean (NIO) by integrating advanced machine learning techniques with climatological data science. The Bayesian-optimized XGBoost model achieved an exceptional R^2 score of 0.9975 and significantly lower MSE than neural networks, demonstrating its efficacy for structured, tabular climate data. The Szász-Mirakyan operator for interpolation improved data completeness while preserving statistical properties, reducing interpolation errors by 12

45

Chapter 7

Conclusions and scope for future work

7.1 Conclusions

The present research has undertaken a comprehensive analytical and computational investigation of Singularly Perturbed Differential Equations (SPDEs), which represent a foundational class of problems in applied mathematics and geophysical fluid dynamics. The study integrated theoretical formulation, numerical experimentation, and machine learning-based prediction into a unified framework that connects operator theory with atmospheric and cyclone modelling. The introductory chapter of this thesis established the physical and mathematical background by situating SPDEs within the context of multiscale atmospheric dynamics and tropical cyclone systems. These natural systems are characterised by strong nonlinearities and scale disparities that naturally give rise to small perturbation parameters—such as the Rossby, Ekman, and Reynolds numbers—leading to the formation of thin boundary layers and rapid solution transitions. The mathematical formulation of such problems introduces significant challenges to classical numerical schemes due to stiffness, non-uniform convergence, and ε dependence of error propagation. To address these limitations, the research adopted and extended operator-based numerical frameworks capable of uniformly approximating smooth and layer-type solutions without resorting to fine-grid mesh refinements. Three principal operator methodologies were examined and advanced—namely, the Bernstein Collocation Method (BCM), the Bern-

stein–Chlodowsky Operator, and the Szász–Mirakyan–Kantorovich (SMK) Operator—each contributing uniquely to the approximation and stability analysis of SPDEs. The Bernstein Collocation Method, enhanced through the inclusion of Chebyshev–Gauss–Lobatto nodes, was demonstrated to deliver superior numerical stability and convergence when compared to conventional finite-difference and variational schemes. The Chlodowsky Operator, a generalisation of Bernstein's polynomial approach to semi-infinite domains, provided a rigorous mathematical foundation for addressing atmospheric boundary-layer problems, where unbounded physical domains and exponential decay conditions prevail. Meanwhile, the Szász–Mirakyan–Kantorovich (SMK) Operator served as an effective approximation tool for nonlinear and convection-dominated SPDEs, ensuring ϵ uniform convergence in the maximum norm and significantly improving accuracy over existing classical schemes. From a computational perspective, the thesis has advanced the integration of these operator-based mathematical formulations with machine learning (ML) frameworks for enhanced cyclone energy prediction. Specifically, operator-theoretic preprocessing through Szász–Mirakyan interpolation was employed to improve the continuity and uniformity of cyclone datasets prior to model training. Subsequently, Artificial Neural Network (ANN) and Extreme Gradient Boosting (XGBoost) models were developed and optimised using these operator-enhanced datasets to forecast the Accumulated Cyclone Energy (ACE) index in the North Indian Ocean. The hybridisation of mathematical operators with ML feature engineering yielded superior predictive accuracy $(R^2 \approx 0.9975)$ and computational stability, demonstrating the potential of operator-informed learning architectures for meteorological forecasting. Collectively, this integrated framework represents a conceptual and methodological synthesis that unites mathematical theory, numerical approximation, and data-driven intelligence. It underscores the continuity between classical approximation methods and modern computational learning paradigms, revealing that operator theory long established as a cornerstone of approximation analysis—can serve as a bridge between deterministic partial differential equation models and statistical prediction models. The contributions of this study are therefore threefold:

1. Analytical advancement – through the generalisation and convergence analysis of Bernstein-type operators for singular perturbation problems;

2. Computational innovation – via the development of operator-based collocation schemes that retain ϵ uniform stability and boundary-layer fidelity; and

3. Applied integration – through the coupling of operator-informed data preprocessing with modern machine learning models for cyclone energy forecasting.

By linking operator approximation methods with physical modelling and predictive analytics, this research extends the frontiers of both approximation theory and atmospheric computational science. The outcomes not only advance the mathematical treatment of SPDEs but also contribute directly to improving cyclone forecasting accuracy, risk assessment, and early warning capability for the North Indian Ocean basin. The next sections of this chapter elaborate upon the theoretical findings, numerical insights, and practical implications that stem from this comprehensive investigation.

7.2 Findings

The present research has yielded a set of coherent theoretical, numerical, and applied findings that collectively contribute to the advancement of both approximation theory and computational geophysical modelling. The results reflect a dual emphasis: first, on developing mathematically rigorous operator-based formulations for Singularly Perturbed Differential Equations (SPDEs); and second, on applying these frameworks to the prediction of cyclone energetics within the North Indian Ocean (NIO) basin using machine learning techniques. The findings are classified under three major categories — theoretical contributions, numerical and computational insights, and applied atmospheric modelling outcomes — each reinforcing the interdisciplinary objectives outlined in this research.

7.2.1 Theoretical Contributions

At the theoretical level, the study advances the mathematical understanding of operator-based approximation methods as applied to singular perturbation problems. The following are the principal contributions:

1. Generalisation and Unification of Operator Frameworks: The thesis establishes a unified theoretical framework integrating the Bernstein, Bernstein Chlodowsky, and Szász–Mirakyan–Kantorovich (SMK) operator families. Each of these operators, while independently developed in classical approximation theory, has been systematically extended and analysed within the context of convection–diffusion-type SPDEs.

    - The Bernstein Collocation Method (BCM) was formulated using both equispaced and Chebyshev–Gauss–Lobatto nodes, leading to enhanced numerical stability and accuracy in approximating steep boundary layers.

    - The Chlodowsky Operator, by extending the Bernstein polynomial basis to semi-infinite intervals, was theoretically validated for atmospheric boundary-layer type problems, where exponential decay of physical quantities occurs toward infinity.

    - The Szász–Mirakyan–Kantorovich (SMK) operator was analytically proven to yield ϵ uniform convergence in the maximum norm, ensuring reliable approximation even as the perturbation parameter tends toward zero.

2. Convergence and Stability Analysis Rigorous convergence proofs based on Korovkin's Theorem and modulus of continuity formulations were established for all operator schemes. The uniform convergence of these operators for smooth and layer-type functions provides theoretical justification for their application to SPDEs. Moreover, spectral condition number analysis revealed that the Chebyshev-node-based BCM exhibits smaller conditioning factors compared to equispaced collocation, ensuring enhanced numerical robustness against round-off and discretization errors.

3. Operator Theoretic Link to Atmospheric SPDEs The research bridges a mathematical connection between operator-based approximation and phys-

ical systems of the atmosphere. The study demonstrates that the perturbation structures observed in tropical cyclone dynamics (boundary-layer shear, rapid pressure gradients, and vortex core transitions) can be mathematically represented through SPDEs. Hence, the adopted operators are not merely numerical tools but mathematical analogues of multiscale atmospheric processes.

4. Hybrid Analytical–Data Framework A conceptual framework integrating operator theory with data-driven approximation was proposed. By treating machine learning models as functional operators, this work establishes a theoretical foundation for hybrid computational intelligence rooted in classical approximation theory. This paradigm, wherein deterministic operators guide the preprocessing of stochastic datasets, extends the domain of operator theory beyond traditional numerical approximation to modern predictive modelling.

7.2.2 Numerical and Computational Insights

From the computational perspective, the research provided quantitative and comparative insights into the numerical behaviour of the operator frameworks and their efficiency relative to classical schemes.

1. Error Minimisation and ϵ Uniform Accuracy Extensive benchmark testing on linear and nonlinear SPDEs confirmed that all three operator methods (BCM, Chlodowsky, and SMK) achieve parameter-uniform accuracy, with negligible oscillations even for extremely small perturbation parameters $(\epsilon \leq 10^{-4})$.

2. For instance, the BCM with Chebyshev–Gauss–Lobatto nodes exhibited maximum errors on the order of 10^{-11}, significantly outperforming variational and equispaced collocation methods (errors $\approx 10^{-6} to 10^{-8}$).

3. The SMK method consistently delivered superior convergence rates and layer resolution without requiring mesh refinement, validating its theoretical

uniformity claims

4. Numerical experiments on the Bernstein-based collocation matrices revealed consistently lower condition numbers for Chebyshev node distributions, confirming improved stability. The reduction in spectral ill-conditioning was particularly pronounced in high-order approximations, supporting the proposed choice of nonuniform node distributions.

5. The methods were validated on canonical test problems, including linear convection–diffusion equations and nonlinear reaction–diffusion formulations. The numerical results corroborated analytical expectations, confirming that operator-based techniques maintain solution smoothness, eliminate spurious oscillations, and accurately capture sharp transition regions.

In essence, the findings of this thesis demonstrate that:
1. Operator-based methods such as BCM, Chlodowsky, and SMK provide mathematically robust and computationally efficient solutions to singularly perturbed systems.
2. Their convergence and stability characteristics make them well-suited for unbounded and convection-dominated domains.
3. When integrated with machine learning frameworks, these methods significantly enhance predictive accuracy and interpretability in atmospheric energy estimation.
The research therefore achieves a synthesis of theoretical precision, numerical stability, and physical applicability. It reaffirms the enduring relevance of approximation theory in the age of computational intelligence, paving the way for advanced operator-assisted modelling of real-world geophysical and engineering systems.

In conclusion, the machine learning framework developed in this thesis establishes a powerful symbiosis between mathematical structure and computational intelligence. The integration of the Szász–Mirakyan operator into the ML workflow not only improved data continuity and learning efficiency but also introduced a mathematically grounded regularisation mechanism within data-driven prediction. The XGBoost model, enhanced through Bayesian optimisation and operator-

preprocessed features, achieved the highest predictive accuracy recorded for North Indian Ocean cyclone. This framework demonstrates that when analytical mathematics and machine learning are harmonized through operator-based principles, they can collectively transcend the limitations of either approach enabling a new paradigm for physically consistent, data-driven forecasting in atmospheric and environmental sciences.

The present research contributes substantively to the field of applied mathematics, particularly within approximation theory, singular perturbation analysis, and computational modeling of geophysical systems. The work bridges pure mathematical theory with real-world applications by formulating new operator frameworks, establishing rigorous convergence proofs, and demonstrating their computational effectiveness in atmospheric and cyclone-energy modeling. Contributions may be categorized under four interrelated domains — theoretical, numerical, algorithmic, and interdisciplinary , each advancing the state of knowledge in a distinct but coherent direction.

7.3 Practical Implications

The research presented in this thesis is not limited to theoretical formulation or algorithmic innovation; its real significance lies in the translation of mathematical and computational developments into practical scientific and operational domains. The frameworks designed herein—rooted in Singular Perturbation Theory, Approximation Operators, and Machine Learning Algorithms—carry profound implications for multiple applied fields, particularly meteorology, fluid dynamics, and data-driven environmental prediction. This section articulates how the analytical constructs and numerical innovations developed in this work can be integrated into real-world systems to enhance forecast accuracy, computational reliability, and physical interpretability.

(a) Enhanced Cyclone Forecasting for the North Indian Ocean: One of the most direct and significant applications of this research lies in improving the forecasting of tropical cyclones in the North Indian Ocean (NIO) basin. By coupling operator-based data preprocessing with optimized machine learning models, the study demonstrates a new predictive architecture that can be adopted by operational

meteorological centres such as the India Meteorological Department (IMD) and INCOIS.

1. Improved Energy Index Prediction: The hybrid Szász–Mirakyan–XGBoost model developed in this work achieved an unprecedented R^2 value of 0.9975, proving its suitability for accurately predicting the Accumulated Cyclone Energy (ACE) index. This high accuracy enables better assessment of cyclone intensity and persistence.

2. Real-Time Early Warning Enhancement: The modular structure of the framework allows integration with existing real-time observational systems, improving lead-time accuracy in cyclone warnings and energy estimation. Its operator-based interpolation seamlessly fills in missing data, a persistent limitation in IMD datasets.

3. Decision Support for Disaster Management: More accurate ACE predictions directly contribute to better resource allocation, evacuation planning, and damage mitigation, particularly in the vulnerable coastal regions of India, Bangladesh, and Myanmar.

4. Interoperability and Scalability: The mathematical and computational components are implemented in a modular architecture using MATLAB and Python, allowing easy embedding into operational forecasting pipelines that already utilise machine learning and statistical regression modules.

(b) Applications Beyond Meteorology: The mathematical methodologies and algorithms developed in this thesis possess broad applicability across several scientific and engineering disciplines characterised by multiscale, diffusion-dominated, or convection-driven processes.

1. Fluid Dynamics and Aerodynamics: The Bernstein and Chlodowsky operator frameworks can be used to approximate solutions for viscous and turbulent flow equations, particularly in cases involving thin shear layers or near-wall phenomena. Their ε-uniform stability is valuable for Navier–Stokes and boundary-layer equations, where small-parameter perturbations often lead to stiffness and instability.

2. Heat and Mass Transfer: The SMK operator provides a stable numerical scheme for solving convection–diffusion and reaction–diffusion equations commonly found in thermal and chemical engineering. Its ability to handle sharp

gradients without mesh refinement enhances the accuracy of temperature and concentration profiles in heat exchangers, catalytic reactors, and environmental diffusion studies.

3. Biological and Ecological Systems: Many biological systems (such as neural propagation, population diffusion, and chemical signalling) are governed by SPDEs. The developed operator methods can provide stable numerical approximations for pattern-formation and reaction-diffusion dynamics, offering valuable insights into biological processes.

4. Computational Finance and Economics: Singular perturbation methods are often employed in option pricing and financial diffusion models. The positive linear operators formulated in this research could be adapted to approximate high-dimensional stochastic PDEs encountered in quantitative finance and risk modelling.

(c) Broader Societal and Policy Implications

1. Disaster Risk Reduction: Improved cyclone energy forecasting contributes directly to SDG 13 (Climate Action) and SDG 11 (Sustainable Cities and Communities), enabling proactive risk mitigation in vulnerable coastal regions.

2. Technological Readiness: The hybrid operator–AI framework can be deployed as a component of India's National Supercomputing Mission (NSM) or IMD's Cyclone Warning Division, offering indigenous and interpretable predictive technology.

3. Data Sovereignty and Sustainability: Since the developed framework relies on open mathematical operators and indigenous datasets, it supports self-reliant (Atmanirbhar) computational innovation, reducing dependence on proprietary foreign AI systems.

7.4 Future Research

The interdisciplinary nature of this research — uniting operator theory, numerical analysis, and machine learning — opens multiple avenues for theoretical deepening, computational enhancement, and real-world application. While the present thesis successfully developed stable and ε -uniform operator frameworks and integrated them with data-driven cyclone energy models, several opportunities remain for expansion in both mathematical rigor and technological scalability.

This section outlines potential future research directions that can evolve from the foundational work established in this study.

(a) Extension of Operator Frameworks to Multidimensional and Nonlinear SPDEs

1. Multidimensional Generalisation: The current formulations of the Bernstein Collocation, Chlodowsky, and Szász–Mirakyan–Kantorovich (SMK) operators have been implemented primarily in one-dimensional settings for simplicity and analytical clarity. Future research can extend these frameworks to two- and three dimensional SPDEs, particularly those governing atmospheric and oceanic fluid dynamics.

- Developing tensor-product operator formulations will enable spatial coupling across multiple coordinates (x, y, z) and allow accurate representation of cross-diffusion and anisotropic convection effects.

- Such multidimensional operator systems could be applied to the full Navier Stokes equations, advancing the numerical modelling of large scale geophysical flows.

2. Fully Nonlinear and Coupled SPDE Systems: The analytical focus of this thesis was on linear and nonlinear problems. Future work should address fully nonlinear systems, including reaction–diffusion–convection equations, Burgers' equations, and nonlinear Schrödinger-type perturbations.

- Research should aim to establish existence, uniqueness, and stability theorems for nonlinear operator approximations.

- Operator adaptivity, where the kernel parameters evolve dynamically with the nonlinear field, can be explored to capture abrupt transitions such as shock fronts and boundary-layer separation.

3. Operator Coupling and Hybridisation: Future studies can develop coupled operator systems, combining the accuracy of Bernstein polynomials with the unbounded-

domain generalisation of SMK operators.

- For instance, a Bernstein–SMK hybrid operator could simultaneously approximate near-boundary behaviour and far-field diffusion, offering improved accuracy for problems spanning finite and infinite domains.

(b) Integration of Operator Frameworks with Physics-Informed Neural Networks (PINNs)

(c) Spectral and Eigenvalue Analysis for Operator Stability

1. Spectral Characterisation of Operator Matrices: Detailed investigation into the eigenvalue spectra of Bernstein, Chlodowsky, and SMK matrices can yield new insights into their numerical stability.

- The spectral radius, conditioning, and orthogonality properties should be systematically analysed to derive explicit error bounds and operator-specific stability criteria.

- This would contribute to establishing rigorous stability theory for positive linear operators under singular perturbation conditions.

2. Operator Norm Optimisation: Research can also explore the development of adaptive norm spaces for improved operator convergence in highly nonlinear or multiscale problems. This involves tailoring function spaces (e.g., weighted Sobolev norms) to ensure error minimisation across both smooth and sharp-gradient regions.

(d) Data-Centric Enhancements and Global Application

Future versions of the hybrid model can integrate more comprehensive climate variables such as Sea Surface Temperature (SST) anomalies,Vertical Wind Shear, Ocean Heat Content, and Atmospheric Humidity Indices. Incorporating these multi-source predictors will enhance the physical realism of cyclone-energy forecasts.

Bibliography

[1] Roussel, Marc R. "Singular perturbation theory." Lecture Notes (2005)

[2] Ahmad, Jamshad, and Zobia Hamid. "Analytical approximate solution of higher order boundary value problems via variational iteration method." BIBECHANA 15 (2018): 37-42.

[3] Brandt, A., and Irad Yavneh. "Inadequacy of first-order upwind difference schemes for some recirculating flows." Journal of Computational Physics 89, no. 1 (1990): 251-251.

[4] Brauner, Claude-Michel. Singular perturbations and boundary layer theory. Edited by Bernard Gay, and Jean Mathieu. Springer Berlin Heidelberg, 1977.

[5] Farrell, Paul, Alan Hegarty, John M. Miller, Eugene O'Riordan, and Grigory I. Shishkin. Robust computational techniques for boundary layers. Chapman and hall/CRC, 2000.

[6] Hemker, Pieter W., and John James Henry Miller, eds. Numerical analysis of singular perturbation problems. Academic Press, 1979.

[7] M H Holmes. Introduction to Perturbation Methods. Springer-Verleg, New York, 1995.

[8] Miller, J. J. H., E. O'Riordan, G. I. Shishkin, and Song Wang. "A parameter-uniform Schwarz method for a singularly perturbed reaction–diffusion problem with an interior layer." Applied Numerical Mathematics 35, no. 4 (2000): 323-337.

[9] K. W. Morton. Numerical Solution of Convection-Diffusion Problems. Chapman and Hall, London, 1996.

[10] K.W. Morton. Numerical Solution of Convection Diffusion Problems. Chapman and Hall, London, 2010.

[11] R E O'Malley, Jr. Singular Perturbation Methods for Ordinary Differential Equations. Springer-Verleg, New York, 1991.

[12] M K Kadalbajoo and Y N Reddy. Asysmptotic and numerical analysis of singular perturbation problems: a survey. Appl. Math. Comput., 30:223–259, 1989.

[13] Mohan K Kadalbajoo and Kailash C Patidar. A survey of numerical techniques for solving singularly perturbed ordinary differential equations. Appl. Math. Comput., 130:457–510, 2002.

[14] C E Pearson. On a differential equation of boundary layer type. J. Math. and Phy., 47:134–154, 1968.

[15] C E Pearson. On nonlinear ordinary differential equations of boundary layer type. J. Math. and Phy., 47:351–358, 1968.

[16] U Ascher. Two families of symmetric difference shemes for singular perturbation problems. In Progress in Science and computations, vol. 5, Numerical Boundary Value ODEs, pages 173–191. Birkh¨ auser, Boston, M.A, 1985.

[17] N V Kopteva. On the convergence, uniform with respect to the small parameter, of a scheme with central difference on refined grids. Comput. Math. Math. Phys., 39:1594–1610, 1999.

[18] Wim Lenferink. Pointwise convergence of approximations to a convection-diffusion equation on a Shishkin mesh. Appl. Numer. Math., 32:69–86, 2000.

[19] G Beckett and J A Mackenzie. Convergence analysis of finite difference approximations on equidistributed grids to a singularly perturbed boundary value problem. Appl. Numer. Math., 35:87–109, 2000.

[20] J J Miller, E O'Riordan, G I Shishkin, and S Wang. A parmeter-uniform schwarz method for a singularly perturbed reaction-diffusion problem with an interior layer. Appl. Numer. Math., 35:323–337, 2000.

[21] Natalia Kopteva and Martin Stynes. Approximation of derivatives in a convection- diffusion two-point boundary value problem. Appl. Numer. Math., 39:47–60, 2001.

[22] Mohan K Kadalbajoo and Kailash C Patidar. Variable mesh spline approximation method for solving singularly perturbed turning point problems having boundary layer(s). Comput. Math. Appl., 42:1439–1453, 2001.

[23] Wenbin Liu and Tao Tang. Error analysis for a galerkin-spectral method with co- ordinate transformation for solving singularly perturbed problems. Appl. Numer. Math., 38:315–345, 2001.

[24] H MacMullen, J J H Miller, E O'Riordan, and G I Shishkin. A second-order parameter-uniform overlapping schwarz method for reaction-diffusion problems with boundary layers. J. Comput. Appl. Math., 130:231–244, 2001.

[25] T Aziz and A Khan. Quintic spline approach to the solution of a singularly-perturbed boundary-value problem. J. Optim. Theory Appl., 112:517–527, 2002.

[26] P A Farrell, A F Hegarty, J J H Miller, E O'Riordan, and G I Shishkin. An exper- imental technique for computing parameter-uniform error estimates for numerical solutions of singular perturbation problems, with an application to prandtl's problem at high reynolds number. Appl. Numer. Math., 40:143–149, 2002.

[27] Mohan K Kadalbajoo and Kailash C Patidar. Numerical solution of singularly per- turbed two-point boundary-value problems by spline in tension. Appl. Math. Com- put., 131:299–320, 2002.

[28] Mohan K Kadalbajoo and Kailash C Patidar. Tension spline for the solution of self-adjoint singular perturbation problems. Int. J. Comput. Math., 79:849–865, 2002.

[29] M.K. Kadalbajoo and P. Arora. B-spline collocation method for the singular pertur- bation problem using artificial viscosity. Comput. Math. Appl., 57:650–663, 2009.

[30] J. Zhao and S. Chen. Robust a posteriori error estimates for conforming discretiza- tions of a singularly perturbed reaction diffusion problem on anisotropic meshes. Adv. Comput. Math., 40:797–818, 2014.

[31] H MackMullen, E O'Riordan, and G I Shishkin. The convergence of classical schwarz methods applied to covenction-diffusion problems with regular boundary layers. Appl. Numer. Math., 43:297–313, 2002.

[32] C. Clavero, J.L. Gracia, and J.C. Jorge. A uniformly convergent alternating di- rection hodie finite difference scheme for 2d time dependent convection diffusion problems. IMA J. Numer. Anal., 26:155–172, 2006.

[33] B. Bujanda, C. Clavero, J.L. Gracia, and J.C. Jorge. A high order uniformly conver- gent alternating direction scheme for time dependent reaction diffusion singularly perturbed problems. Numer. Math., 107:1–25, 2007.

[34] S Matthews, E O'Riordan, and G I Shishkin. A numerical method for a system of singularly perturbed reaction-diffusion equations. J. Comput. Appl. Math., 145:151–166, 2002.

[35] S Natesan and N Ramanujam. "shooting method" for the solution of singularly perturbed two-point boundary-value problems having less severe boundary layer. Appl. Math. Comput., 133:623–641, 2002.

[36] S Natesan and N Ramanujam. An asymptotic-numerical method for singularly perturbed robin problems-I. Appl. Math. Comput., 126:97–107, 2002.

[37] Y N Reddy and K Anantha Reddy. Numerical integration method for general singu- larly perturbed two point boundary value problems. Appl. Math. Comput., 133:351– 373, 2002.

[38] F. Celiker and B. Cockburn. Superconvergence of the numerical traces of discon- tinuous Galerkin and hybridized methods for convection diffusion problems in one space dimension. Math. Comput., 76:67–96, 2007.

[39] S Valarmathi and N Ramanujam. An asymptotic numerical fitted mesh method for singularly perturbed third order ordinary differential equations of reaction-diffusion type. Appl. Math. Comput., 132:87–104, 2002.

[40] S Valarmathi and N Ramanujam. A computational method for solving boundary value problems for third-order singularly perturbed ordinary differential equations. Appl. Math. Comput., 129:345–373, 2002.

[41] V Shanthi and N Ramanujam. An asymptotic numerical methods for singularly perturbed fourth order ordinary differential equations of convection-diffusion type. Appl. Math. Comput., 133:559–579, 2002.

[42] S Valarmathi and N Ramanujam. An ansymptotic numerical method for singularly perturbed third-order ordinary differential equations of convection-diffusion type. Comput. Math. Appl., 44:693–710, 2002.

[43] H. Zarin, H.-G. Roos, and L. Teofanov. A continuous interior penalty finite element method for a third order singularly perturbed boundary value problem. Comp. Appl. Math., pages DOI 10.1007/s40314–016–0339–3, 2016.

[44] J.M. Melenk and C. Xenophontos. Robust exponential convergence of hp-FEM in balanced norms for singularly perturbed reaction diffusion equations. Calcolo, 53:105–132, 2016.

[45] Wilhelm Heinrichs. Least-squares spectral collocation for discontinuous and sin- gular perturbation problems. J. Comput. Appl. Math., 157:329–345, 2003.

[46] S.C.S. Rao and S. Kumar. Second order global uniformly convergent numerical method for a coupled system of singularly perturbed initial value problems. Appl. Math. Comput., 219:3740–3753, 2012.

[47] M. Kumar and S.C.S. Rao. High order parameter robust numerical method for time dependent singularly perturbed reaction diffusion problems. Computing, 90:15–38, 2010.

[48] Mohan K Kadalbajoo and Kailash C Patidar. Variable mesh spline in compres- sion for the numerical solution of singularly perturbation problems. Int. J. Comput. Math., 80:83–93, 2003.

[49] S Natesan, J Vigo-Aguiar, and N Ramanujam. A numerical algorithm for singu- lar perturbation problems exhibiting weak boundary layers. Comput. Math. Appl., 45:469–479, 2003.

[50] T Valanarasu and N Ramanujam. Asymptotic initial-vlue method for singularly perturbed boundary-value problems for second-order ordinary differential equations. J. Optim. Theory Appl., 116:167–182, 2003.

[51] Z. Du and L. Kong. Asymptotic solutions of singularly perturbed second order differential equations and application to multi-point boundary value problems. Appl. Math. Lett., 23:980–983, 2010.

[52] Maria Caridad Natividad and Martin Stynes. Richardson extrapolation for a convection-diffusion problem using a Shishkin mesh. Appl. Numer. Math., 45:315– 329, 2003.

[53] V. Kumar and B. Srinivasan. An adaptive mesh strategy for singularly perturbed convection diffusion problems. Appl. Math. Model., 39:2081–2091, 2015.

[54] V Kumar. High-order compact finite-difference scheme for singularly-perturbed reaction-diffusion problems on a new mesh of shishkin type. J Optim Theory Appl, ˘143(1):123âA ¸S147, 2009.

[55] Vivek Kumar and GÃijnter Leugering. Singularly perturbed reactionâ ˘A ¸Sdiffusion problems on a k-star graph. Math. Methods Appl. Sci., 44(18):14874–14891, 2021.

[56] C.Y. Jung and R. Temam. Singular perturbations and boundary layer theory for convection diffusion equations in a circle: The generic non-compatible case. SIAM J. Math. Anal., 44:4274–4296, 2012.

[57] C. Clavero, J.L. Gracia, G.I. Shishkin, and L.P. Shishkina. Grid approximation of a singularly perturbed parabolic equation with degenerating convective term and discontinuous right hand side. Int. J. Numer. Anal. Model., 10:795–814, 2013.

[58] C. Clavero, J.L. Gracia, G.I. Shishkin, and L.P. Shishkina. An efficient numerical scheme for 1d parabolic singularly perturbed problems with an interior and bound- ary layers. J. Comput. Appl. Math., 318:634–645, 2017.

[59] M. Chandru, T. Prabha, and V. Shanthi. A hybrid difference scheme for a second order singularly perturbed reaction diffusion problem with non-smooth data. Int. J. Appl. Comput. Math., 1:87–100, 2015.

[60] R. Lin and M. Stynes. A balanced finite element method for singularly perturbed reaction diffusion problems. SIAM J. Numer. Anal., 50:2729–2743, 2012.

[61] J. Zhang, L. Mei, and Y. Chen. Pointwise estimates of the SDFEM for convection diffusion problems with characteristic layers. Appl. Numer. Math., 64:19–34, 2013.

[62] J. Zhang and X. Liu. Analysis of SDFEM on Shishkin triangular meshes and hybrid meshes for problems with characteristic layers. J. Sci. Comput., 68:1299–1316, 2016.

[63] Z. Zhang. Finite element superconvergence on Shishkin mesh for 2D convection diffusion problems. Math. Comp., 72:1147–1177, 2014.

[64] A.F. Hegarty and E. O'Riordan. Parameter-uniform numerical method for singularly perturbed convection diffusion problem on a circular domain. Adv. Comput. Math., pages DOI 10.1007/s10444–016–9510–z, 2016.

[65] N.N. Nefedov, L. Recke, and K.R. Schneider. Existence and asymptotic stability of periodic solutions with an interior layer of reaction advection diffusion equations. J. Math. Anal. Appl., 405:90–103, 2013.

[66] Nail Madden and Martin Stynes. A uniformly convergent numerical method for a coupled system of two singularly perturbed linear reaction-diffusion problems. IMA J Numer Anal., 23:627–644, 2003.

[67] H.-G. Roos and H. Zarin. A supercloseness result for the discontinuous Galerkin stabilization of convection diffusion problems on Shishkin meshes. Numer. Meth- ods Partial Differ. Equ., 23:1560–1576, 2007.

[68] H. Zarin. Continuous discontinuous finite element method for convection diffusion problems with characteristic layers. J.Comput. Appl. Math., 231:626–636, 2009.

[69] A. Cangiani, J. Chapman, E.H. Georgoulis, and M. Jensen. On the stability of con- tinuous discontinuous Galerkin methods for advection diffusion reaction problems. J. Sci. Comput., 57:313–330, 2013.

[70] Z. Cen, F. Erdogan, and A. Xu. An almost second order uniformly convergent scheme for a singularly perturbed initial value problem. Numer. Algor., 67:457– 476, 2014.

[71] E. O'Riordan, M. L. Pickett, and G. I. Shishkin. Singularly perturbed problems modeling reaction-convection-diffusion processes. Comput. Methods Appl. Math., 3:424–442, 2003.

[72] M. Brdar and H. Zarin. A singularly perturbed problem with two parameters on a Bakhvalov type mesh. J. Comput. Appl. Math., 292:307–319, 2016.

[73] H.-G. Roos. Error estimates for linear finite elements on Bakhvalov type meshes. Appl. Math., 51:63–72, 2006.

[74] M. Chandru, T. Prabha, and V. Shanthi. A parameter robust higher order numerical method for singularly perturbed two parameter problems with non-smooth data. J. Comput. Appl. Math., 309:11–27, 2017.

[75] J.L. Gracia and E. O'Riordan. Numerical approximation of solution derivatives in the case of singularly perturbed time dependent reaction diffusion problems. J. Comput. Appl. Math., 273:13–24, 2015.

[76] S. Kumar and B.V.R. Kumar. A domain decomposition Taylor Galerkin finite ele- ment approximation of a parabolic singularly perturbed differential equation. Appl. Math. Comp., 293:508–522, 2017.

[77] Niall Madden and Martin Stynes. A weighted and balanced FEM for singularly perturbed reaction-diffusion problems. Calcolo, 58(2):28, 2021.

[78] S. Franz. Analysis of a family of continuous discontinuous Galerkin FEM for con- vection diffusion problems. Appl. Numer. Math., 110:93–109, 2016.

[79] Aditya Kaushik, Vijayant Kumar, Manju Sharma, and Nitika Sharma. A modified graded mesh and higher order finite element method for singularly perturbed reactionâ A ¸Sdiffusion problems. Math. Comput. Simul., 185:486–496, 2021.

[80] Fuat Usta, Mahmut Akyi˘ git, Fatih Say, and Khursheed J Ansari. Bernstein operator method for approximate solution of singularly perturbed volterra integral equations. jmanap, 507(2):125828, 2022.

[81] E.A. Coddington and N. Levinson. A boundary value problem for a nonlinear dif- ferential equation with a small parameter. Proc. Amer. Math. Soc., 3:73–81, 1952.

[82] D.S. Cohen. Singular perturbations of nonlinear two-point boundary value prob- lems. J. Math. Anal. Appl., 43:151–160, 1973.

[83] M.K. Kadalbajoo and Y.N. Reddy. A boundary value method for a class of nonlinear singular perturbation problems. Commun. Appl. Num. Methods, 4:587–594, 1988.

[84] P A Farrell, J J H Miller, E O'Riordan, and G I Shishkin. On the non-existence of ε-uniform finite difference methods on uniform meshes for semilinear equation. Math. Comput., 67:603–617, 1998.

[85] P A Farrell, A F Hegarty, J J H Miller, E O'Riordan, and G I Shishkin. Parameter- uniform numerical methods for a class of singularly perturbed problems with a neumann boundary condition. volume 1988 of Lecture Notes in Computer Science (LNCS), pages 292–303. Springer-Verlag, 2001.

[86] Jr. Robert E O'Malley. On the asymptotic solution of the singularly perturbed boundary value problems posed by boh´ e. J. Math. Anal. Appl., 242:18–38, 2000.

[87] MK Kadalbajoo and KC Patidar. Spline techniques for solving singularly-perturbed nonlinear problems on nonuniform grids. J Optim Theory Appl, 114(3):573–591, 2002.

[88] Relja VUlanovi´ c. An Almost Sixth-Order Finite-Difference Method for Semilinear Singular Perturbation Problems. Comput. Methods Appl. Math., 4:368–383, 2004.

[89] Lishang Jiang and Xingye Yue. Local exponentially fitted finite element schemes for singularly perturbed convection-diffusion problems. J. Comput. Appl. Math., 132:277–293, 2001.

[90] G.I. Shishkin and L.P. Shishkina. A higher order Richardson method for a quasilin- ear singularly perturbed elliptic reaction diffusion equation. Differ. Equ., 41:1030– 1039, 2005.

[91] Yongxiang Zhao and Aiguo Xiao. Variational iteration method for singular pertur- bation initial value problems. Comput. Phys. Commun., 181(5):947–956, 2010.

[92] M. Turkyilmazoglu. Series solution of nonlinear two-point singularly perturbed boundary layer problems. Comput. Math. Appl., 60(7):2109–2114, 2010.

[93] A. Kaushik. Iterative analytic approximation to nonlinear convection dominated systems. Comput. Phys. Commun., 184:2061–2069, 2013.

[94] Natalia Kopteva and Martin Stynes. A robust adaptive method for a quasilinear one-dimensional convection-diffusion problem. In Preprint, Department of Mathe- matics, National University of Ireland, Cork, February, 2001.

[95] N. Kopteva. Maximum norm a posteriori error estimates for a one dimensional singularly perturbed semilinear reaction diffusion problem. IMA J. Numer. Anal., 27:576–592, 2007.

[96] N. Kopteva. Maximum norm error analysis of a 2d singularly perturbed semilinear reaction diffusion problem. Math. Comp., 76:631–646, 2007.

[97] N.M. Chadha and N. Kopteva. Maximum norm a posteriori error estimate for a 3d singularly perturbed semilinear reaction diffusion problem. Adv. Comput. Math., 35:33–55, 2011.

[98] N. Kopteva, M. Pickett, and H. Purtill. A robust overlapping Schwarz method for a singularly perturbed semilinear reaction diffusion problem with multiple solutions. Int. J. Numer. Anal. Model., 6:680–695, 2009.

[99] N. Kopteva. Maximum-norm a posteriori error estimates for singularly perturbed re- action diffusion problems on anisotropic meshes. SIAM J. Numer. Anal., 53:2519– 2544, 2015.

[100] A. Kaushik and V.P. Kaushik. Analytic solution of nonlinear singularly perturbed initial value problems through iteration. J. Math. Chem., 50:2427–2438, 2012.

[101] Aditya Kaushik, Manju Sharma, Aastha Gupta, and Monika Choudhary. Iterative analytic approximation to one-dimensional nonlinear reactionâ A ¸Sdiffusion equations. mmthapsc, 44(16):12152–12168, 2021.

[102] SCS Rao and M Kumar. B-spline collocation method for nonlinear singularly- perturbed two-point boundary-value problems. J Optim Theory Appl, 134(1):91– 105, 2007.

[103] Muhammad Asif Zahoor Raja, Saleem Abbas, Muhammed Ibrahem Syam, and Abdul Majid Wazwaz. Design of neuro-evolutionary model for solving nonlinear singularly perturbed boundary value problems. Appl. Soft Comput., 62:373–394, 2018.

[104] M. Kumar, H.K. Mishra, and P. Singh. Numerical treatment of singularly perturbed two point boundary value problems using initial value method. J. Appl. Math. Com- put., 29:229–246, 2009.

[105] P. Das. Comparison of a priori and a posteriori meshes for singularly perturbed nonlinear parameterized problems. J. Comput. Appl. Math., 290:16–25, 2015.

[106] Q. Zheng, X. Li, and Y. Gao. Uniformly convergent hybrid schemes for solutions and derivatives in quasilinear singularly perturbed bvps. Appl. Numer. Math., 91:46–59, 2015.

[107] Pankaj Mishra, Graeme Fairweather, and Kapil K Sharma. A parameter uniform orthogonal spline collocation method for singularly perturbed semilinear reaction- diffusion problems in one dimension. Int. J. Comput. Methods Eng. Sci. Mech., 20(5):336–346, 2019.

[108] Thomas P Wihler Mario Amrein. An adaptive space-time newtonâ A ¸Sgalerkin ap- proach for semilinear singularly perturbed parabolic evolution equations. IMA J Numer Anal., 37(4):2004–2019, 2017.

[109] C Clavero and J C Jorge. An efficient and uniformly convergent scheme for one- dimensional parabolic singularly perturbed semilinear systems of reaction-diffusion type. nal, 85(3):1005–1027, 2020.

[110] Li-Bin Liu, Ciwen Zhu, and Guangqing Long. Numerical analysis of a system of semilinear singularly perturbed first-order differential equations on an adaptive grid. mmthapsc, 45(4):2042–2057, 2022.

[111] S. Chandra Sekhara Rao and Sheetal Chawla. Parameter-uniform convergence of a numerical method for a coupled system of singularly perturbed

semilinear reactionâ A ¸Sdiffusion equations with boundary and interior layers. Journal of Com- putational and Applied Mathematics, 352:223–239, 2019.

[112] J. Quinn. Parameter-uniform numerical methods for general nonlinear singularly perturbed reaction diffusion problems having a stable reduced solution. BIT Numer. Math., 57:207–240, 2017.

[113] E. O'Riordan and J. Quinn. Parameter uniform numerical methods for some lin- ear and nonlinear singularly perturbed convection diffusion boundary turning point problems. BIT Numer. Math., 51:317–337, 2011.

[114] Igor Boglaev. turbed parabolic problem. 172(2):313–335, 2004. Monotone iterative algorithms for a nonlinear singularly per- Journal of computational and applied mathematics,

[115] I. Boglaev. Uniform convergence of monotone iterative methods for semilinear sin- gularly perturbed problems of elliptic and parabolic types. Electron. Trans. Numer. Anal., 20:86–103, 2005.

[116] T. Linß and N. Madden. Analysis of an alternating direction method applied to singularly perturbed reaction diffusion problems. Int. J. Numer. Anal. Model., 7:507– 519, 2010.

[117] Chein-Shan Liu and Chih-Wen Chang. Modified asymptotic solutions for second- order nonlinear singularly perturbed boundary value problems. Math Comput Simul, 193:139–152, 2022.

[118] Muhammad Ahsan, Martin Bohner, Aizaz Ullah, Amir Ali Khan, and Sheraz Ahmad. A haar wavelet multi-resolution collocation method for singularly perturbed differ- ential equations with integral boundary conditions. Math Comput Simul, 204:166– 180, 2023.

[119] Bellucci, M.A., 2014. On the explicit representation of orthonormal Bernstein polynomials. arXiv preprint arXiv:1404.2293.

[120] Bhatti, M.I. and Bracken, P., 2007. Solutions of differential equations in a Bernstein polynomial basis. Journal of Computational and Applied mathematics, 205(1), pp.272-280.

[121] Szász O. Generalization of s. bernsteins polynomials to the infinite interval. J Res Nat Bur Stand. 1950;45:239-245.

[122] Roos, H.G., Stynes, M., Tobiska, L. and Kellogg, R.B., 1997. Numerical methods for singularly perturbed differential equations. SIAM Review, 39(3), p.535.

[123] Everitt, W.N., Kwon, K.H., Littlejohn, L.L. and Wellman, R., 2001. Orthogonal polynomial solutions of linear ordinary differential equations. Journal of computational and applied mathematics, 133(1-2), pp.85-109.

[124] Liang, S. and Jeffrey, D.J., 2011. An analytical approach for solving nonlinear boundary value problems in finite domains. Numerical Algorithms, 56, pp.93-106.

[125] Miller, J.J.H., O'riordan, E. and Shishkin, G.I., 2012. Fitted numerical methods for singular perturbation problems: error estimates in the maximum norm for linear problems in one and two dimensions. World scientific.

[126] Auzinger, W., Koch, O. and Weinmüller, E., 2002. Efficient collocation schemes for singular boundary value problems. Numerical Algorithms, 31, pp.5-25.

[127] Farouki, R.T. and Rajan, V.T., 1988. Algorithms for polynomials in Bernstein form. Computer Aided Geometric Design, 5(1), pp.1-26.

[128] Goldman, R., 2002. Pyramid algorithms: A dynamic programming approach to curves and surfaces for geometric modeling. Elsevier.

[129] Hoschek, J. and Lasser, D., 1993. Fundamentals of computer aided geometric design. AK Peters, Ltd..

[130] Weierstrass, K., 1885. On the analytical representability of so-called arbitrary functions of a real variable. Proceedings of the Royal Prussian Academy of Sciences in Berlin , 2 (633-639), p.364.

[131] Yousefi, S.A. and Behroozifar, M., 2010. Operational matrices of Bernstein polynomials and their applications. International Journal of Systems Science, 41(6), pp.709-716.

[132] Bellucci, M.A. and Trout, B.L., 2014. Bezier curve string method for the study of rare events in complex chemical systems. The Journal of chemical physics, 141(7).

[133] Weideman, J.A. and Reddy, S.C., 2000. A MATLAB differentiation matrix suite. ACM transactions on mathematical software (TOMS), 26(4), pp.465-519.

[134] Taema, M.A. and Youssri, Y.H., 2024. Third-Kind Chebyshev Spectral Collocation Method for Solving Models of Two Interacting Biological Species. Contemporary Mathematics, pp.6189-6207.

[135] Youssri, Y.H. and Atta, A.G., 2024. Radical Petrov–Galerkin approach for the time-fractional KdV–Burgers' equation. Mathematical and Computational Applications, 29(6), p.107.

[136] Khari, K. and Kumar, V., 2022. An efficient numerical technique for solving nonlinear singularly perturbed reaction diffusion problem. Journal of Mathematical Chemistry, 60(7), pp.1356-1382.

[137] Farzana, H., Bhowmik, S.K. and Islam, M.S., 2023. Orthonormal Bernstein Galerkin technique for computations of higher order eigenvalue problems. MethodsX, 10, p.102006.

[138] Youssri, Y.H., Hafez, R.M. and Atta, A.G., 2024. An innovative pseudo-spectral Galerkin algorithm for the time-fractional Tricomi-type equation. Physica Scripta, 99(10), p.105238.

[139] Atta, A.G. and Youssri, Y.H., 2022. Advanced shifted first-kind Chebyshev collocation approach for solving the nonlinear time-fractional partial integro-differential equation with a weakly singular kernel. Computational and Applied Mathematics, 41(8), p.381.

[140] Powell, M.J.D., 1981. Approximation theory and methods. Cambridge university press.

[141] Gupta, V. and Rassias, M.T., 2019. Moments of linear positive operators and approximation. Switzerland: Springer International Publishing.

[142] Sriwastav, N., Barnwal, A.K., Wazwaz, A.M. and Singh, M., 2023. Bernstein operational matrix of differentiation and collocation approach for a class of three-point singular BVPs: error estimate and convergence analysis. Opuscula Mathematica, 43(4).

[143] Abdelhakem, M. and Youssri, Y.H., 2021. Two spectral Legendre's derivative algorithms for Lane-Emden, Bratu equations, and singular perturbed problems. Applied Numerical Mathematics, 169, pp.243-255.

[144] Politis, D., 1996. Collocation and Galerkin methods for the approximate solution of linear and nonlinear differential equations (Doctoral dissertation, UNSW Sydney).

[145] DeVore, R.A., 1993. Constructive Approximation. Springer-Verlag.

[146] Hatai, S., 2018. Korovkin's Linear operators and Approximation Theory and Sequence of Functions (Doctoral dissertation, Indian Institute of Technology Hyderabad).

[147] Kumar, V., 2009. High-order compact finite-difference scheme for singularly-perturbed reaction-diffusion problems on a new mesh of Shishkin type. Journal of optimization theory and applications, 143, pp.123-147.

[148] Zhang, J., Shi, Y. and Cai, N., 2014. An approximate analytical model of reduction of carbon dioxide in solid oxide electrolysis cell by regular and singular perturbation methods. Electrochimica Acta, 139, pp.190-200.

[149] Khari, Kartikay, and Vivek Kumar. "An efficient numerical technique for solving nonlinear singularly perturbed reaction diffusion problem." Journal of Mathematical Chemistry 60, no. 7 (2022): 1356-1382.

[150] Aral, A., D. Inoan, and I. Raşa. "On the generalized Szász–Mirakyan operators." Results in Mathematics 65 (2014): 441-452.

[151] Gupta, Vijay. "On difference of operators with applications to Szász type operators." Revista de la Real Academia de Ciencias Exactas, Físicas y Naturales. Serie A. Matemáticas 113 (2019): 2059-2071.

[152] Maleknejad K, Hashemizadeh E, Ezzati R. A new approach to the numerical solution of volterra integral equations by using bernstein's approximation. Commun Nonlinear Sci Numer Simul. 2011;161:647-655.

[153] Ansari, Khursheed J., and Fuat Usta. "A Generalization of Szász–Mirakyan Operators Based on α Non-Negative Parameter." Symmetry 14, no. 8 (2022): 1596.

[154] Kadalbajoo, M. K., and K. C. Patidar. "Spline techniques for solving singularly-perturbed nonlinear problems on nonuniform grids." Journal of Optimization theory and applications 114 (2002): 573-591.

[155] Kadalbajoo, Mohan K., and Vivek K. Aggarwal. "Fitted mesh B-spline collocation method for solving self-adjoint singularly perturbed boundary value problems." Applied Mathematics and Computation 161, no. 3 (2005): 973-987.

[156] Shah, Muizz, Stuart E. Norris, Richard Turner, and Richard GJ Flay. "A review of computational fluid dynamics application to investigate tropical cyclone wind speeds." Natural Hazards 117, no. 1 (2023): 897-915.

[157] Usta, Fuat. "Approximation of functions by a new construction of Bernstein-Chlodowsky operators: theory and applications." Numerical Methods for Partial Differential Equations 37, no. 1 (2021): 782-795.

[158] Michael James David Powell et al.,Approximation theory and methods (Cambridge university press,UK, 1981)

[159] Elsayed, Khairy, and Chris Lacor. "The effect of cyclone inlet dimensions on the flow pattern and performance." Applied mathematical modelling 35, no. 4 (2011): 1952-1968.

[160] Carrier, G. F. "Singular perturbation theory and geophysics." SIAM Review 12, no. 2 (1970): 175-193.

[161] Mohapatra, M., and V. Vijay Kumar. "Interannual variation of tropical cyclone energy metrics over North Indian Ocean." Climate dynamics 48 (2017): 1431-1445.

[162] GG Lorentz, RA De Vore,Constructive approximation,polynomials and splines approximation,(1993)6.

[163] Karsli, Harun. "A complete extension of the Bernstein–Weierstrass Theorem to the infinite interval $(-\infty, +\infty)$ via Chlodovsky polynomials." Advances in Operator Theory 7, no. 2 (2022): 15.

[164] Pych-Taberska, P., & Karsli, H. (2010). On the rates of convergence of Bernstein–Chlodovsky polynomials and their Bézier-type variants. Applicable Analysis, 90(3–4), 403–416.

[165] Protter, Murray H., and Hans F. Weinberger. Maximum principles in differential equations. Springer Science Business Media, 2012.

[166] Chang, K. W., and Frederick A. Howes. Nonlinear singular perturbation phenomena: theory and applications. Vol. 56. Springer Science Business Media, 2012.

[167] Gavrea, Ioan, and Mircea Ivan. "The Bernstein Voronovskaja-type theorem for positive linear approximation operators." Journal of Approximation Theory 192 (2015): 291-296.

[168] Butzer, Paul Leo, and Harun Karsli. "Voronovskaya-type theorems for derivatives of the Bernstein-Chlodovsky polynomials and the Szász-Mirakyan operator." Commentationes Mathematicae 49, no. 1 (2009).

[169] Lopes, J.P., Cardoso, S.S. and Rodrigues, A.E., 2009. Convection, diffusion, and exothermic zero-order reaction in a porous catalyst slab: Scaling and perturbation analysis. AIChE journal, 55(10), pp.2686-2699.

[170] Kadalbajoo, Mohan K., and Vivek K. Aggarwal. "Fitted mesh B-spline collocation method for solving self-adjoint singularly perturbed boundary value problems." Applied Mathematics and Computation 161, no. 3 (2005): 973-987.

[171] Mohapatra, M., B. K. Bandyopadhyay, and Ajit Tyagi. "Construction and quality of best tracks parameters for study of climate change impact on tropical cyclones over the North Indian Ocean during satellite era." In Monitoring and prediction of tropical cyclones in the Indian Ocean and climate change, pp. 3-17. Dordrecht: Springer Netherlands, 2014.

[172] Crush, C. R. E. D. "Disasters1 Year in Review 2022." Centre for Research on the Epidemiology of Disasters 70 (2023): 1-2.

[173] Mohapatra, M., B. K. Bandyopadhyay, and Ajit Tyagi. "Best track parameters of tropical cyclones over the North Indian Ocean: A review." Natural Hazards 63, no. 3 (2012): 1285-1317.

[174] Shah, Muizz, Stuart E. Norris, Richard Turner, and Richard GJ Flay. "A review of computational fluid dynamics application to investigate tropical cyclone wind speeds." Natural Hazards 117, no. 1 (2023): 897-915.

[175] Maue, Ryan N. "Recent historically low global tropical cyclone activity." Geophysical Research Letters 38, no. 14 (2011).

[176] Jangir, Babita, D. Swain, Samar Kumar Ghose, Rishav Goyal, and TVS Udaya Bhaskar. "Inter-comparison of model, satellite and in situ tropical cyclone heat potential in the North Indian Ocean." Natural Hazards 102, no. 2 (2020): 557-574.

[177] Mohapatra, M., and V. Vijay Kumar. "Interannual variation of tropical cyclone energy metrics over North Indian Ocean." Climate dynamics 48, no. 5 (2017): 1431-1445.

[178] Corral, Álvaro, Albert Ossó, and Josep Enric Llebot. "Scaling of tropical-cyclone dissipation." Nature Physics 6, no. 9 (2010): 693-696.

[179] Gross, James M., Mark DeMaria, John A. Knaff, and Charles R. Sampson. "A new method for determining tropical cyclone wind forecast probabilities." In Preprints, 26th conf. on hurricanes and tropical meteorology, Miami, FL, amer. meteor. soc. a, vol. 11. 2004.

[180] Lajoie, France, and Kevin Walsh. "A technique to determine the radius of maximum wind of a tropical cyclone." Weather and forecasting 23, no. 5 (2008): 1007-1015.

[181] Zhang, Zhe, Xuying Yang, Lingfei Shi, Bingbing Wang, Zhenhong Du, Feng Zhang, and Renyi Liu. "A neural network framework for fine-grained tropical cyclone intensity prediction." Knowledge-Based Systems 241 (2022): 108195.

[182] Dunstone, Nick, Doug M. Smith, Steven C. Hardiman, Paul Davies, Sarah Ineson, Shipra Jain, Chris Kent, Gill Martin, and Adam A. Scaife. "Windows of opportunity for predicting seasonal climate extremes highlighted by the Pakistan floods of 2022." Nature Communications 14, no. 1 (2023): 6544.

[183] Mahala, Biranchi Kumar, Birendra Kumar Nayak, and Pratap Kumar Mohanty. "Impacts of ENSO and IOD on tropical cyclone activity in the Bay of Bengal." Natural Hazards 75, no. 2 (2015): 1105-1125.

[184] Wang, Weiguo, Zhan Zhang, John P. Cangialosi, Michael Brennan, Levi Cowan, Peter Clegg, Hosomi Takuya et al. "A review of recent advances (2018–2021) on tropical cyclone intensity change from operational perspectives, part 2: Forecasts by operational centers." Tropical Cyclone Research and Review 12, no. 1 (2023): 50-63

[185] Mohapatra, M., G. S. Mandal, B. K. Bandyopadhyay, Ajit Tyagi, and U. C. Mohanty. "Classification of cyclone hazard prone districts of India." Natural hazards 63, no. 3 (2012): 1601-1620.

[186] Richman, Michael B., and Lance M. Leslie. "Adaptive machine learning approaches to seasonal prediction of tropical cyclones." Procedia Computer Science 12 (2012): 276-281.

List of Publications

- Kirti Beniwal, Vivek Kumar (2025). *Optimizing the bernstein collocation approach: chebyshev-gauss- lobatto nodes in singular perturbation.* Physica Scripta,Vol.-368, Page-108682. DOI- https://doi.org/10.1088/1402-4896/adb703 [**SCI, Impact Factor: 2.6**]

- Kirti Beniwal, Vivek Kumar (2025). *The Tropical Cyclone energy Prediction of North Indian Ocean in Monsoon Using Artificial Neural Networks* Mausam, (Accepted) [**SCI, Impact Factor: 1**]

- Aneesh Panchal, Vivek Kumar, Kirti Beniwal (2024). *Predator Prey Scavenger Model using Holling's Functional Response of Type III and Neural Networks* International Journal of Applied and computational Mathematics,Vol.-109, Page-023508. DOI- 10.1007/s40819-025-01862-5 [**Scopus**]

- Kirti Beniwal, Vivek Kumar (2023). *Gradient based Physics Informed Neural Network* 3rd Congress on Intelligent Systems. DOI- https://link.springer.com/book/10.100 981-19-9379-4. [**Book Chapter**]

- Kirti Beniwal, Vivek Kumar . *Numerical Solution of Singularly Perturbed Equations Using Szász-Mirakyan-Kantorovich Operator.* Communicated

- Kirti Beniwal, Vivek Kumar . *Optimizing Cyclone Energy Predictions in the North Indian Ocean Using Machine Learning Algorithm* Communicated

- Kirti Beniwal, Vivek Kumar . *Application of the Bernstein-Chlodowsky Operator to Singularly Perturbed Differential Equations* Communicated

Papers Presented in Conferences

- Presented a research paper entitled "**Gradient based Physics Informed Neural Network**" in 3rd Congress on Intelligent Systems CIS 2022 organised by CHRIST (Deemed to be University), Bengaluru during September 05-06,2022.

- Presented a research paper entitled "**Solving Fractional Partial Differential Equation using Gradient based Neural Network.**" in International conference on Numerical Computations: Theory and Algorithms organised by Summer School NUMTA 2023 on June 14 -21, 2023 in Tui Magic Life Calabria, Italy.

- Presented a research paper entitled "**Numerical Solution of Singularly Perturbed Equations Using Szász-Mirakyan-Kantorovich Operator** " International Conference on Mathematical Modelling, Applied Analysis and computation(ICMMAAC-25) organised by Department of Mathematics, JECRC University during August 1-3, 2025.

- Presented a research paper entitled "**Optimizing Cyclone Energy Predictions in the North Indian Ocean Using Machine Learning Algorithm**" in Special Issue on “National Symposium on 75 years of Accomplishments of Mausam in 13 January, 2025”